Title
Direct targeting of connexin-43 to adherens junctions and SK channel regulation of granulocyte reactive oxygen species production

Author
Fay, Alexander James

Publication Date
2006

Peer reviewed|Thesis/dissertation

Direct Targeting of Connexin-43 to Adherens Junctions and SK Channel Regulation of Granulocyte Reactive Oxygen Species Production

By

Alexander James Fay

DISSERTATION

Submitted in partial satisfaction of the requirements for the degree of

DOCTOR OF PHILOSOPHY

in

BIOPHYSICS

in the

GRADUATE DIVISION

of the

UNIVERSITY OF CALIFORNIA, SAN FRANCISCO

Acknowledgments

I am thankful to have had the opportunity to work under Dr. Lily Y. Jan and Dr. Yuh Nung Jan over the course of my graduate career. Their scientific reputations that attract a talented group of scientists to the lab, and their broad interests in channel biology and neurobiology make the lab a stimulating place to work. Lily, in particular, has given me the freedom to pursue my scientific interests, even when they were outside of the mainstream of the lab, and I am thankful for the chance to have become a more independent scientist, in the process. Throughout the course of my graduate work, Lily has helped me to make sense of new data, and to place my work in the larger context of channel biology. I also appreciate Lily's support for my pursuing medical education.

Dr. Robin Shaw has been not only a scientific collaborator, but also a mentor to me. Our gap junction work would not exist without him, as he brought his interest in cardiac electrophysiology and gap junctions to the lab several years ago. It has been a privilege to work with him, as he brings both a rigorous, quantitative mind and an optimistic outlook to research. He fearlessly jumps at opportunities to learn and incorporate new techniques, and our work has benefited immeasurably from his enthusiasm and technical skill. He has been a good friend and has given me much advice and support during the medical school application process.

Xiang Qian performed the electrophysiological experiments on granulocytes. I appreciate his taking the time to discuss my data with me, and for giving me a healthy dose of optimism. Monika Jain has provided valuable technical support over the past several months of the gap junction project. She is a talented and organized

experimentalist, and has been a great help in bringing this work to a close. I have also enjoyed her friendship and our many conversations over the past two years.

Toral Surti, Helen Lai, and Patrick Haddick have been in graduate school and the Jan lab with me for most of the last five years, and are three of my closest friends. Toral is an amazingly kind and generous person, and has helped me through some difficult times in graduate school. Helen is a persistent and organized scientist, but also a very thoughtful person, and I enjoyed our many long conversations in the lab. Patrick and I have shared lab space since we began over five years ago, and he has provided much comic relief through his unique sense of humor and musical taste. Friederike Haass has also been a good friend and has helped me with experiments and reagents many times. I thank Nita Srinivas for her friendship and support, especially during the final few weeks of preparing my thesis. In addition, I wish to thank Delphine Bichet and Franck Chatelain, Michael Grabe, Kim Raab-Graham, and Hee Jung Chung for their companionship and scientific insights.

I have appreciated having my parents, James and Stephanie, close by over the past few years. They have given me many welcome dinner breaks from lab work on weekend evenings. They are also my inspiration for pursuing long term education, as they both were in school well into their thirties. I would also like to thank my brother Eric and Krysia for welcoming me on my many trips to Poland. I have enjoyed getting to know their daughters Veronica, Victoria, and Natalia, and look forward to watching them grow up.

Lily Y. Jan, a co-author for Chapters 2-4, directed and supervised the research that forms the basis for this dissertation. Yuh Nung Jan, a co-author on Chapters 2-4, also advised this research. Xiang Qian performed the electrophysiological measurements in Figure 2 of Chapter 2. Alex Fay performed all other experiments and analyses for Chapter 2. Robin Shaw, a co-author on Chapters 3 and 4, collaborated in the experimental design of both projects and performed experiments together with Alex Fay. This work is comparable to work for a standard thesis awarded by the University of California, San Francisco.

Lily Yeh Jan

Abstract

Membrane channels permit the movement of ions and small molecules across cell membranes, and are essential for electrical activity and solute homeostasis. Potassium channels are a class of ion channel that is selective for K+, and mediate the recovery phase of neuronal and cardiac action potentials, in addition to their roles in salt balance, volume regulation, calcium signaling, and apoptosis in non-excitable cells. Chapter 2 of this thesis explores the role of a small-conductance, calcium-actiavted K+ channel (SK) in reactive oxygen species (ROS) production by neutrophils, immune cells that use ROS and antimicrobial proteins to kill pathogenic microbes. This study shows that increasing SK activity in neutrophils and the neutrophil-like PLB-985 cell line enhances ROS formation by an NADPH-oxidase-independent pathway, and also increases PLB-985 apoptosis. A second study, in Chapter 3, focuses on the localization of gap junctions, clusters of connexin (Cx) proteins that span the membranes of adjacent cells and allow cells to exchange cytoplasmic small molecules. Deconvolution microscopy, imaging of live and fixed cells, and siRNA knockdown of the proteins β-catenin, EB1, and p150(Glued) are used to probe the interactions between Cx-43, microtubule plus-ends, and the adherens junction. This work proposes a novel mechanism for gap junction protein delivery directly to cell-cell borders, mediated by the capture of microtubule plus-ends by adherens junction proteins. A third study finds that nuclei can co-localize to cell-cell borders with gap junctions, and shows by nuclear microinjection that gap junctions can mediate the exchange of small molecules between the nuclei of adjacent cells.

Table of Contents

List of Figures

Chapter 1

Voltage-Gated Potassium Channels

Introduction

Cells create differences in voltage and ion concentration across membranes through the action of ATP-dependent ion pumps, and the dissipation of these electrochemical gradients through ion channels underlies the generation and propagation of action potentials, release of hormones and neurotransmitters, and many other functions essential for cellular signaling and homeostasis. Mammalian cell membranes typically maintain a resting membrane potential of –50 to –90 mV, a range that is close to the equilibrium potential for potassium (K^+) and far from the equilibrium potentials for sodium (Na^+) and calcium (Ca^{2+}). Relatively voltage-insensitive background K^+ channels maintain hyperpolarized membrane potentials at rest, resisting the depolarizing shifts in membrane potential that open voltage-dependent Na^+, K^+, and Ca^{2+} channels.

A sufficiently strong depolarizing stimulus, such as a sodium current through an ionotropic glutamate receptor, can precipitate an action potential by initiating the sequential opening and closing of voltage-gated ion channels. Voltage-gated Na^+ channels open earliest and further depolarize the membrane before they inactivate and become non-conductive. More slowly activating voltage-gated K^+ channels then open and return the membrane towards its resting potential before they inactivate. Voltage-gated Ca^{2+} channels also open upon depolarization, stimulating neurotransmitter release as well as longer term (e.g., transcriptional) effects that depend on calcium as a second messenger.

It is clear from the roles of voltage-gated ion channels in the neuronal action potential that channels must be selective for a specific ion, and must open and inactivate within the proper voltage range. The conformational changes that lead to opening and closing of channels are known as "gating," and occur in response to stimuli such as ligands or voltage. Selectivity and gating depend on structural elements of the channel proteins, and X-ray crystallographic studies in the last few years have provided the first high-resolution insights into the 3-dimensional organization and functional properties of channels. However, before the channels can affect cellular physiology, they must fold properly, co-assemble with homologous or auxiliary subunits, and reach the plasma membrane through the secretory pathway. While gating and selectivity have been tractable properties to study with electrophysiological techniques for decades, only recently have genetic, molecular biological, biochemical, and immunological approaches enabled channel biologists to understand the pre- and post-translational modification, assembly, and trafficking of ion channels.

With so many levels of regulation of ion channel activity, one can imagine that mutations of ion channels at critical amino acid residues could lead to various defects in channel folding, trafficking, or conduction. Indeed, a number of ion channel-related diseases, or channelopathies, have been described, including epilepsy, arrhythmia, myotonia, diabetes, and even cancer, in humans. In addition, animal models, particularly mouse and the fruit fly *Drosophila melanogaster*, have helped to reveal the physiological roles of both wild-type and mutant channels.

As the roles that channels play in pathophysiology become clearer, the importance of developing pharmacological tools to manipulate channel function grows. Nature has

provided many highly specific channel blockers in the form of peptide toxins from venomous snakes, spiders, sea snails, scorpions, and other species. While useful for laboratory studies, these toxins have poor bioavailability, so the identification and development of organic small molecule blockers and openers has become an important goal of pharmacological research.

This review will give an overview of the current state of knowledge about the structures of ion channels; the mechanisms of selectivity and gating; the cell biology of ion channels, including co-assembly of channel subunits with other proteins and trafficking of ion channels; the physiological functions of ion channels and their roles in disease; and pharmacological tools available for the manipulation of ion channels *in vitro* and *in vivo*. While a vast array of ion channels exists with different selectivities and mechanisms of activation, these channel classes are reviewed elsewhere, and this chapter will focus on voltage-gated K^+ channels.

Cloning and Evolutionary Relationships

Cloning of the first voltage-gated ion channel, from the eel *Electrophorus electricus*, showed four repeats of a six transmembrane segment (TMS) topology, with a highly charged fourth TMS in each repeat [1]. Further cloning of other voltage-gated channels indicated that an amphipathic alpha-helix, with an arginine residue approximately every fourth residue, is a conserved motif among voltage-gated ion channels. This charged helix appeared to be a region of the channel that might be sensitive to changes in transmembrane potential.

Identification of the genes for voltage-gated K^+ channels, beginning with the *Shaker* mutant of *Drosophila* [2, 3], revealed an evolutionary relationship among voltage-gated ion channels. Whereas the Na^+ and Ca^{2+} channels contain four pseudorepeating domains (DI-IV), each containing six TMS, the voltage-gated K^+ channels are made up of only one domain of six TMS and assemble as tetramers. Thus, it appears that voltage-gated sodium and Ca^{2+} channels emerged evolutionarily by successive gene duplications from a K^+ channel precursor. With the sequencing of genomes of organisms from all kingdoms of life, it is clear that voltage-gated ion channel genes are both ancient and ubiquitous. Na^+ channels of 24TMS topology have been found in some lower organisms, such as cnidarians and ctenophores [4], and one 24TMS voltage-gated Ca^{2+} channel is present in the yeast *Saccharomyces cerevisiae* [5]. Among the voltage-gated cation channels, only K^+ channels are present in prokaryotes, though a Na^+ channel of 6TM topology from *Bacillus halodurans* has been cloned and characterized [6]. Bacterial K^+ channels that can be over-expressed and purified in large quantities provided the raw materials for the X-ray crystallographic studies that show the details of ion selectivity and voltage-sensing at an atomic level.

Nomenclature

The naming of ion channels has been an idiosyncratic process over the years, as researchers named channels for mutant or knockout phenotypes, or with acronyms derived from channel functional properties. For example, K^+ channels related to the *Shaker* channel from *Drosophila* have alternately been called Shaker, $K_v1.x$, or KCNA channels. In the interest of consistency, we will follow IUPHAR nomenclature for

voltage-gated sodium (Na_v) [7] and Ca^{2+} channels (Ca_v) [8]. For voltage-gated K^+ channels, we use K_v names for the A-type and delayed rectifier channels $K_v1.x$, $K_v2.x$, $K_v3.x$, $K_v4.x$, $K_v5.1$, $K_v6.x$, $K_v8.1$, and $K_v9.x$. We use the more common literature names for the KCNQ1-5 channels and for the calcium-activated K^+ channels of large (BK), intermediate (IK), and small (SK) conductance. The more widely used, *Drosophila*-derived names EAG, ERG, and ELK are employed instead of KCNH1-8 or $K_v10.x/K_v11.x/K_v12.x$ [9].

Potassium Channels

K^+ channels are essential in both excitable and non excitable cells for the control of membrane potential, regulation of cell volume, and the secretion of salt, neurotransmitters and hormones. They allow the selective, diffusional passage of potassium ions across biological membranes, and are capable of up to 10,000-fold selectivity of potassium over sodium. Voltage-gated K^+ channels, unlike the related voltage-gated Na^+ and Ca^{2+} channels, are expressed not only in heart, neurons, and muscle cells, but also in many non-excitable cells.

While best known for their role in repolarizing the membrane of neurons and cardiomyocytes during an action potential, K^+ channels are, in fact, expressed in most mammalian cell types. They play a critical role in such diverse processes as epithelial salt balance across epithelial cells, particularly in the kidney and colon, T cell signaling, and insulin release by pancreatic beta cells. Accordingly, a growing number of K^+ channels are potential targets for treatment of diseases. For example, missense mutations in KCNQ2 or KCNQ3 that reduce M-channel current cause an autosomal dominant form of

seizure disorder, benign neonatal familial convulsions. And a number of voltage-gated K^+ channel mutations can cause arrhythmias by delaying the repolarization phase of the cardiac action potential.

With the sequencing of the human genome, over 80 K^+ channels genes have now been identified, and can be grouped into several classes based on their transmembrane topologies. The inwardly-rectifying K^+ channels have two TMS flanking the highly conserved pore region, or P loop, which confers potassium selectivity (see "Selectivity," below), and assemble as tetramers. The two-P, or KCNK channels, consist of two inward recitifier-type domains linked together, and function as dimers. The voltage-gated and calcium-activated K^+ channels have an inward rectifier-type topology, containing the conserved P loop, preceded by four transmembrane domains (five, in the case of BK channels). A highly charged fourth TMS functions as the voltage sensor in the voltage-gated channels. The N- and C-terminal domains of K^+ channels are cytoplasmic and can regulate channel electrophysiological properties and trafficking, and can be a platform for phosphorylation, channel-lipid interactions, and co-assembly with other proteins. In addition to these pore-forming, or α-subunits, a number of cytosolic and transmembrane proteins co-assemble with K^+ channels and alter channel sensitivity to various ligands or to voltage, or regulate subcellular localization of the channel complex.

The last six years have brought high-resolution structures of several bacterial K^+ channels, as well as cytoplasmic domains and beta subunits of several mammalian channels. The structure of KcsA in 1998 [10] showed the atomic details of potassium coordination by the selectivity filter. While the KcsA structure shows a channel in the closed state, the structure of the calcium-activated MthK [11] revealed the conformation

of an open channel. A structure of the voltage-gated K^+ channel, K_vAP, was published in 2003 [12], but there is still much debate regarding the organization of transmembrane helices of this class of channels and the conformational changes involved in voltage gating [13]. The increasing use of structural biology as a tool for studying ion channels will allow for more detailed understanding of gating, selectivity, disease-causing mutations, as well as the interactions between channels and the drugs that modulate them.

A vast pharmacology exists for K^+ channels, including many peptide toxins isolated from microbes and venomous animals, and therapeutically more useful small organic compounds. Many of these agents act on multiple K^+ channels subtypes, on account of the conserved structural elements among K^+ channels, while others show potent specificity for a single channel subtype.

Voltage-Gated K^+ Channels

Voltage-gated K^+ channels are generally divided into subgroups depending on sequence homology and the ability to heteromultimerize. The three Shal K^+ channels (K_v4.1-4.3 or KCND1-3), for example, can co-assemble with each other but not with Shaker (K_v1.1-1.8 or KCNA1-8) K^+ channels. The K_v channels activate upon depolarization and inactivate either through fast or slow inactivation, and are also known as delayed rectifiers, since upon depolarization they repolarize the membrane after a delay. Other voltage-gated K^+ channels, the KCNQ channels and KCNH (HERG, EAG, ELK) channels, activate more slowly and are known as slow delayed rectifiers. While electrophysiological studies have demonstrated the diverse activation and inactivation properties of voltage–gated K^+ channels, high resolution structural studies and

spectroscopy are beginning to provide detailed molecular models for the voltage-dependent properties of these channels.

Selectivity

The region of K^+ channels responsible for selectivity, the P-loop, was identified more than a decade ago by sequence alignment and mutagenesis studies, and a tripeptide motif Gly-Tyr-Gly, was found to be crucial for distinguishing potassium from other monovalent cations [14]. It was not until MacKinnon and colleagues solved the crystal structure of the KcsA channel from *Streptomyces lividans* [10] that the geometry of potassium coordination by the channel pore became clear. The four subunits of the K^+ channel symmetrically surround the permeating potassium ions of the structure, with the channel reaching its narrowest point at the GYG region of the P-loop. In this region, known as the selectivity filter, rings of four carbonyl oxygens coordinate potassium ions as they move through the constriction in single-file. The oxygens, in effect, mimic the hydration sphere of a potassium ion in solution, and therefore lower the dehydration energy required to move the ion from bulk solvent into the protein channel. The geometry of the pore provides a more favorable coordination sphere for potassium than for sodium, which has a smaller atomic radius and a higher dehydration energy. Some have argued recently, though, that the channel pore may not be rigid, and that the nature of carbonyl dipole moments themselves favor potassium over sodium [15].

Conduction occurs in the direction of the electrochemical gradient for potassium at rates approaching the diffusion limit. Repulsion between closely-spaced potassium ions in the selectivity filter facilitates such rapid conduction [10]. The narrow selectivity

filter makes up less than a third of the distance of the conduction pathway, and the rest of the channel pore is wide enough to contain water molecules that hydrate ions as they pass through the inner cavity. Thus, each ion is only briefly dehydrated. Ions in the water-filled cavity below the selectivity filter are further stabilized by the orientation of negative dipoles of the four pore helices towards the cavity.

Voltage-Activation

With the cloning and sequencing of the first voltage-gated K^+ channels, *Shaker* from *Drosophila melanogaster* in 1987 [3], and the previously cloned voltage-gated sodium and Ca^{2+} channels, it became clear that the charged S4 TMS was likely to be important for voltage sensing. Electrophysiological studies had already shown that a "gating current" of 12-13 charges precedes the conduction of ions through the channel, indicating that a charged part of the channel protein moves across the transmembrane electric field in a voltage-dependent manner [16]. Site-directed mutagenesis of basic residues in S4 confirmed the importance of S4 in voltage gating [17]. Later experiments showed that acidic residues in the S2 and S3 segments are important for stabilizing S4 basic residues within the membrane [18]. Based on the presumed topology of the channel and the magnitude of gating currents, several models for voltage sensor movement were proposed [4]. The S4 helix might undergo a simple translation, altering the register of S2-S4 and S3-S4 interactions, and exposing some S4 residues to the extracellular solution. Alternatively, voltage sensing could be a combination of helical translation and rotation of S4. Resonance energy transfer experiments measured relatively small changes in the distance of S4 segments relative to one another, results not consistent with dramatic

conformational changes [19, 20]. A way to reconcile the measured distances with the necessity of moving 12-13 charges through the transmembrane electric field is a thinning of the membrane around S4, such that four basic residues could move from the cytoplasmic side of the membrane to the extracellular side with only a modest translation and rotation.

The structure of the bacterial voltage-gated K^+ channels K_vAP showed an unexpected orientation of S1-S4, with an S3-S4 voltage-sensing "paddle" on the outer edge of each subunit and touching lipid [12]. The data led MacKinnon and colleagues to propose that the voltage paddle is flexible and can swing across the bilayer upon voltage activation [21]. A caveat of the crystallization procedure, however, was the use of an antibody against the S3-S4 region to co-crystallize with the channel. The antibody likely distorted the voltage-sensing portion of channel so that it may not be resting in its normal position for the depolarized state (assuming that crystallization in detergent mimics the zero mV state of the channel). In addition, parts of the structure that appear to be on the cytoplasmic side of the membrane in the structure are glycosylated in homologous mammalian channels, suggesting that they are unlikely to move through the membrane [13]. Thus, the mechanics of voltage-sensing are still an open question that will require more high resolution structural and computational studies before it can be answered definitively.

Gating

Diverse stimuli can cause channel opening and closing, a process known as "gating," and their effects must ultimately affect potassium movement through the

permeation pathway of the channel. Structural and spectroscopic studies, coupled with measurements of the solvent accessibility of residues in open versus closed states have identified two "gates" that restrict ion permeation. One is at the cytoplasmic face of the channel, where the inner pore-lining helices constrict and can block ion passage through the narrow opening. This region was mapped through the differential accessibility of cysteine-modifying reagents to cytseine mutations in S6 in the open and closed states [22]. Structures of the KcsA channel, which is presumably in the closed state [10], and MthK, a calcium-sensitive channel in the open state [11], confirmed this result. The KcsA structure has straight pore-lining helices that constrict at the cytoplasmic side to limit access to the selectivity filter. MthK, when opened by calcium, swings open its pore helices around a glycine hinge in M2 (S6), such that there is an opening of 12 Angstroms from the cytoplasm to the inner pore. While voltage-gated K^+ channels may make use of this glycine hinge, they also have a Pro-X-Pro motif (though K_vAP lacks this element) at the cytoplasmic mouth of the channel that acts as a hinge and may make the opening narrower than that of MthK [23]. Interestingly, this more constricted opening may explain in part the ten-fold lower conductance of K_v channels compared to MthK.

The second gate is at the selectivity filter, which can adopt a conformation that prevents permeation of ions. This kind of gating underlies C-type (slow) inactivation of K_v channels, an inactivation mechanism that persists in the absence of fast inactivation (see below) and is dependent on the extracellular potassium concentration. The structure of KcsA in the presence of low potassium (3 mM) shows a collapsed structure that coordinates fewer potassium ions than the high potassium (200mM) structure [24]. The structure of a bacterial inwardly-rectifying K^+ channels has a slightly different pore

structure, and also appears to be a non-conducting form [25] that may represent a C-type inactivated conformation.

A related question for voltage-gated channels is how voltage sensing is coupled to the channel gates to allow for opening following the movement of a gating current. During voltage-sensing, the S4 domain's charged residues move outwards, likely exerting tension on the S4-S5 linker. Some studies have suggested that this linker interacts with the C-terminal end of S6 in the HERG K^+ channels [26].

Fast Inactivation

A-type, or rapidly inactivating, K^+ channels inactivate on a scale of tens to hundreds of milliseconds after depolarization. This inhibition is mediated by a peptide of about 30 amino acids either at the N-terminus of the channel or at the N-terminus of a β-subunit. The peptide binds to the cytoplasmic side of the K^+ channel pore and prevents ion conduction until it is reversed by repolarization [27]. Although no structure of the inactivation peptide bound to the pore has been solved, the prevailing model has been the "ball-and-chain." The N-terminal "ball" of basic and hydrophobic residues is tethered by a "chain" of linker residues to the T1 domain or β-subunit, and probably snakes through the space between the T1 domain and the membrane in order to reach the pore [28]. The "ball" residues are not well conserved among channels, but hydrophobic residues seem to be of particular importance in binding to the pore [29].

Interacting Proteins

There are many cytoplasmic proteins that have been found to interact with voltage-gated K^+ channels, and to alter the electrophysiological properties or localization of the pore-forming α-subunits. The β-subunits exist in three forms, β1-3, β1 and β3 having several splice variants, and co-assemble with K_v α-subunits in the endoplasmic reticulum [30]. While β1 and β3 are capable of converting slowly-inactivating delayed rectifiers to transient A-type currents [31], β2 seems primarily to increase K_v surface expression. These subunits are members of the aldo-keto reductase family and bind NADPH. The function of the co-factor is not clear, and while mutation of catalytic residues seems to have no effect on trafficking of β2 subunits, disruption of the cofactor binding site leads to improper targeting of alpha subunits [32]. Large-conductance calcium-activated K^+ (BK) channels interact with another type of β-subunit, which has two transmembrane segments and modifies the voltage activation and calcium sensitivity of the BK α-subunits.

A second class of proteins that directly affect voltage-gated potassium activity is the KChIPs (K^+ Channel Interacting Proteins), which interact primarily with members of the K_v4 (*Shal*) sub-family. KChIPs are cytoplasmic calcium-binding proteins that have four EF-hand Ca^{2+}-binding motifs, and bind to the N-terminal domain of $K_v4.x$ channels. KChIPs1-3 affect α-subunit activity similarly, by increasing current density, shifting the voltage activation curve to more hyperpolarized potentials, speeding up recovery from inactivation, and slowing the time constant of inactivation [33]. KChIP4 may compete competitively with other KChIPs, fails to increase current density, and can remove rapid inactivation from $K_v4.x$ currents [34].

KCNE (MinK and MiRP) proteins are a class of transmembrane subunits that modulate voltage-gated K^+ channel function. They contain a single transmembrane helix with a glycosylated, extracellular N-terminus and a cytoplasmic C-terminal domain. KCNE1 assembles with KCNQ1 to form the slow component of the cardiac delayed rectifier K^+ current (IK_s), part of the repolarization phase of the cardiac action potential. Its effect on KCNQ1 is to slow voltage activation and increase conductance, and mutations in KCNE1 that reduce KCNQ1/KCNE1 conductance can be arrhythmogenic [35]. KCNE1 can also interact with $K_v4.3$ and decreases its activation and inactivation rates while increasing current density [36], while KCNE3 has been found to co-immunoprecipitate with and affect the electrophysiological properties of $K_v2.1$ and $K_v3.1$ [37].

Cytoskeletal and scaffolding proteins may help to target or maintain voltage-gated K^+ channels at specific sub-cellular locations. Filamin, an actin-binding protein, co-localizes with $K_v4.2$ and may aid in the synaptic targeting of this channel [38]. Integrins, a type of cell adhesion molecule, may help to maintain $K_v4.x$ channel complexes at the neuromuscular junction [39], and interact with $K_v1.3$ in T lymphocytes. The scaffolding protein PSD-95 can mediate synaptic clustering of K_v channels with other channels and signaling proteins [40].

K_v Channels: Physiological Functions, Disease Relevance, Pharmacology

Threshold of voltage activation and localization play key roles in the physiological function of the various K_v subunits. K^+ channels that activate at subthreshold potentials will tend to resist excitation near the resting potential, while

channels that activate at more depolarized potentials will tend to play a more important role in the repolarization phase of an action potential. Axonal or axon terminal K^+ channels shape action potentials and modulate neurotransmitter release, whereas somatodendritic channels affect synaptic integration and shape backpropagating action potentials.

K_v1 channels are predominantly localized to axonal nodes of Ranvier (the juxtaparanodal region) and nerve terminals [41], though they have also been found in somatodendritic membranes [42]. Their main functions at axonal locations are repolarization during an action potential and spike broadening at the terminal in order to regulate calcium influx, and thereby neurotransmitter release. K_v1 channels form sustained currents, except when they contain a $K_v1.4$ subunit or $\beta1$ subunits that confer fast inactivation. $K_v1.5$ is expressed in the heart, where it makes up the ultra-rapidly activating K^+ current [43], a part of the repolarization phase of the cardiac action potential, while $K_v1.3$ modulates T-lymphocyte activation by promoting calcium influx at hyperpolarized potentials [44].

K_v2 channels produce sustained currents that are localized predominantly in the cell body and dendritic membranes. $K_v2.1$ has a more restricted distribution in the soma and proximal dendrites [45], while $K_v2.2$ is found along the length of dendrites [46]. The α-subunits $K_v5.1$, 6.1-6.3, 8.1, and 9.1-9.3 are all non-functional when expressed alone in heterologous systems. However, many of them can co-assemble with K_v2 channels, acting as dominant negatives in some cases and increasing conductance in others [47, 48].

The four K_v3 channels can make up either transient or sustained currents, and have more depolarized thresholds for voltage activation (>-10 mV) than most other K_v channels. Coupled with their rapid deactivation (within milliseconds), this high threshold makes these channels suited to their role in high-frequency spiking neurons [49]. Accordingly, K_v3 expression has been observed in most types of high-frequency firing neurons, such as neocortical interneurons [50] and auditory principal neurons [51].

The three K_v4 channels all form A-type currents that are expressed predominantly in somatodendritic membrane. This localization implies that K_v4 channels play a role in synaptic integration and backpropagating action potentials, which are of particular importance for informing dendritic membranes of neuronal firing activity. Their coincidence with sub-threshold post-synaptic inputs can lead to synaptic plasticity through long-term potentiation. Immunohistochemistry [52] and electrophysiological studies [53] suggest that K_v4 channels, especially $K_v4.2$, are likely to mediate the A-type currents in dendrites of hippocampal pyramidal neurons. These currents increase in density with distance from the soma, leading to a dampening of backpropagating action potential amplitude in distal dendrites [54]. The inhibition of A-type potassium currents by neurotransmitter receptor-coupled phosphorylation [55] provides a mechanism for increasing backpropagating action potential frequency and NMDA receptor activation. K_v4 channels are also responsible for the transient outward potassium current ($I_{K,to}$) during the repolarization of the cardiac action potential, as $K_v4.2$ knockout mice lack this $I_{K,to}$ [56]. This current likely consists of $K_v4.2/3$ subunits and KChIP2, since a gradient in KChIP2 expression across the ventricular wall reflects the increase in $I_{K,to}$ in the epicardium compared to the endocardium [57].

Despite their ubiquitous expression in both excitable and non-excitable cells, K_v channel mutations have been implicated in a relatively small number of diseases. Mutations in $K_v1.1$ can cause episodic ataxia type-1 (EA-1), an autosomal dominant disorder characterized by stress- or alcohol-induced attacks of imbalance and loss of coordination. EA-1 and its associated loss of function mutations cause an increase in action potential duration, repetitive firing, and elevated neurotransmitter release. These EA-1 mutations either yield non-functional channels or channels with impaired $K_v\beta1$-mediated N-type inactivation [58]. An intriguing pharmacological mystery with episodic ataxia is the ability of the carbonic anhydrase inhibitor acetazolamide to relieve attacks [59]. In addition to this $K_v1.1$ disorder, $K_v4.3$, in accordance with its importance in the cardiac transient outwardly-rectifying K^+ channels, has been found to be down-regulated in paroxysmal atrial fibrillation [60].

The most potent blockers of K_v channels are toxins from a variety of venomous creatures, which can block either a single channel type or a range of voltage-gated channels with high affinity. Since peptide toxins make poor pharmaceutical agents, however, the channel blockers used clinically are smaller, less specific organic compounds. The least specific blockers, Ba^{2+}, Cs^+ and tetraethylammonium (TEA) are simply cationic species that block the conduction pathway, whether they are applied to the inner or outer face of the channel. Another general blocker of K^+ channels is 4-aminopyridine, which blocks voltage-gated channels at micromolar to millimolar concentrations and likely acts at the cytoplasmic opening of the channel [61]. A slightly more potent inhibitor is quinidine, an antiarrhythmic derivative of the antimalarial drug quinine, and a voltage-dependent open channel blocker [62].

Dendrotoxins are potent peptide toxins from the venom of mamba snakes that have nanomolar affinities for K_v channels. Dendrotoxin K is specific for $K_v1.1$, while α-dendrotoxin targets A-type potassium currents and β- and γ-dendrotoxins block primarily non-inactivating potassium currents. The scorpion peptide margatoxin and stichodactyla toxin from sea anemone inhibit $K_v1.3$ at nanomolar concentrations, and can block experimental autoimmune encephalomyelitis [63]. The prospect of $K_v1.3$ blockers as immunosuppressants has made the development of small molecule inhibitors a promising endeavor [64, 65]. Other selective peptide toxins include BDS-I and BDS-II, from sea anemone, which block $K_v3.4$, and the spider toxin heteropodatoxin-2 and phrixotoxin-2 from tarantula, which are selective for K_v4 channels.

Large Conductance Calcium-Activated K^+ channels: Physiological Functions, Disease Relevance, Pharmacology

Large-conductance calcium-activated K^+ (BK) channels are voltage-dependent, have an intrinsic calcium sensing ability and a conductance ranging from 100-250 pS, and play diverse roles in neuronal and non-neuronal tissues. In hippocampal neurons, they mediate both the repolarizing phase of an action potential and the fast afterhyperpolarization, and respond directly to calcium influx through N-type Ca^{2+} channels [66]. And in adrenal chromaffin cells, the hypothalamic-pituitary-adrenocortical stress axis modulates epinephrine release by alternative splicing of mRNA of BK channels, which regulate hormone release [67]. In the cochlea, a gradient of BK splice variants/β-subunit complexes with varying kinetics underlies frequency tuning along the cochlear hair cell membrane [68]. The gradient makes those hair cells with more slowly gating BK channels (more β-subunit) tuned to lower frequencies, while hair cells

sensitive to higher frequencies have faster-gating BK channels (less β-subunit). Deletion of BK causes hearing loss in knockout mice, and seems to be correlated with down-regulated KCNQ4 expression in outer hair cell membrane that leads to degeneration of those cells [69]. BK is the most abundant channel in vascular smooth muscle, and channel composition is important in regulating vascular tone, since impaired β-subunit expression leads to increased vasoconstriction and hypertension [70]. More recently, BK channels have been found to be essential for killing of certain microorganisms by neutrophils, and may function by promoting the release of microbicidal serine proteases into the phagosome [71].

There are several peptide toxins that block BK channels specifically, including iberiotoxin, slotoxin, and BmBKTx1, all of which are from scorpion venom. Charybdotoxin, another scorpion toxin, has also been used as a BK blocker, but it inhibits some voltage-gated K^+ channels, as well as the intermediate conductance calcium-activated K^+ channels (IK). Non-peptide inhibitors include the indole diterpenes paxilline, penitrem A, and verruculogen. There are several activators of the benzimidazolone family, such as NS-1619 and NS-004, that have only moderate specificity for BK. The opener BMS-204352 may limit ischemic damage during stroke [72], while NS-8 may be a useful as a treatment for incontinence [73]. BK activators may also be useful in the treatment of erectile dysfunction [74], since arousal stimulates increased BK current, causing hyperpolarization and relaxation of the cavernosal smooth muscle cell membranes.

Intermediate Conductance Calcium-Activated K^+ channels: Physiological Functions, Disease Relevance, and Pharmacology

Intermediate conductance (IK) and small conductance (SK) calcium-activated K^+ channels are both voltage-insensitive 6TM K^+ channels, and derive their calcium sensitivity from calmodulin, which is constitutively bound to the channel C-terminal domain. IK channels have conductances of 20-80 pS, are found mostly in non-neuronal tissues, and are often important for secretion and volume regulation. In red blood cells, increased IK channel activity can lead to cell shrinkage that promotes the concentration and aggregation of hemoglobin S in sickle cell anemia patients [75]. In T lymphocytes, IK channels are up-regulated upon mitogen stimulation [76], and maintain cytoplamic calcium concentrations necessary for activation [77]. The importance of IK in T-cell activation could make it a potentially useful target for auto-immune diseases such as multiple sclerosis and rheumatoid arthritis [78].

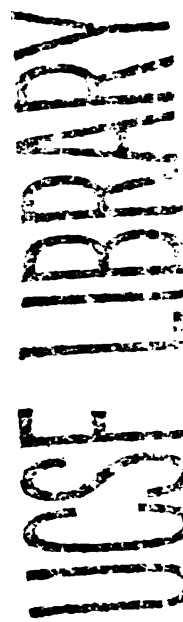

The only peptide toxin that inhibits IK channels potently is charybdotoxin, but, as was mentioned above, it is not specific. The antifungal clotrimazole blocks IK at micromolar concentrations, but has the undesirable property of also being a cytochrome P450 inhibitor. An analogue that does not affect cytochrome activity, TRAM-34, has been reported [79], and may be a more promising pharmaceutical candidate. IK blockers have been proposed as possible treatments for sickle cell anemia [80], diarrhea, and rheumatoid arthritis [81]. As is the case with $K_v1.3$ blockers, IK inhibitors may be useful as immunosuppressants. Activators include 1-ethyl-2-benzimidazolinone (1-EBIO), a more potent analogue NS309, chlorzoxanone, and zoxazolamine, and may be useful in treating cystic fibrosis and vascular disorders [81].

Small Conductance Calcium-Activated K^+ channels: Physiological Functions, Disease Relevance, and Pharmacology

SK channels have conductances of 4-20 pS, and are best known for mediating the neuronal afterhyperpolarization (AHP) of medium duration. This current activates within milliseconds and has a duration on the order of hundreds of milliseconds. Depending on channel localization, the SK AHP can regulate bursting behavior in neuronal firing, set a tonic firing frequency or instantaneous firing rate, modulate rhythmic oscillations in activity, or affect spike frequency adaptation [82]. The three SK genes, SK1-3, have varying sensitivities to the bee venom peptide toxin apamin, a property that has helped in distinguishing these channels eletrophysiologically. Apamin-blocked AHP has been proposed to play a role in learning and memory [83], and hippocampi of Alzheimer's disease patients have been found to have reduced numbers of apamin binding sites [84]. SK activity can also regulate catecholamine release in adrenal chromaffin cells [85]. And genetic studies have suggested SK3 involvement in schizophrenia [86] and anorexia nervosa [87].

Apamin is the most potent blocker of SK channels, and more recently, the scorpion peptide toxins scyllatoxin [88] and BmSKTx [89] have been identified as selective blockers of SK channels. Tubocurarine, a plant-derived, non-peptide inhibitor of the nicotinic acetylcholine receptor, also blocks SK channels at the same site as apamin [90]. Dequalinium and bicuculline are other non-peptide blockers of SK channels, but the former is a mitochondrial poison and the latter blocks GABA-A chloride channels. Synthesis of bisquinolinium cyclophane compounds related to dequalinium has yielded

blockers such as UCL-1684, which is at least 100-fold more potent than dequalinium [91]. SK activators, such as 1-EBIO, NS309, and chlorzoxanone, also stimulate IK channel activity, and are thought to act by increasing the interaction between SK and calmodulin [92].

KCNQ Channels: Physiological Functions, Disease Relevance, and Pharmacology

Channels of the KCNQ family are voltage-gated, activate slowly, and play critical roles in cardiac, neuronal, and auditory function. Mutations in four of the five KCNQ channels (KCNQ1-4) underlie genetic disorders in humans. The first member of the family, KCNQ1, was cloned as a gene associated with long-QT syndrome type 1 [93]. KCNQ1, co-assembled with KCNE1, was subsequently identified as the slow delayed-rectifier current of the cardiac action potential. KCNQ1 was later also found to form a prominent current in colonic crypt cells (with KCNE3) [94] that mediates intestinal chloride homeostasis, and to modulate potassium recycling in the inner ear (with KCNE1) [95].

Long-QT syndrome type 1 is caused by mutations in either KCNQ1 or KCNE1 that lead to non-functional or smaller currents than wild-type. These mutations are located throughout the channel [96]. The reduced channel activity leads to a prolongation of the repolarization phase of the cardiac action potential and lengthening of the QT phase of the electrocardiogram. The result can be *torsade de pointes*, a life-threatening arrhythmia. Autosomal-dominant LQT1, or Romano-Ward syndrome, is the result of dominant negative mutations in KCNQ1 or KCNE1, while the rarer Jervall-Lange-Nielsen syndrome is recessive and causes both LQT1 and congenital bilateral deafness.

Deafness results from a failure of mutant channels to maintain high endolymph K^+ concentration. Auditory stimulation leads to potassium influx into hair cells from the endolymph, followed by K^+ exit from the basal side of hair cells and recycling to the endolymph through the stria vascularis. This last step in recycling occurs through KCNQ1/KCNE1 channels, so reduced channel activity leads to reduced endolymph potassium levels and reduced endolymph potential, which diminishes sensitivity to auditory stimuli. Potassium leaves hair cells through KCNQ4 channels on the basal side of the outer hair cell membrane [97], and a loss of this channel's function can lead to outer hair cell degeneration [98]. KCNQ4 is expressed almost exclusively in the inner ear, and mutations in this channel cause nonsyndromic autosomal dominant deafness-2 (DFNA-2) [99]. Several DFNA-2-associated mutations in KCNQ4 cluster around the pore region [100].

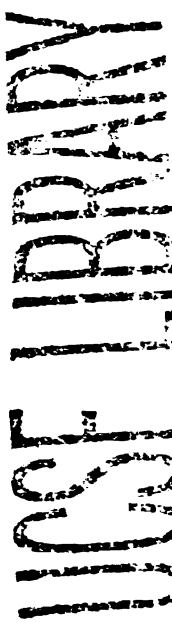

Two other members of the KCNQ family, KCNQ2 and KCNQ3, make up the M-current, a neuronal current that is activated sub-threhold and inhibited by muscarinic acetylcholine receptor activation, and affects neuronal excitability. While KCNQ2 and KCNQ3 expressed alone produce relatively small currents, together they form channels with over ten times the current expected from summing their individual conductances [101]. In addition to M1 muscarinic receptors, other receptors that can mediate M-current inhibition include B2 bradykinin receptors, substance P, and luteinizing hormone-releasing hormone receptors [102]. This coupling is a way for neurotransmitters to excite the post-synaptic membrane, by inhibiting a potassium conductance that resists excitation. While knockout of KCNQ2 is lethal, a mouse with a dominant negative KCNQ2 restricted to neurons has increased hippocampal pyramidal neuron excitability,

reduced spike frequency adaptation, spontaneous seizures, and behavioral hyperexcitability [103].

Mutations in KCNQ2 and KCNQ3 are associated with a seizure disorder in neonates, benign neonatal familial convulsions (BNFC), and predispose affected individuals to epilepsy later in life. BFNC caused by KCNQ2/3 mutations can be the result of relatively modest (25 %) reductions in current [104]. Mutations that cause loss of channel function in BNFC include pore mutations and frameshift truncations of KCNQ2 and KCNQ3 that yield non-functional channels, and do not act as dominant negatives [96]. KCNQ4 and KCNQ5 can also co-assemble with KCNQ3, and may contribute to the diversity of M-currents found in the nervous system [105].

The cardiac I_{Ks} and the neuronal M-current are the two major pharmaceutical targets in the KCNQ family, and there are specific pharmacologies for each. Several anti-arrhythmic drugs can block KCNQ1/KCNE1 complexes selectively, particularly the chromanols HMR1556 and chromanol 293B, and can prolong the cardiac action potential and block ventricular tachycardia by prolonging I_{Ks} [106]. These blockers are both enantioselective, (-)3R,4S being the potent enantiomer in each case [107], and both more potently inhibit KCNQ1/KCNE1 complexes than KCNQ1 tetramers [108, 109]. Benzodiazapenes such as L-768673 and L-7 also block I_{Ks} [110]. Mefenemic acid and the chloride channel blocker DIDS non-specifically activate KCNQ1.

Linopirdine is a relatively specific M-current inhibitor, and was shown to enhance learning and cognition in a mouse model [111], but failed to show a clear affect in a human Alzheimer's disease trial [112]. The M-current is also blocked by XE991, though this drug inhibits KCNQ1 and KCNQ4, as well. An activator of KCNQ2/3, retigabine, is

in clinical trials as an anticonvulsant to treat epilepsy, and may also be useful in treating neuropathic pain [113]. The BK activator BMS-204352 also stimulates M-current.

KCNH K^+ Channels: Physiological Functions, Disease Relevance, Pharmacology

Channels of the KCNH family include EAG (ether-à-go-go), HERG (human ether-à-go-go-related gene), and ELK (ether-à-go-go-like gene). These names derive from the channels' homology to the *Drosophila ether-à-go-go* channel, and are characterized by their slow activation and direct activation by cyclic nucleotides. Another important property of these channels is that they are voltage-dependent and activate at sub-threshold or near-threshold potentials, suggesting that they could play a role in resting membrane potential regulation [114] and spike frequency adaptation [115]. HERG is best known for its role in the fast delayed rectifier current (I_{Kr}) of the cardiac action potential, where it carries a large portion of the outward current during repolarization. The channel has an unusual, bell-shaped current-voltage curve, with increasing currents up to +10 mV, then progressively smaller currents at more depolarized potentials [116]. This behavior is the result of slow voltage activation coupled with unusually fast C-type inactivation at depolarized potentials [117]. Mutations in HERG are associated with long-QT syndrome, type 2, and account for the reduced potassium currents that lead to prolongation of the cardiac QT phase.

In general, the function of KCNH channels in the mammalian nervous system is not well characterized, despite the well-studied role of these channels in *Drosophila* neuromuscular function. ERG mRNA is present throughout the brain [118], and has been suggested to play a role in firing frequency and spike frequency adaptation in cerebellar

Purkinje neurons [119]. The three ELK channels have predominantly neuronal expression, and can co-assemble with one another. Although their functional importance is unknown, their activation at potentials near the resting potential suggests a role in neuronal excitability. EAG channels are expressed predominantly in non-neuronal tissues, and are notably up-regulated in various tumors. Transfection of normal cells with the gene encoding EAG can lead to transformation to tumor cells [120], and EAG expression has been reported to be a marker for cervical cancer [121]. HERG also has oncogenic potential in neoplastic hematopoietic cells [122]. This unexpected role for ion channels in cell proliferation is likely related to cell cycle-dependent changes in channel activity [123].

The rapid delayed rectifier potassium current of the heart, I_{Kr}, is a major drug target for the treatment of arrhythmia, and the class III methanesulfonalide antiarrhythmics block this current carried by HERG/KCNE2. The methanesulfonalides include dofetilide, E-4031, ibutilide, D-solatol, and MK-499. They are open channel blockers that enter the cytoplasmic mouth of channel and bind to residues in the central cavity [124]. Class III antiarrhythmics prolong the ventricular action potential by increasing the QT phase. While these drugs can work by pore block, there are also reports that they can rescue channel mutants with folding defects and increase trafficking to the plasma membrane [125]. Unfortunately, many of these drugs are associated with drug-induced long QT syndrome, an increased risk for torsade de pointes, and sudden cardiac death [126]. Still, the class III antiarrhythmics are useful as a therapy for atrial fibrillation or flutter [127].

Antihistamines (astemizole, terfenadine), antipsychotics (chlorpromazine, haloperidol), some antibiotics, and gastrointestinal prokinetic agents (cisapride) have also been found to cause drug-induced long QT syndrome and ventricular arrhythmia [126]. Peptide toxins that block other voltage-gated K^+ channels are generally not effective against HERG, but recently two scorpion peptides, Ergtoxin and BeKm-1, have been identified, and specifically inhibit HERG, but not ELK or EAG channels [128, 129].

Although relatively little is known about EAG and ELK pharmacology relative to HERG's, EAG is a potential target for anti-tumor therapies, as both the antihistamine astemizole [130] and the tricyclic antidepressant imipramine [131] can inhibit EAG-mediated cell proliferation. The physiological roles of ELK channels are still unknown, and the search for their function would be aided by specific pharmacological tools.

Other Sub-Families of K^+ Channels: Inwardly-Rectifying and Two-P K^+ Channels

The inward rectifier sub-family contains the basic transmembrane unit of a K^+ channels, two TMS flanking the P-loop. The unique electrophysiological feature of these channels is inward rectification: a larger conductance at membrane potentials favoring inward current than at potentials favoring outward current. This property is the result of blockade of the cytoplasmic side of the pore by magnesium or polyamines at depolarized potentials. These channels are open around the resting potential and resist small depolarizations, but are blocked upon stronger depolarizations, such as those following the opening of voltage-gated Na^+ channels.

Inwardly-rectifying K^+ channels help to set the resting membrane potential of excitable cells, and play more specialized roles other cells types. The ATP-inhibited

K_{ATP}, channel, for example, is an octamer of four Kir 6.1 or 6.2 subunits and four sulfonylurea receptor (SUR) subunits. Inhibition of K_{ATP} in pancreatic beta cells promotes insulin release. Another class of inward rectifier is the GIRK channels, which are opened by binding to the G-protein $G_{\beta\gamma}$ subunit, and so are linked to the activity of G-protein coupled receptors.

The two-P, or KCNK, channels [132] have only recently been identified, and make up a sub-family of fourteen members in humans. Their topology consists of two inward rectifier channels linked in tandem, so they contain two P loops per subunit and presumably assemble as dimers. Functionally, the two-P channels are thought to carry background, or leak, potassium conductances, which set the resting potential of many cell types and can modulate the excitability of neurons, heart and muscle cells, and endocrine cells. While no high-affinity, specific agents for two-P channels have been identified, a number of physiological stimuli, such as mechanical stretch, acid, and polyunsaturated fatty acids do affect channel open probability. Some neurotransmitters can inhibit two-P channels, further enhancing membrane excitability through second messenger pathways [133]. Two-P channels may also be a target for general anesthetics, as agents such as halothane and chloroform open some KCNK channels at clinically relevant concentrations [134].

References

1. Noda, M., S. Shimizu, T. Tanabe, T. Takai, T. Kayano, T. Ikeda, H. Takahashi, H. Nakayama, Y. Kanaoka, N. Minamino, et al. (1984). Primary structure of Electrophorus electricus sodium channel deduced from cDNA sequence. *Nature*, 312:121-127.
2. Papazian, D. M., T. L. Schwarz, B. L. Tempel, Y. N. Jan, L. Y. Jan (1987). Cloning of genomic and complementary DNA from Shaker, a putative potassium channel gene from Drosophila. *Science*, 237:749-753.

3. Tempel, B. L., D. M. Papazian, T. L. Schwarz, Y. N. Jan, L. Y. Jan (1987). Sequence of a probable potassium channel component encoded at Shaker locus of Drosophila. *Science*, 237:770-775.
4. Hille, B., *Ion channels of excitable membranes*, 3rd ed. Sinauer. Sunderland, Mass., 2001
5. Paidhungat, M., S. Garrett (1997). A homolog of mammalian, voltage-gated calcium channels mediates yeast pheromone-stimulated Ca2+ uptake and exacerbates the cdc1(Ts) growth defect. *Mol Cell Biol*, 17:6339-6347.
6. Ren, D., B. Navarro, H. Xu, L. Yue, Q. Shi, D. E. Clapham (2001). A prokaryotic voltage-gated sodium channel. *Science*, 294:2372-2375.
7. Catterall, W. A., A. L. Goldin, S. G. Waxman (2003). International Union of Pharmacology. XXXIX. Compendium of voltage-gated ion channels: sodium channels. *Pharmacol Rev*, 55:575-578.
8. Catterall, W. A., J. Striessnig, T. P. Snutch, E. Perez-Reyes (2003). International Union of Pharmacology. XL. Compendium of voltage-gated ion channels: calcium channels. *Pharmacol Rev*, 55:579-581.
9. Gutman, G. A., K. G. Chandy, J. P. Adelman, J. Aiyar, D. A. Bayliss, D. E. Clapham, M. Covarriubias, G. V. Desir, K. Furuichi, B. Ganetzky, M. L. Garcia, S. Grissmer, L. Y. Jan, A. Karschin, D. Kim, S. Kuperschmidt, Y. Kurachi, M. Lazdunski, F. Lesage, H. A. Lester, D. McKinnon, C. G. Nichols, I. O'Kelly, J. Robbins, G. A. Robertson, B. Rudy, M. Sanguinetti, S. Seino, W. Stuehmer, M. M. Tamkun, C. A. Vandenberg, A. Wei, H. Wulff, R. S. Wymore (2003). International Union of Pharmacology. XLI. Compendium of voltage-gated ion channels: potassium channels. *Pharmacol Rev*, 55:583-586.
10. Doyle, D. A., J. Morais Cabral, R. A. Pfuetzner, A. Kuo, J. M. Gulbis, S. L. Cohen, B. T. Chait, R. MacKinnon (1998). The structure of the potassium channel: molecular basis of K+ conduction and selectivity. *Science*, 280:69-77.
11. Jiang, Y., A. Lee, J. Chen, M. Cadene, B. T. Chait, R. MacKinnon (2002). The open pore conformation of potassium channels. *Nature*, 417:523-526.
12. Jiang, Y., A. Lee, J. Chen, V. Ruta, M. Cadene, B. T. Chait, R. MacKinnon (2003). X-ray structure of a voltage-dependent K+ channel. *Nature*, 423:33-41.
13. Cohen, B. E., M. Grabe, L. Y. Jan (2003). Answers and questions from the KvAP structures. *Neuron*, 39:395-400.
14. Heginbotham, L., Z. Lu, T. Abramson, R. MacKinnon (1994). Mutations in the K+ channel signature sequence. *Biophys J*, 66:1061-1067.
15. Noskov, S. Y., S. Berneche, B. Roux (2004). Control of ion selectivity in potassium channels by electrostatic and dynamic properties of carbonyl ligands. *Nature*, 431:830-834.
16. Armstrong, C. M., F. Bezanilla (1973). Currents related to movement of the gating particles of the sodium channels. *Nature*, 242:459-461.
17. Papazian, D. M., L. C. Timpe, Y. N. Jan, L. Y. Jan (1991). Alteration of voltage-dependence of Shaker potassium channel by mutations in the S4 sequence. *Nature*, 349:305-310.
18. Papazian, D. M., X. M. Shao, S. A. Seoh, A. F. Mock, Y. Huang, D. H. Wainstock (1995). Electrostatic interactions of S4 voltage sensor in Shaker K+ channel. *Neuron*, 14:1293-1301.

19. Cha, A., G. E. Snyder, P. R. Selvin, F. Bezanilla (1999). Atomic scale movement of the voltage-sensing region in a potassium channel measured via spectroscopy. *Nature*, 402:809-813.
20. Glauner, K. S., L. M. Mannuzzu, C. S. Gandhi, E. Y. Isacoff (1999). Spectroscopic mapping of voltage sensor movement in the Shaker potassium channel. *Nature*, 402:813-817.
21. Jiang, Y., V. Ruta, J. Chen, A. Lee, R. MacKinnon (2003). The principle of gating charge movement in a voltage-dependent K+ channel. *Nature*, 423:42-48.
22. Liu, Y., M. Holmgren, M. E. Jurman, G. Yellen (1997). Gated access to the pore of a voltage-dependent K+ channel. *Neuron*, 19:175-184.
23. Webster, S. M., D. Del Camino, J. P. Dekker, G. Yellen (2004). Intracellular gate opening in Shaker K+ channels defined by high-affinity metal bridges. *Nature*, 428:864-868.
24. Zhou, M., J. H. Morais-Cabral, S. Mann, R. MacKinnon (2001). Potassium channel receptor site for the inactivation gate and quaternary amine inhibitors. *Nature*, 411:657-661.
25. Kuo, A., J. M. Gulbis, J. F. Antcliff, T. Rahman, E. D. Lowe, J. Zimmer, J. Cuthbertson, F. M. Ashcroft, T. Ezaki, D. A. Doyle (2003). Crystal structure of the potassium channel KirBac1.1 in the closed state. *Science*, 300:1922-1926.
26. Tristani-Firouzi, M., J. Chen, M. C. Sanguinetti (2002). Interactions between S4-S5 linker and S6 transmembrane domain modulate gating of HERG K+ channels. *J Biol Chem*, 277:18994-19000.
27. Demo, S. D., G. Yellen (1991). The inactivation gate of the Shaker K+ channel behaves like an open-channel blocker. *Neuron*, 7:743-753.
28. Gulbis, J. M., M. Zhou, S. Mann, R. MacKinnon (2000). Structure of the cytoplasmic beta subunit-T1 assembly of voltage-dependent K+ channels. *Science*, 289:123-127.
29. Murrell-Lagnado, R. D., R. W. Aldrich (1993). Interactions of amino terminal domains of Shaker K channels with a pore blocking site studied with synthetic peptides. *J Gen Physiol*, 102:949-975.
30. Nagaya, N., D. M. Papazian (1997). Potassium channel alpha and beta subunits assemble in the endoplasmic reticulum. *J Biol Chem*, 272:3022-3027.
31. Rettig, J., S. H. Heinemann, F. Wunder, C. Lorra, D. N. Parcej, J. O. Dolly, O. Pongs (1994). Inactivation properties of voltage-gated K+ channels altered by presence of beta-subunit. *Nature*, 369:289-294.
32. Campomanes, C. R., K. I. Carroll, L. N. Manganas, M. E. Hershberger, B. Gong, D. E. Antonucci, K. J. Rhodes, J. S. Trimmer (2002). Kv beta subunit oxidoreductase activity and Kv1 potassium channel trafficking. *J Biol Chem*, 277:8298-8305.
33. An, W. F., M. R. Bowlby, M. Betty, J. Cao, H. P. Ling, G. Mendoza, J. W. Hinson, K. I. Mattsson, B. W. Strassle, J. S. Trimmer, K. J. Rhodes (2000). Modulation of A-type potassium channels by a family of calcium sensors. *Nature*, 403:553-556.
34. Shibata, R., H. Misonou, C. R. Campomanes, A. E. Anderson, L. A. Schrader, L. C. Doliveira, K. I. Carroll, J. D. Sweatt, K. J. Rhodes, J. S. Trimmer (2003). A fundamental role for KChIPs in determining the molecular properties and trafficking of Kv4.2 potassium channels. *J Biol Chem*, 278:36445-36454.

35. Sesti, F., S. A. Goldstein (1998). Single-channel characteristics of wild-type IKs channels and channels formed with two minK mutants that cause long QT syndrome. *J Gen Physiol*, 112:651-663.
36. Deschenes, I., G. F. Tomaselli (2002). Modulation of Kv4.3 current by accessory subunits. *FEBS Lett*, 528:183-188.
37. McCrossan, Z. A., A. Lewis, G. Panaghie, P. N. Jordan, D. J. Christini, D. J. Lerner, G. W. Abbott (2003). MinK-related peptide 2 modulates Kv2.1 and Kv3.1 potassium channels in mammalian brain. *J Neurosci*, 23:8077-8091.
38. Birnbaum, S. G., A. W. Varga, L. L. Yuan, A. E. Anderson, J. D. Sweatt, L. A. Schrader (2004). Structure and function of Kv4-family transient potassium channels. *Physiol Rev*, 84:803-833.
39. Vasilyev, D. V., M. E. Barish (2003). Regulation of an inactivating potassium current (IA) by the extracellular matrix protein vitronectin in embryonic mouse hippocampal neurones. *J Physiol*, 547:859-871.
40. Sheng, M., M. Wyszynski (1997). Ion channel targeting in neurons. *Bioessays*, 19:847-853.
41. Wang, H., D. D. Kunkel, T. M. Martin, P. A. Schwartzkroin, B. L. Tempel (1993). Heteromultimeric K+ channels in terminal and juxtaparanodal regions of neurons. *Nature*, 365:75-79.
42. Wang, H., D. D. Kunkel, P. A. Schwartzkroin, B. L. Tempel (1994). Localization of Kv1.1 and Kv1.2, two K channel proteins, to synaptic terminals, somata, and dendrites in the mouse brain. *J Neurosci*, 14:4588-4599.
43. Feng, J., B. Wible, G. R. Li, Z. Wang, S. Nattel (1997). Antisense oligodeoxynucleotides directed against Kv1.5 mRNA specifically inhibit ultrarapid delayed rectifier K+ current in cultured adult human atrial myocytes. *Circ Res*, 80:572-579.
44. Lin, C. S., R. C. Boltz, J. T. Blake, M. Nguyen, A. Talento, P. A. Fischer, M. S. Springer, N. H. Sigal, R. S. Slaughter, M. L. Garcia, et al. (1993). Voltage-gated potassium channels regulate calcium-dependent pathways involved in human T lymphocyte activation. *J Exp Med*, 177:637-645.
45. Du, J., J. H. Tao-Cheng, P. Zerfas, C. J. McBain (1998). The K+ channel, Kv2.1, is apposed to astrocytic processes and is associated with inhibitory postsynaptic membranes in hippocampal and cortical principal neurons and inhibitory interneurons. *Neuroscience*, 84:37-48.
46. Hwang, P. M., M. Fotuhi, D. S. Bredt, A. M. Cunningham, S. H. Snyder (1993). Contrasting immunohistochemical localizations in rat brain of two novel K+ channels of the Shab subfamily. *J Neurosci*, 13:1569-1576.
47. Kramer, J. W., M. A. Post, A. M. Brown, G. E. Kirsch (1998). Modulation of potassium channel gating by coexpression of Kv2.1 with regulatory Kv5.1 or Kv6.1 alpha-subunits. *Am J Physiol*, 274:C1501-1510.
48. Salinas, M., J. de Weille, E. Guillemare, M. Lazdunski, J. P. Hugnot (1997). Modes of regulation of shab K+ channel activity by the Kv8.1 subunit. *J Biol Chem*, 272:8774-8780.
49. Rudy, B., C. J. McBain (2001). Kv3 channels: voltage-gated K+ channels designed for high-frequency repetitive firing. *Trends Neurosci*, 24:517-526.

50. Erisir, A., D. Lau, B. Rudy, C. S. Leonard (1999). Function of specific K(+) channels in sustained high-frequency firing of fast-spiking neocortical interneurons. *J Neurophysiol*, 82:2476-2489.
51. Li, W., L. K. Kaczmarek, T. M. Perney (2001). Localization of two high-threshold potassium channel subunits in the rat central auditory system. *J Comp Neurol*, 437:196-218.
52. Sheng, M., M. L. Tsaur, Y. N. Jan, L. Y. Jan (1992). Subcellular segregation of two A-type K+ channel proteins in rat central neurons. *Neuron*, 9:271-284.
53. Song, W. J., T. Tkatch, G. Baranauskas, N. Ichinohe, S. T. Kitai, D. J. Surmeier (1998). Somatodendritic depolarization-activated potassium currents in rat neostriatal cholinergic interneurons are predominantly of the A type and attributable to coexpression of Kv4.2 and Kv4.1 subunits. *J Neurosci*, 18:3124-3137.
54. Hoffman, D. A., J. C. Magee, C. M. Colbert, D. Johnston (1997). K+ channel regulation of signal propagation in dendrites of hippocampal pyramidal neurons. *Nature*, 387:869-875.
55. Yuan, L. L., J. P. Adams, M. Swank, J. D. Sweatt, D. Johnston (2002). Protein kinase modulation of dendritic K+ channels in hippocampus involves a mitogen-activated protein kinase pathway. *J Neurosci*, 22:4860-4868.
56. Barry, D. M., H. Xu, R. B. Schuessler, J. M. Nerbonne (1998). Functional knockout of the transient outward current, long-QT syndrome, and cardiac remodeling in mice expressing a dominant-negative Kv4 alpha subunit. *Circ Res*, 83:560-567.
57. Rosati, B., Z. Pan, S. Lypen, H. S. Wang, I. Cohen, J. E. Dixon, D. McKinnon (2001). Regulation of KChIP2 potassium channel beta subunit gene expression underlies the gradient of transient outward current in canine and human ventricle. *J Physiol*, 533:119-125.
58. Maylie, B., E. Bissonnette, M. Virk, J. P. Adelman, J. G. Maylie (2002). Episodic ataxia type 1 mutations in the human Kv1.1 potassium channel alter hKvbeta 1-induced N-type inactivation. *J Neurosci*, 22:4786-4793.
59. Zasorin, N. L., R. W. Baloh, L. B. Myers (1983). Acetazolamide-responsive episodic ataxia syndrome. *Neurology*, 33:1212-1214.
60. Brundel, B. J., I. C. Van Gelder, R. H. Henning, A. E. Tuinenburg, M. Wietses, J. G. Grandjean, A. A. Wilde, W. H. Van Gilst, H. J. Crijns (2001). Alterations in potassium channel gene expression in atria of patients with persistent and paroxysmal atrial fibrillation: differential regulation of protein and mRNA levels for K+ channels. *J Am Coll Cardiol*, 37:926-932.
61. Kirsch, G. E., C. C. Shieh, J. A. Drewe, D. F. Vener, A. M. Brown (1993). Segmental exchanges define 4-aminopyridine binding and the inner mouth of K+ pores. *Neuron*, 11:503-512.
62. Fedida, D. (1997). Gating charge and ionic currents associated with quinidine block of human Kv1.5 delayed rectifier channels. *J Physiol*, 499 (Pt 3):661-675.
63. Beeton, C., H. Wulff, J. Barbaria, O. Clot-Faybesse, M. Pennington, D. Bernard, M. D. Cahalan, K. G. Chandy, E. Beraud (2001). Selective blockade of T lymphocyte K(+) channels ameliorates experimental autoimmune encephalomyelitis, a model for multiple sclerosis. *Proc Natl Acad Sci U S A*, 98:13942-13947.
64. Koo, G. C., J. T. Blake, K. Shah, M. J. Staruch, F. Dumont, D. Wunderler, M. Sanchez, O. B. McManus, A. Sirotina-Meisher, P. Fischer, R. C. Boltz, M. A. Goetz, R.

Baker, J. Bao, F. Kayser, K. M. Rupprecht, W. H. Parsons, X. C. Tong, I. E. Ita, J. Pivnichny, S. Vincent, P. Cunningham, D. Hora, Jr., W. Feeney, G. Kaczorowski, et al. (1999). Correolide and derivatives are novel immunosuppressants blocking the lymphocyte Kv1.3 potassium channels. *Cell Immunol*, 197:99-107.
65. Vennekamp, J., H. Wulff, C. Beeton, P. A. Calabresi, S. Grissmer, W. Hansel, K. G. Chandy (2004). Kv1.3-blocking 5-phenylalkoxypsoralens: a new class of immunomodulators. *Mol Pharmacol*, 65:1364-1374.
66. Marrion, N. V., S. J. Tavalin (1998). Selective activation of Ca2+-activated K+ channels by co-localized Ca2+ channels in hippocampal neurons. *Nature*, 395:900-905.
67. Lovell, P. V., D. P. McCobb (2001). Pituitary control of BK potassium channel function and intrinsic firing properties of adrenal chromaffin cells. *J Neurosci*, 21:3429-3442.
68. Ramanathan, K., T. H. Michael, G. J. Jiang, H. Hiel, P. A. Fuchs (1999). A molecular mechanism for electrical tuning of cochlear hair cells. *Science*, 283:215-217.
69. Ruttiger, L., M. Sausbier, U. Zimmermann, H. Winter, C. Braig, J. Engel, M. Knirsch, C. Arntz, P. Langer, B. Hirt, M. Muller, I. Kopschall, M. Pfister, S. Munkner, K. Rohbock, I. Pfaff, A. Rusch, P. Ruth, M. Knipper (2004). Deletion of the Ca2+-activated potassium (BK) alpha-subunit but not the BKbeta1-subunit leads to progressive hearing loss. *Proc Natl Acad Sci U S A*, 101:12922-12927.
70. Amberg, G. C., A. D. Bonev, C. F. Rossow, M. T. Nelson, L. F. Santana (2003). Modulation of the molecular composition of large conductance, Ca(2+) activated K(+) channels in vascular smooth muscle during hypertension. *J Clin Invest*, 112:717-724.
71. Ahluwalia, J., A. Tinker, L. H. Clapp, M. R. Duchen, A. Y. Abramov, S. Pope, M. Nobles, A. W. Segal (2004). The large-conductance Ca2+-activated K+ channel is essential for innate immunity. *Nature*, 427:853-858.
72. Jensen, B. S. (2002). BMS-204352: a potassium channel opener developed for the treatment of stroke. *CNS Drug Rev*, 8:353-360.
73. Tanaka, M., K. Takahashi, T. Saika, I. Kobayashi, T. Ueno, J. Kumazawa (1998). Development of fluoroquinolone resistance and mutations involving GyrA and ParC proteins among Neisseria gonorrhoeae isolates in Japan. *J Urol*, 159:2215-2219.
74. Archer, S. L. (2002). Potassium channels and erectile dysfunction. *Vascul Pharmacol*, 38:61-71.
75. Brugnara, C., L. de Franceschi, S. L. Alper (1993). Inhibition of Ca(2+)-dependent K+ transport and cell dehydration in sickle erythrocytes by clotrimazole and other imidazole derivatives. *J Clin Invest*, 92:520-526.
76. Ghanshani, S., H. Wulff, M. J. Miller, H. Rohm, A. Neben, G. A. Gutman, M. D. Cahalan, K. G. Chandy (2000). Up-regulation of the IKCa1 potassium channel during T-cell activation. Molecular mechanism and functional consequences. *J Biol Chem*, 275:37137-37149.
77. Fanger, C. M., H. Rauer, A. L. Neben, M. J. Miller, H. Wulff, J. C. Rosa, C. R. Ganellin, K. G. Chandy, M. D. Cahalan (2001). Calcium-activated potassium channels sustain calcium signaling in T lymphocytes. Selective blockers and manipulated channel expression levels. *J Biol Chem*, 276:12249-12256.
78. Jensen, B. S., M. Hertz, P. Christophersen, L. S. Madsen (2002). The Ca2+-activated K+ channel of intermediate conductance:a possible target for immune suppression. *Expert Opin Ther Targets*, 6:623-636.

79. Wulff, H., M. J. Miller, W. Hansel, S. Grissmer, M. D. Cahalan, K. G. Chandy (2000). Design of a potent and selective inhibitor of the intermediate-conductance Ca2+-activated K+ channel, IKCa1: a potential immunosuppressant. *Proc Natl Acad Sci U S A*, 97:8151-8156.
80. Brugnara, C., L. De Franceschi, C. C. Armsby, N. Saadane, M. Trudel, Y. Beuzard, A. Rittenhouse, N. Rifai, O. Platt, S. L. Alper (1995). A new therapeutic approach for sickle cell disease. Blockade of the red cell Ca(2+)-activated K+ channel by clotrimazole. *Ann N Y Acad Sci*, 763:262-271.
81. Shieh, C. C., M. Coghlan, J. P. Sullivan, M. Gopalakrishnan (2000). Potassium channels: molecular defects, diseases, and therapeutic opportunities. *Pharmacol Rev*, 52:557-594.
82. Stocker, M. (2004). Ca(2+)-activated K+ channels: molecular determinants and function of the SK family. *Nat Rev Neurosci*, 5:758-770.
83. Messier, C., C. Mourre, B. Bontempi, J. Sif, M. Lazdunski, C. Destrade (1991). Effect of apamin, a toxin that inhibits Ca(2+)-dependent K+ channels, on learning and memory processes. *Brain Res*, 551:322-326.
84. Ikeda, M., D. Dewar, J. McCulloch (1991). Selective reduction of [125I]apamin binding sites in Alzheimer hippocampus: a quantitative autoradiographic study. *Brain Res*, 567:51-56.
85. Nagayama, T., Y. Fukushima, M. Yoshida, M. Suzuki-Kusaba, H. Hisa, T. Kimura, S. Satoh (2000). Role of potassium channels in catecholamine secretion in the rat adrenal gland. *Am J Physiol Regul Integr Comp Physiol*, 279:R448-454.
86. Tomita, H., V. G. Shakkottai, G. A. Gutman, G. Sun, W. E. Bunney, M. D. Cahalan, K. G. Chandy, J. J. Gargus (2003). Novel truncated isoform of SK3 potassium channel is a potent dominant-negative regulator of SK currents: implications in schizophrenia. *Mol Psychiatry*, 8:524-535, 460.
87. Koronyo-Hamaoui, M., Y. Danziger, A. Frisch, D. Stein, S. Leor, N. Laufer, C. Carel, S. Fennig, M. Minoumi, A. Apter, B. Goldman, G. Barkai, A. Weizman, E. Gak (2002). Association between anorexia nervosa and the hsKCa3 gene: a family-based and case control study. *Mol Psychiatry*, 7:82-85.
88. Auguste, P., M. Hugues, B. Grave, J. C. Gesquiere, P. Maes, A. Tartar, G. Romey, H. Schweitz, M. Lazdunski (1990). Leiurotoxin I (scyllatoxin), a peptide ligand for Ca2(+)-activated K+ channels. Chemical synthesis, radiolabeling, and receptor characterization. *J Biol Chem*, 265:4753-4759.
89. Xu, C. Q., L. L. He, B. Brone, M. F. Martin-Eauclaire, E. Van Kerkhove, Z. Zhou, C. W. Chi (2004). A novel scorpion toxin blocking small conductance Ca2+ activated K+ channel. *Toxicon*, 43:961-971.
90. Ishii, T. M., J. Maylie, J. P. Adelman (1997). Determinants of apamin and d-tubocurarine block in SK potassium channels. *J Biol Chem*, 272:23195-23200.
91. Rosa, J. C., D. Galanakis, C. R. Ganellin, P. M. Dunn, D. H. Jenkinson (1998). Bis-quinolinium cyclophanes: 6,10-diaza-3(1,3),8(1,4)-dibenzena-1,5(1,4)-diquinolinacyclodecaphane (UCL 1684), the first nanomolar, non-peptidic blocker of the apamin-sensitive Ca(2+)-activated K+ channel. *J Med Chem*, 41:2-5.
92. Pedarzani, P., J. Mosbacher, A. Rivard, L. A. Cingolani, D. Oliver, M. Stocker, J. P. Adelman, B. Fakler (2001). Control of electrical activity in central neurons by

modulating the gating of small conductance Ca2+-activated K+ channels. *J Biol Chem*, 276:9762-9769.
93. Wang, Q., M. E. Curran, I. Splawski, T. C. Burn, J. M. Millholland, T. J. VanRaay, J. Shen, K. W. Timothy, G. M. Vincent, T. de Jager, P. J. Schwartz, J. A. Toubin, A. J. Moss, D. L. Atkinson, G. M. Landes, T. D. Connors, M. T. Keating (1996). Positional cloning of a novel potassium channel gene: KVLQT1 mutations cause cardiac arrhythmias. *Nat Genet*, 12:17-23.
94. Schroeder, B. C., S. Waldegger, S. Fehr, M. Bleich, R. Warth, R. Greger, T. J. Jentsch (2000). A constitutively open potassium channel formed by KCNQ1 and KCNE3. *Nature*, 403:196-199.
95. Nicolas, M., D. Dememes, A. Martin, S. Kupershmidt, J. Barhanin (2001). KCNQ1/KCNE1 potassium channels in mammalian vestibular dark cells. *Hear Res*, 153:132-145.
96. Ashcroft, F. M., *Ion channels and disease : channelopathies*. Academic Press. San Diego, 2000
97. Kharkovets, T., J. P. Hardelin, S. Safieddine, M. Schweizer, A. El-Amraoui, C. Petit, T. J. Jentsch (2000). KCNQ4, a K+ channel mutated in a form of dominant deafness, is expressed in the inner ear and the central auditory pathway. *Proc Natl Acad Sci U S A*, 97:4333-4338.
98. Nouvian, R., J. Ruel, J. Wang, M. J. Guitton, R. Pujol, J. L. Puel (2003). Degeneration of sensory outer hair cells following pharmacological blockade of cochlear KCNQ channels in the adult guinea pig. *Eur J Neurosci*, 17:2553-2562.
99. Kubisch, C., B. C. Schroeder, T. Friedrich, B. Lutjohann, A. El-Amraoui, S. Marlin, C. Petit, T. J. Jentsch (1999). KCNQ4, a novel potassium channel expressed in sensory outer hair cells, is mutated in dominant deafness. *Cell*, 96:437-446.
100. Van Hauwe, P., P. J. Coucke, R. J. Ensink, P. Huygen, C. W. Cremers, G. Van Camp (2000). Mutations in the KCNQ4 K+ channel gene, responsible for autosomal dominant hearing loss, cluster in the channel pore region. *Am J Med Genet*, 93:184-187.
101. Wang, H. S., Z. Pan, W. Shi, B. S. Brown, R. S. Wymore, I. S. Cohen, J. E. Dixon, D. McKinnon (1998). KCNQ2 and KCNQ3 potassium channel subunits: molecular correlates of the M-channel. *Science*, 282:1890-1893.
102. Cooper, E. C., L. Y. Jan (2003). M-channels: neurological diseases, neuromodulation, and drug development. *Arch Neurol*, 60:496-500.
103. Peters, H. C., H. Hu, O. Pongs, J. F. Storm, D. Isbrandt (2005). Conditional transgenic suppression of M channels in mouse brain reveals functions in neuronal excitability, resonance and behavior. *Nat Neurosci*, 8:51-60.
104. Schroeder, B. C., C. Kubisch, V. Stein, T. J. Jentsch (1998). Moderate loss of function of cyclic-AMP-modulated KCNQ2/KCNQ3 K+ channels causes epilepsy. *Nature*, 396:687-690.
105. Robbins, J. (2001). KCNQ potassium channels: physiology, pathophysiology, and pharmacology. *Pharmacol Ther*, 90:1-19.
106. Tamargo, J., R. Caballero, R. Gomez, C. Valenzuela, E. Delpon (2004). Pharmacology of cardiac potassium channels. *Cardiovasc Res*, 62:9-33.
107. Yang, I. C., M. W. Scherz, A. Bahinski, P. B. Bennett, K. T. Murray (2000). Stereoselective interactions of the enantiomers of chromanol 293B with human voltage-gated potassium channels. *J Pharmacol Exp Ther*, 294:955-962.

108. Busch, A. E., G. L. Busch, E. Ford, H. Suessbrich, H. J. Lang, R. Greger, K. Kunzelmann, B. Attali, W. Stuhmer (1997). The role of the IsK protein in the specific pharmacological properties of the IKs channel complex. *Br J Pharmacol*, 122:187-189.
109. Wang, H. S., B. S. Brown, D. McKinnon, I. S. Cohen (2000). Molecular basis for differential sensitivity of KCNQ and I(Ks) channels to the cognitive enhancer XE991. *Mol Pharmacol*, 57:1218-1223.
110. Seebohm, G., J. Chen, N. Strutz, C. Culberson, C. Lerche, M. C. Sanguinetti (2003). Molecular determinants of KCNQ1 channel block by a benzodiazepine. *Mol Pharmacol*, 64:70-77.
111. Schnee, M. E., B. S. Brown (1998). Selectivity of linopirdine (DuP 996), a neurotransmitter release enhancer, in blocking voltage-dependent and calcium-activated potassium currents in hippocampal neurons. *J Pharmacol Exp Ther*, 286:709-717.
112. van Dyck, C. H., C. H. Lin, R. Robinson, J. Cellar, E. O. Smith, J. C. Nelson, A. F. Arnsten, P. B. Hoffer (1997). The acetylcholine releaser linopirdine increases parietal regional cerebral blood flow in Alzheimer's disease. *Psychopharmacology (Berl)*, 132:217-226.
113. Dost, R., A. Rostock, C. Rundfeldt (2004). The anti-hyperalgesic activity of retigabine is mediated by KCNQ potassium channel activation. *Naunyn Schmiedebergs Arch Pharmacol*, 369:382-390.
114. Overholt, J. L., E. Ficker, T. Yang, H. Shams, G. R. Bright, N. R. Prabhakar (2000). HERG-Like potassium current regulates the resting membrane potential in glomus cells of the rabbit carotid body. *J Neurophysiol*, 83:1150-1157.
115. Chiesa, N., B. Rosati, A. Arcangeli, M. Olivotto, E. Wanke (1997). A novel role for HERG K+ channels: spike-frequency adaptation. *J Physiol*, 501 (Pt 2):313-318.
116. Sanguinetti, M. C., C. Jiang, M. E. Curran, M. T. Keating (1995). A mechanistic link between an inherited and an acquired cardiac arrhythmia: HERG encodes the IKr potassium channel. *Cell*, 81:299-307.
117. Smith, P. L., T. Baukrowitz, G. Yellen (1996). The inward rectification mechanism of the HERG cardiac potassium channel. *Nature*, 379:833-836.
118. Papa, M., F. Boscia, A. Canitano, P. Castaldo, S. Sellitti, L. Annunziato, M. Taglialatela (2003). Expression pattern of the ether-a-gogo-related (ERG) K+ channel-encoding genes ERG1, ERG2, and ERG3 in the adult rat central nervous system. *J Comp Neurol*, 466:119-135.
119. Sacco, T., A. Bruno, E. Wanke, F. Tempia (2003). Functional roles of an ERG current isolated in cerebellar Purkinje neurons. *J Neurophysiol*, 90:1817-1828.
120. Pardo, L. A., D. del Camino, A. Sanchez, F. Alves, A. Bruggemann, S. Beckh, W. Stuhmer (1999). Oncogenic potential of EAG K(+) channels. *Embo J*, 18:5540-5547.
121. Farias, L. M., D. B. Ocana, L. Diaz, F. Larrea, E. Avila-Chavez, A. Cadena, L. M. Hinojosa, G. Lara, L. A. Villanueva, C. Vargas, E. Hernandez-Gallegos, I. Camacho-Arroyo, A. Duenas-Gonzalez, E. Perez-Cardenas, L. A. Pardo, A. Morales, L. Taja-Chayeb, J. Escamilla, C. Sanchez-Pena, J. Camacho (2004). Ether a go-go potassium channels as human cervical cancer markers. *Cancer Res*, 64:6996-7001.
122. Smith, G. A., H. W. Tsui, E. W. Newell, X. Jiang, X. P. Zhu, F. W. Tsui, L. C. Schlichter (2002). Functional up-regulation of HERG K+ channels in neoplastic hematopoietic cells. *J Biol Chem*, 277:18528-18534.

123. Pardo, L. A., A. Bruggemann, J. Camacho, W. Stuhmer (1998). Cell cycle-related changes in the conducting properties of r-eag K+ channels. *J Cell Biol*, 143:767-775.
124. Tristani-Firouzi, M., M. C. Sanguinetti (2003). Structural determinants and biophysical properties of HERG and KCNQ1 channel gating. *J Mol Cell Cardiol*, 35:27-35.
125. Rajamani, S., C. L. Anderson, B. D. Anson, C. T. January (2002). Pharmacological rescue of human K(+) channel long-QT2 mutations: human ether-a-go-go-related gene rescue without block. *Circulation*, 105:2830-2835.
126. Vandenberg, J. I., B. D. Walker, T. J. Campbell (2001). HERG K+ channels: friend and foe. *Trends Pharmacol Sci*, 22:240-246.
127. VerNooy, R. A., J. P. Mounsey (2004). Antiarrhythmic drug therapy of atrial fibrillation. *Cardiol Clin*, 22:21-34.
128. Gurrola, G. B., B. Rosati, M. Rocchetti, G. Pimienta, A. Zaza, A. Arcangeli, M. Olivotto, L. D. Possani, E. Wanke (1999). A toxin to nervous, cardiac, and endocrine ERG K+ channels isolated from Centruroides noxius scorpion venom. *Faseb J*, 13:953-962.
129. Korolkova, Y. V., S. A. Kozlov, A. V. Lipkin, K. A. Pluzhnikov, J. K. Hadley, A. K. Filippov, D. A. Brown, K. Angelo, D. Strobaek, T. Jespersen, S. P. Olesen, B. S. Jensen, E. V. Grishin (2001). An ERG channel inhibitor from the scorpion Buthus eupeus. *J Biol Chem*, 276:9868-9876.
130. Ouadid-Ahidouch, H., X. Le Bourhis, M. Roudbaraki, R. A. Toillon, P. Delcourt, N. Prevarskaya (2001). Changes in the K+ current-density of MCF-7 cells during progression through the cell cycle: possible involvement of a h-ether.a-gogo K+ channel. *Receptors Channels*, 7:345-356.
131. Gavrilova-Ruch, O., K. Schonherr, G. Gessner, R. Schonherr, T. Klapperstuck, W. Wohlrab, S. H. Heinemann (2002). Effects of imipramine on ion channels and proliferation of IGR1 melanoma cells. *J Membr Biol*, 188:137-149.
132. Goldstein, S. A., D. Bockenhauer, I. O'Kelly, N. Zilberberg (2001). Potassium leak channels and the KCNK family of two-P-domain subunits. *Nat Rev Neurosci*, 2:175-184.
133. Talley, E. M., Q. Lei, J. E. Sirois, D. A. Bayliss (2000). TASK-1, a two-pore domain K+ channel, is modulated by multiple neurotransmitters in motoneurons. *Neuron*, 25:399-410.
134. Patel, A. J., E. Honore, F. Lesage, M. Fink, G. Romey, M. Lazdunski (1999). Inhalational anesthetics activate two-pore-domain background K+ channels. *Nat Neurosci*, 2:422-426.

Chapter 2

SK Channels Mediate NADPH Oxidase-Independent ROS Production and Apoptosis in Granulocytes

Alex J. Fay[1], Xiang Qian[2], Yuh-Nung Jan[2,3], and Lily Y. Jan[2,3]

[1] Graduate Group in Biophysics, University of California, San Francisco, CA 94143, USA

[2] Department of Physiology, University of California, San Francisco, CA 94143, USA

[3] Howard Hughes Medical Institute and Department of Biochemistry, University of California, San Francisco, CA 94143, USA

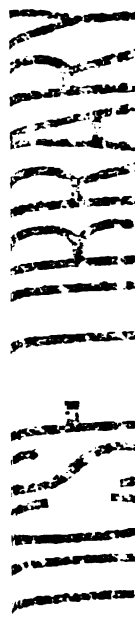

Abstract

Neutrophils are inflammatory cells that bind to, engulf, and destroy bacterial and fungal pathogens in infected tissue. Killing involves both oxidative and non-oxidative processes, both of which have been linked to ion channel activity. The oxidative pathway involves the electrogenic production of superoxide by the membrane-bound NADPH oxidase complex, which requires a compensatory ion flow to prevent electrostatic inhibition. A variety of stimuli, from bacterial chemotactic peptides and cell wall components to complement- or IgG-opsonized microbes, can stimulate the production of reactive oxygen species (ROS) by neutrophils, presumably via NADPH oxidase. We report here that 1-EBIO, an activator of calcium-activated potassium channels of small conductance (SK) and intermediate conductance (IK), causes production of superoxide and hydrogen peroxide by neutrophils and granulocyte-differentiated PLB-985 cells. This response, furthermore, can be partially inhibited by the SK blocker apamin. Apamin also inhibits an outward current evoked by the bacterial chemotactic peptide fMLF, and analysis of RNA transcripts indicates that channels encoded by the SK3 gene carry this

current. The effects of 1-EBIO and apamin are independent of the NADPH oxidase pathway, as demonstrated using a PLB-985 cell line lacking the gp91phox subunit. Rather, 1-EBIO and apamin appear to modulate intracellular ROS production. Consistent with the enhanced ROS production and K+ efflux mediated by 1-EBIO, we found that this SK opener increased apoptosis of PLB-985 cells. Together, these findings indicate a novel mechanism for the regulation of neutrophil reactive oxygen species production and programmed cell death.

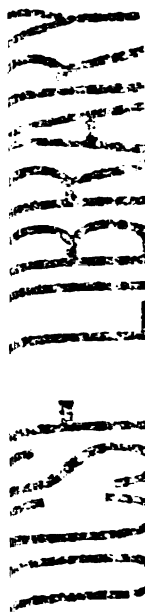

Introduction

Neutrophils, as key players in the innate immune response, must be able to identify, phagocytose, and neutralize a broad array of pathogenic microbes [1]. Killing usually involves isolation of bacteria or fungi within the phagosome, though neutrophils can release their toxic contents into their surroundings to kill extracellular microbes [1]. These toxic contents include reactive oxygen species (ROS), such as hydrogen peroxide and hypochlorous acid, as well as proteases and antimicrobial peptides. Since these toxins can also damage host cells, limiting their release and clearing apoptotic neutrophils are ultimately necessary for resolving an infection [2]. Understanding how neutrophils regulate the production of oxidants is, therefore, important for both resisting pathogens and controlling inflammation.

While ion channels are best known for their roles in neuronal and cardiac action potentials, their importance in some immune cells, particularly neutrophils, has begun to emerge over the past few years [1, 3-5]. The NADPH oxidase of neutrophils produces large amounts of superoxide at the plasma and phagosomal membranes, resulting in an

electrogenic efflux of electrons from the cytoplasm [6]. An extensive literature indicates that a proton channel, whose molecular identity has recently been identified [7, 8], carries a compensating cationic current that prevents depolarization of the cell membrane to potentials that inhibit the NADPH oxidase [9]. Stimulation of neutrophil oxidative activity also activates a large conductance, calcium-activated potassium channel (BK), which maintains a slightly alkaline pH in the phagosome and may also mediate release of cationic proteases from azurophilic granules [10]. Still, relatively few ion channels have been identified in neutrophils, and the roles of observed ionic currents in neutrophil functions remain unclear.

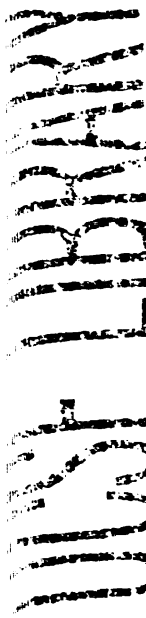

We present evidence here for a small conductance, calcium activated potassium channel in neutrophils and neutrophil-like PLB-985 cells that modulates reactive oxygen species production. Activation of SK/IK channels with 1-EBIO potentiates superoxide production stimulated by the bacterial chemotactic peptide fMLF, or by IgG-opsonized *S. aureus*. The specific SK blocker apamin, but not the IK blocker clotrimazole, reduces both of these effects of 1-EBIO, and also diminishes peroxide production following fMLF or IgG-opsonized *S. aureus* activation of the respiratory burst. Using whole cell patch clamp electrophysiology, we found that the bacterial fMLF stimulates an apamin-sensitive current in PLB-985 cells, suggesting the presence of a small conductance, calcium-activated K^+ channel (SK). We also found SK3 mRNA to be present in both neutrophils and PLB-985 cells by RT-PCR. The enhancement of ROS production by 1-EBIO is independent of the NADPH oxidase inhibitor dipheylene iodonium (DPI), and is present even in a cell line lacking the gp91*phox* subunit of NADPH oxidase. Instead, these reactive oxygen species are likely of mitochondrial origin. Consistent with

increased the ROS production in the presence of 1-EBIO, the SK/IK opener also increased the rate of apoptosis in both undifferentiated and differentiated PLB-985 cells. Together, these results point towards a pathway for intracellular ROS regulation parallel to but independent of NADPH oxidase activity in neutrophils and PLB-985 cells, a novel pathway regulated by small conductance calcium-activated potassium channels. This pathway may be important for neutrophil apoptosis, which is critical to resolving inflammation [2].

Materials and Methods

Culture of PLB-985 Cells

PLB-985 cells (UCSF Cell Culture Facility) and PLB-X-CGD cells [11] were grown in RPMI-1640 with 20 mM HEPES (UCSF CCF), supplemented with 10 % heat-inactivated fetal bovine serum (UCSF CCF) and penicillin-streptomycin (UCSF CCF), at 37 °C and 5 % CO_2. Cells were passaged every 3-4 days at an approximate density of 1-2 x 10^6 cells/ml. For differentiation to granulocytes, cells were cultured in the medium above at 1-2 x 10^6 cells/ml with either 10 % DMSO (Sigma) or 0.5 % DMF (Sigma) for 5-9 days.

Purification of Human Neutrophils

Fresh human blood collected under informed consent was anti-coagulated with heparin or citrate-dextrose solution (ACD) (Sigma), layered over an equal volume of Polymorphprep (Axis-Shield) and centrifuged for 30 min. at room temperature and 500 x g with no brake in a swinging bucket centrifuge. The neutrophil layer was removed and washed three times with Hanks' Balanced Saline Solution -Ca^{2+}/-Mg^{2+} with 20 mM HEPES, pH 7.3. Red blood cells were lysed by resuspending the cell pellet in 10 mM HEPES, pH 7.3 + 0.2 % NaCl + 1 % BSA for 10 seconds, then adding an equal volume

of 10 mM HEPES, pH 7.3 + 1.6 % NaCl + 1 % BSA. Neutrophils were resuspended in HBSS -Ca^{2+}/-Mg^{2+} until ready for use.

Detection of SK and IK Transcripts by RT-PCR

Total RNA was isolated from PLB-985 cells, HL-60 cells, or neutrophils using an RNEasy Mini Kit (Qiagen, Valencia, CA), according to the manufacturer's instructions. Following purification, RNA was treated with DNase I (Ambion, Austin, TX) in order to digest genomic DNA. cDNA was made by synthesizing the first strand from RNA with oligo-dT primers and Stratascript Reverse Transcriptase (Stratagene, La Jolla, CA), according the manufacturer's protocol. The first strand was then used as a template for PCR with primers specific to human SK1, SK2, Sk3, or IK. Primer pairs (Integrated DNA Technologies, Coralville, IA) were as follows: SK1 forward 5'-GGGCGGCCTGCAGCGAGC-3', reverse 5'- TGCCGGCCTCATCTTCCTCATCA-3'; SK2 forward 5'- GCGGCCGCTCAGCAACTTG-3', reverse 5'-CCGTGCCCGCTCCCTCCA-3'; SK3 forward 5'-CGGGGGTGGGGGACTTGGATG-3', reverse 5'-GGCGGTGGAGTTGGACGAAGGTG-3'; IK forward 5'-GGGGATCTGGTGCTTGGCCTGG-3', reverse 5'-CGCCCCTAAATCCTGCACGCAC-3'. In addition, a second set of SK3 primers (Elim biopharmaceuticals, Inc., Hayward, CA) was used to validate amplification by the first primer set: forward 5'-TGTTATGGTGATAGAGACCGAGCTC-3', reverse 5'-TGGACAGACTGATAAGGCATTTCA-3'.

Measurement of Reactive Oxygen Species Production by Neutrophils and PLB-985 Cells

After washing cells to remove culture medium, PLB-985 cells or neutrophils were resuspended in HBSS + 0.2 % BSA with either 500 nM DHR 123, 5 μM DHE, or 7.7 μM PF1 [12] in the presence or absence of drugs. Cells were then rotated at 37 °C for 10 min. in order to allow uptake of fluorescent probes. In order to stimulate cells, 100 nM fMLF (Sigma-Aldrich, St. Luois, MO) was added and cells were incubated for 10 min. longer at 37 °C before quenching on ice. For stimulation with opsonized bacteria, approximately 4 mg of heat-killed S. aureus (Invitrogen, Carlsbad, CA) was washed and incubated for 2-3 hrs. in PBS + 10 mg/ml human IgG (Sigma) at 37 °C. The opsonized bacteria were then washed with PBS and added to neutrophils or PLB-985 cells to a ratio of approximately 10-20 bacteria/granulocyte. The suspension was centrifuged briefly at 500 x *g* in order to promote binding and phagocytosis, and then incubated again at 37 °C for 10-15 min. before quenching on ice. Fluorescence spectra were measured using a Fluoromax-3 (Jobin Yvon Horiba, Edison, NJ). For DHR 123 experiments, excitation was at 501 nm and emission measured from 510-600 nm (531 nm maximum), DHE was excited at 492 with emission spectra collected from 525-650 nm (600 nm maximum), and PF1 was excited at 488 nm with 500-600 nm emission (518 nm maximum).

Measuring Apoptosis of PLB-985 Cells

Undifferentiated cells or PLB-985 cells differentiated for 6 days with 0.5 % DMF (10^6 cells) were treated for 6 hrs. at 37 °C, 5 % CO_2 with staurosporine (EMD Biosciences, San Diego, CA) with or without 1-EBIO or apamin. Cells were washed and resuspended in cold PBS + 10 nM Yo-pro-1 + 1 ug/ml propidium iodide, and incubated on ice for 30

min. Fluorescence of 10,000 cells was analyzed using a FACSort (BD Biosciences, San Jose, CA) flow cytometer.

Whole-Cell Patch Clamp Electrophysiology

Recording electrodes were pulled from thin-walled borosilicate glass with an internal filament (MTW150F-3, World Precision Instruments) using a P-87 Flaming Brown puller (Sutter Instrument) and were fire polished to a resistance of 5–10 MΩ. The bath solution consisted of 110 mM KCl, 1.44 mM $MgCl_2$, 30 mM KOH, 10 mM EGTA, 10 mM HEPES, pH to 7.2. The intrapipette solution consisted of 140 mM KCl, 1.2 mM $MgCl_2$, 2.6 mM $CaCl_2$, 10 mM HEPES, pH to 7.4. All patches were voltage-clamped at −100 mV intracellularly. Currents were recorded with Axopatch 200A patch-clamp amplifier (Axon Instruments) and were low-pass filtered (3 dB, 2 kHz) with an 8-pole Bessel filter (Frequency Devices).

Results

In order to assay neutrophil and PLB-985 reactive oxygen species production, we measured the amount of conversion of dihydrorhodamine 123 (DHR 123) to rhodamine 123 in the presence of various drugs that affect channel activity. DHR 123 is oxidized to its fluorescent derivative by several reactive oxygen species, but most prominently by hydrogen peroxide in the presence of a peroxidase (such as myeloperoxidase or glutathione peroxidase). While most potassium channel blockers had no effect, the SK blocking toxin apamin was found to partially reduce peroxide levels when cells were stimulated with either IgG-opsonized, heat-killed *S. aureus* or with the bacterial chemotactic peptide fMLF (Figure 1A). Another SK blocker, d-tubocurarine [13], also decreased oxidation of DHR123. On the other hand, the SK activator 1-EBIO potently

increased rhodamine 123 formation by both neutrophils and PLB-985 cells (Figure 1B). These effects were also present when a peroxidase-independent hydrogen peroxide sensor, PF1 [12], was used as a fluorogenic probe (Figure 1C). These effects suggested a potential role for SK channels in peroxide formation.

Since 1-EBIO is believed to potentiate SK and IK currents by increasing the affinity of $Ca2^{+}$-calmodulin for the SK channel subunit, thus causing greater current at lower calcium concentrations, we hypothesized that the effects of 1-EBIO should be increased by a rise in cytosloic calcium. Indeed, treatment of cells with ionomycin, a calcium ionophore, enhanced the effects of 1-EBIO on rhodamine 123 formation, even though ionomycin itself had no effect on resting levels of rhodamine 123 formation (Figure 1D).

Given the pharmacological evidence for SK channel involvement in ROS production, we set out to demonstrate the presence of an apamin-sensitive current in the promyelocytic leukemia PLB-985 cell line. Stimulation of neutrophils or differentiated promyelocytic cell lines with inflammatory agonists, such as the PKC activator phorbol 12-myristate 13-acetate (PMA) or the bacterial chemotactic peptide fMLF, is known to alter plasma membrane potential by affecting ion channel activity [14-16]. Using whole cell voltage clamp electrophysiology, we found that fMLF activated an outward current in PLB-985 cells with a reversal potential consistent with a potassium-selective channel. This current could be selectively inhibited by the bee venom-derived peptide toxin apamin (Figure 2), a specific blocker of small conductance, calcium-activated potassium channels [17]. An outward current could also be activated by 1-EBIO, an opener of SK and intermediate conductance, calcium-activated potassium channels (IK) [18, 19]. The

1-EBIO-dependent current was sensitive to both apamin and the IK blocker clotrimazole. Given these effects on SK/IK currents activated by fMLF, which is a stimulator of NADPH oxidase-mediated superoxide production, we set out to determine which of the three cloned SK genes, SK1-3 [20], is expressed in neutrophils and neutrophil-like cell lines.

After purifying RNA from human neutrophils, PLB-985 cells, and HL-60, we used reverse transcription and primers specific for SK1, SK2, SK3, or IK to amplify any transcript present for these channels. While no transcript was detected for either SK1 or SK2, SK3 was present in all three cell types tested (Figure 3). Interestingly, SK3 is transcribed in both differentiated and undifferentiated (not shown) PLB-985 cells. In addition, IK transcript was detected in PLB-985 cells, but not neutrophils or HL-60 cells (Figure 3). Thus, it appears that SK3 is the most likely candidate for mediating the apamin and 1-EBIO effects on ROS production described above.

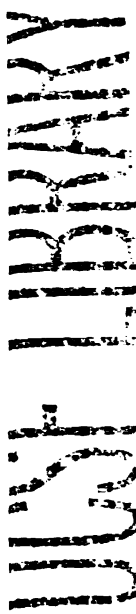

Because superoxide is, in most cases, the precursor to hydrogen peroxide, we also measured the effects of apamin and 1-EBIO on superoxide production, using the superoxide-specific probe dihydroethidine (DHE). DHE is oxidized to red fluorescent ethidium by superoxide and then preferentially associates with DNA. 1-EBIO caused a clear increase in superoxide production, which could be partially inhibited by apamin, consistent with the results obtained using DHR 123 (Figure 4A). Oxidation of DHE following 1-EBIO treatment was enhanced by ionomycin, consistent with 1-EBIO's activation of a calcium-activated channel (Figure 4B). Furthermore, neither drug had an effect on extracellular reduction of cytochrome c by superoxide, while the NADPH oxidase blocker diphenylene iodonium (DPI) blocked almost all cytochrome c reduction

(Figure 4C), indicating that SK channels increase superoxide production without activating the NADPH oxidase.

While DPI is a relatively specific inhibitor of NADPH oxidase, the only way to unequivocally scrutinize whether the oxidase is involved in apamin and 1-EBIO-mediated effects is to knock out one of the subunits of the oxidase. This genotype of patients with chronic granulomatous disease [21] has been mimicked in PLB-985 cells by targeted deletion, and we used this gp91*phox* knockout cell line (PLB-X-CGD) [11] in order to determine whether the NADPH oxidase is necessary for 1-EBIO to increase and for apamin to decrease neutrophil ROS production. Whereas PLB-985 wild-type cells have a fMLF-stimulated respiratory burst, PLB-X-CGD cells do not respond to the chemotactic peptide. Remarkably, 1-EBIO induced DHR 123 oxidation in both cell lines (Figure 5). In addition, while the NADPH oxidase inhibitor DPI decreases ROS production in wild-type cells, DPI increases CGD cells' formation of superoxide and peroxide (Figure 5). This enhancement of ROS production is likely due to inhibition of complex I (NADH dehydrogenase) [22] of the mitochondrial electron transport chain by DPI, since another complex I inhibitor, rotenone [23], had the same effect. These findings point to SK channel regulation of NADPH oxidase-independent ROS production by neutrophils and strongly indicate that the source of the observed ROS effects is the mitochondrial oxidative phosphorylation cascade.

In order to more specifically probe the involvement of mitochondria in the effects of 1-EBIO and apamin, we used MitoSOX [24], a superoxide-specific probe, to explore ROS production within the mitochondria. The timecourse of superoxide production is clearly sensitive to rotenone, a complex I inhibitor that is known to increase superoxide

production in the mitochondrial matrix by forcing the electron transport chain to run in reverse. 1-EBIO also causes an increase in the rate of mitochondrial superoxide production, an effect that can be inhibited by apamin (Figure 6). The fact that these results are qualitatively similar to those obtained with DHR 123, DHE, and PF1 strongly suggests that all of these probes are reporting on the same pathway of ROS production, and that the mitochondria is the most likely source of these ROS. Neither apamin nor 1-EBIO, however, altered the mitochondrial membrane potential, as measured by the inner membrane-localized, potential-sensitive probe MitoTracker Red.

Given the central role that both mitochondrial ROS generation and plasma membrane K^+ efflux play in apoptosis, we wondered whether SK channel activity might affect programmed cell death. Using an assay for apoptosis, based on the differential binding by the DNA-intercalating dyes Yo-Pro [25] and propidium iodide (PI), we showed that 1-EBIO increased and apamin inhibited staurosporine-induced apoptosis, indicating that SK activity can mediate its effects through a well-characterized apoptotic pathway (Figure 7). Neither apamin nor 1-EBIO alone affected apoptosis of PLB-985 cells.

Discussion

While SK channels have been extensively characterized in neurons, where they mediate the afterhyperpolarization [17, 26, 27], and in some endocrine cells [28-30], where they are thought to regulate hormone secretion, the functions of ionic fluxes in non-excitable cells, particularly immune cells [31, 32], are only beginning to emerge. The specialized functions of neutrophils require that they release large quantities of

reactive oxygen species, proteases, and basic antimicrobial peptides. Electrogenic superoxide release by the NADPH oxidase has long been thought to be coupled to a voltage-gated proton channel that provides charge balance and prevents voltage-dependent inhibition of the oxidase [9]. The recent cloning of a zinc-and voltage-sensitive proton channel expressed in immune cells [7, 8] should help to resolve this issue definitively. For protease release, Segal and co-workers have proposed that the large conductance, calcium-activated potassium channel (BK) compensates part of the superoxide flux [10], allowing for potassium-dependent release of basic proteins from the granule proteoglycan matrix [33]. Blocking BK channels impairs maintenance of phagosomal pH, protease-dependent digestion of microbial proteins, and killing of various microbes [10].

Mitochondria are a second, less prominent source of reactive oxygen species [34] in neutrophils. Since neutrophils rely predominantly on the hexose monophosphate shunt for NAD(P)H production [35], it has been assumed that mitochondria are superfluous for neutrophil function. However, more recent studies have shown that neutrophil mitochondrial activity, while not essential for phagocytosis or respiratory burst initiation, does affect chemotaxis [36] and apoptosis [37, 38]. Neutrophil phagocytosis may even involve incorporation of some mitochondrial components into the phagosome [39]. It is clear from our results that neutrophil mitochondria can produce substantial quantities of reactive oxygen species, and that plasma membrane SK3 channels modulate this process.

We set out, initially, to characterize the effects of potassium channel blockers on respiratory burst production, and found that apamin, a specific peptide toxin blocker of SK channels from bee venom, inhibits oxidation of dihydrorhodamine 123 (Figure 1A).

This finding indicated an effect of SK channels on neutrophil peroxide production. It is the first identification of an apamin-sensitive SK current in neutrophils. Whereas studies suggest that calcium-activated potassium channels affect granule release and reactive oxygen species production by eosinophils [40-42] and microglia [43], a link between potassium channels, ROS production, and apoptosis has not been established previously.

The most robust of the pharmacological effects observed is the potentiation of hydrogen peroxide formation by 1-EBIO (Figure 1), as measured by oxidation of DHR 123. Even without activating the respiratory burst with a physiological stimulus such as fMLF or opsonized bacteria, the SK/IK opener dramatically increased rhodamine 123 fluorescence. This effect was calcium-dependent, since the calcium ionophore ionomycin potentiated the response to 1-EBIO (Figure 1D). In addition, apamin, but not the IK blockers clotrimazole (not shown) or charybdotoxin (Figure 1A), was able to partially reduce the 1-EBIO effect, indicating that 1-EBIO is acting primarily or exclusively through SK channels to increase ROS production. This inability of apamin to entirely inhibit the effect of 1-EBIO is consistent with electrophysiological studies of SK [44] and may be due to heterogeneity of glycosylation of SK channels, some of which may respond to the cytosolic 1-EBIO but not to the cell-impermeant peptide apamin.

While DHR 123 is a widely used probe for studying the respiratory burst in neutrophils, it is important to employ several different probes in this study because DHR 123 is susceptible to oxidation by several other reactive oxygen species in addition to hydrogen peroxide. DHR 123 is readily oxidized by peroxide in the presence of a peroxidase, but is also sensitive to hydroxyl radical, peroxynitrite, and hypochlorous acid. A more recently characterized probe, PF1 [12], is converted from a non-fluorescent form

to fluorescein in the presence of peroxide (independent of peroxidase), responds less to hydroxyl radical, and is insensitive to hypochlorous acid and peroxynitrite. Using PF1 to measure peroxide formation in PLB-985 cells stimulated with opsonized bacteria, we found that the effects of 1-EBIO and apamin were qualitatively similar to those obtained with DHR 123: that is, 1-EBIO stimulates peroxide production and apamin inhibits it (Figure 1C). These experiments were carried out in the presence of the peroxidase inhibitor 4-aminobenzoic acid hydrazide, since peroxidase has been shown to bleach fluorescein fluorescence [45]. Thus, experiments performed with two distinct probes for hydrogen peroxide indicate that apamin and 1-EBIO alter hydrogen peroxide levels. Hydroxyl radical is unlikely to be a contaminating species, given production of this species requires free ferrous ion, which must be added exogenously to detect hydroxyl radical in neutrophils [46].

Since peroxide is made directly from superoxide radical by superoxide dismutase, drugs that target SK should have similar effects on superoxide production if channel activity somehow regulates ROS production. Indeed, we found that the superoxide-specific probe dihydroethidine also showed an increased conversion to its fluorescent, oxidized form, ethidium, in the presence of 1-EBIO (Figure 4). In addition, this effect could be partially inhibited by apamin. Oxidation of this probe required stimulation with fMLF or opsonized bacteria, though its conversion to ethidium could also be initiated by addition of the mitochondrial complex I inhibitor rotenone (not shown). Thus, this probe appears to be a sensor for superoxide from both NADPH oxidase activity and from mitochondrial sources.

In order to distinguish between NADPH oxidase-dependent and -independent pathways of granulocyte ROS production, it is necessary to remove NADPH oxidase activity. While the NADPH oxidase inhibitor DPI is a potent pharmacological tool, it also inhibits the NADH dehydrogenase of complex I of the mitochondrial respiratory chain [47]. Thus, it is important to perform additional tests on the possible involvement of NADPH oxidase. Patients with the X-linked chronic granulomatous disease [21] have neutrophils that are incapable of producing a respiratory burst in response to stimuli such as fMLF, opsonized microbes, or PMA, rendering them susceptible to infections by pathogenic bacteria and fungi. The molecular basis for this disease is a non-functional NADPH oxidase [48], most commonly resulting from mutations in the gp91*phox* subunit [49]. Dinauer and colleagues have made a stable line of PLB-985 cells, which can be differentiated to neutrophil-like cells, with targeted knockout of the gp91*phox* subunit [11]. This line has the same deficiencies in ROS production as do the neutrophils from CGD patients and has been used for studies of the cell biology of neutrophil ROS production. As expected, we found that the CGD line did not respond to fMLF and that DPI increased ROS production (Figure 5B), likely due to its ability to inhibit mitochondrial NADH dehydrogenase. Potentiation of ROS production 1-EBIO, in contrast, was the same in wild-type and CGD cell lines, demonstrating that the actions of this drug is independent of NADPH oxidase (Figure 5).

NADPH oxidase is the source of ROS involved in oxidative microbial killing and possibly in the release of serine proteases [50], but mitochondria provide another, less well characterized source of ROS in neutrophils [34, 51]. Mitochondria produce superoxide as a consequence of leakage of electrons, which escape the electron transport

chain and react with oxygen [50]. This leakage is thought to occur primarily at complex I [22], but also at complex III [52]. Superoxide released into the mitochondrial matrix can be converted to hydrogen peroxide by mitochondrial MnSOD, while superoxide that reaches the intermembrane space and cytoplasm reacts with CuZnSOD [53]. Inhibition of either complex I or complex III actually increases superoxide formation, presumably by causing greater flavoprotein autooxidation and electron leakage [54]. In most cells, mitochondria are the predominant source of ROS, and disruption of the electron transport chain by complex I inhibitors like rotenone can trigger apoptosis [55, 56]. Even in neutrophils, which are capable of much greater ROS production than other cells, mitochondria are involved in apoptosis [37], and neutrophil apoptotic pathways can be triggered by ROS [37].

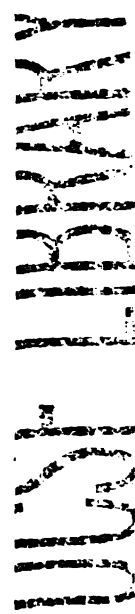

It is likely that the probes used to detect total ROS production in this study are being oxidized by ROS derived from the mitochondria, since the probes are all membrane-permeant, as is hydrogen peroxide. DHR 123 can be oxidized by hydrogen peroxide in the presence of a peroxidase, such as mitochondrial glutathione peroxidase or myeloperoxidase, which is synthesized in the endoplasmic reticulum before becoming incorporated into azurophilic granules. The oxidized form of this probe, rhodamine 123, tends to accumulate in mitochondria. PF1 could react with peroxide either inside or outside of mitochondria, while DHE would likely react with superoxide in mitochondria and then bind to DNA in the nucleus and mitochondria.

In order to more directly detect mitochondrial ROS production, we used a probe, MitoSOX [24], which localizes to mitochondria and is specific for superoxide. 1-EBIO caused an increased rate of superoxide production in the mitochondria, as did rotenone

(not shown), and apamin decreased the 1-EBIO effect (Figure 6). Thus, mitochondria are the most likely source of the reactive oxygen species in cells with elevated SK channel activity.

We next used electrophysiology and RT-PCR to confirm the presence of an apamin-sensitive SK channel in PLB-985 cells and neutrophils. While BK channels have been recently identified in neutrophils [10], earlier electrophysiological studies showed the presence of a calcium-activated potassium channel of lower conductance in neutrophils [57], but used no pharmacological tools to further identify the channel. We were able to show the presence of a current stimulated by the bacterial chemotactic peptide fMLF, which could be inhibited by apamin (Figure 2), a specific peptide toxin blocker of SK channels [17] from bee venom.

To further specify the molecular identity of this channel, we purified RNA from neutrophils, PLB-985 cells, and HL-60 cells, and used reverse transcription and PCR with primers specific for SK1-3 and IK to amplify any transcripts present. Only SK3 was present in all of these cells, while neither SK1 nor SK2 was detected in any of them (Figure 3). Thus, we conclude that SK3 is mediating the apamin-sensitive current recorded, as well as the apamin- and 1-EBIO-sensitive production of reactive oxygen species measured in these cells.

A common feature of apoptotic cells is a reduction in volume, where the loss of water is triggered by an efflux of K^+ and Cl^-, the most abundant cytoplasmic ions [58]. This volume loss, and in particular the drop in cytoplasmic K^+ concentration, can activate both proteases and nucleases involved in programmed cell death, while the activities of these enzymes may be suppressed at normal cytoplasmic K^+ concentrations [59]. Up-

regulation of K^+ channels has been associated with apoptosis in neurons [60], tumor cells [61], vascular smooth muscle cells [62], erythrocytes [63], T lymphocytes [64, 65], and many other cell types. Reactive oxygen species are common triggers for apoptosis, and in neutrophils they are known to activate formation of a death receptor complex that leads to a drop in cellular glutathione levels and the commencement of programmed cell death [38, 66]. Loss of the mitochondrial membrane potential, release of cytochrome c from the mitochondrial matrix, and the formation of mitochondrial ROS often accompany apoptosis, even in neutrophils, which are not dependent on mitochondria for most metabolic activity [36, 51]. Our findings that the SK opener 1-EBIO enhances staurosporine-mediated apoptosis (Figure 7) are clearly consistent with potassium loss and reactive oxygen species formation causing cell death. The SK channel pathway appears to be NADPH oxidase-independent, since 1-EBIO can trigger ROS even in gp91*phox*-deficient PLB-985-CGD cells (Figure 5B), but its stimulation of ROS production could potentially be upstream of chloride channel activation [67]. Our work represents the first reported involvement of a specific K^+ channel in neutrophil apoptosis.

One of the unexpected findings from this study is that a plasma membrane channel can affect intracellular ROS generation, most likely by mitochondria. Apamin, because it is membrane-impermeant, does not have access to organellar membranes except through endocytosis, so it most likely inhibits only plasma membrane channels. Since neither apamin nor 1-EBIO altered cytoplasmic calcium levels, either in resting cells or in fMLF-stimulated cells, it is unlikely that SK channels are affecting calcium release. A possible explanation is that the K^+ efflux stimulated by 1-EBIO affects cellular energy homeostasis, which leads to a reduction in the NADPH/$NADP^+$ ratio, and

a more oxidizing intracellular environment. This could enhance the oxidation of fluorescent ROS probes in compartments such as the mitochondria and endoplasmic reticulum, which maintain oxidizing environments. Activation of K^+ efflux could, for example, alter the metabolic oscillations present in neutrophils [68] or increase glutathione efflux [69], as it has been found to do in airway epithelia [70]. Further experiments will be necessary to fully characterize the mechanism of SK channel regulation of neutrophil ROS production and apoptosis.

This work identifies, for the first time, the presence of a small conductance, calcium-activated potassium channel in neutrophils and the granulocytic cell-line PLB-985, and shows that SK channel activity affects reactive oxygen species production by these cells. The SK blocker apamin reduces peroxide formation, as measured by oxidation of dihydrorhodamine 123 or PF1, and the SK/IK activator 1-EBIO increases peroxide production in these assays and in tests for detect superoxide formation. Apamin partially compensates for the effects of 1-EBIO, consistent with SK channel pharmacology. An apamin-sensitive current is present in PLB-985 cells, and RT-PCR shows that SK3 is the likely molecular correlate to this current. Since the effects of SK channels seem to mediate ROS production in the mitochondria, rather than through the NADPH oxidase, it is unlikely that this pathway has a direct effect on microbial killing. However, we find that triggering the opening of SK channels enhances apoptosis, the first demonstration of a role for a K^+ channel in neutrophil programmed cell death. Given the critical role of mitochondrial ROS in cell signaling and redox homeostasis, SK channels may also be important for regulating neutrophil turnover or differentiation.

References

1. Segal, A. W. (2005). How neutrophils kill microbes. *Annu Rev Immunol*, 23:197-223.
2. Serhan, C. N., J. Savill (2005). Resolution of inflammation: the beginning programs the end. *Nat Immunol*, 6:1191-1197.
3. Panyi, G., Z. Varga, R. Gaspar (2004). Ion channels and lymphocyte activation. *Immunol Lett*, 92:55-66.
4. Cahalan, M. D., H. Wulff, K. G. Chandy (2001). Molecular properties and physiological roles of ion channels in the immune system. *J Clin Immunol*, 21:235-252.
5. DeCoursey, T. E. (2004). During the respiratory burst, do phagocytes need proton channels or potassium channels, or both? *Sci STKE*, 2004:pe21.
6. Henderson, L. M., J. B. Chappell, O. T. Jones (1987). The superoxide-generating NADPH oxidase of human neutrophils is electrogenic and associated with an H+ channel. *Biochem J*, 246:325-329.
7. Ramsey, I. S., M. M. Moran, J. A. Chong, D. E. Clapham (2006). A voltage-gated proton-selective channel lacking the pore domain. *Nature*.
8. Sasaki, M., M. Takagi, Y. Okamura (2006). A Voltage Sensor-Domain Protein is a Voltage-Gated Proton Channel. *Science*.
9. DeCoursey, T. E., D. Morgan, V. V. Cherny (2003). The voltage dependence of NADPH oxidase reveals why phagocytes need proton channels. *Nature*, 422:531-534.
10. Ahluwalia, J., A. Tinker, L. H. Clapp, M. R. Duchen, A. Y. Abramov, S. Pope, M. Nobles, A. W. Segal (2004). The large-conductance Ca2+-activated K+ channel is essential for innate immunity. *Nature*, 427:853-858.
11. Zhen, L., A. A. King, Y. Xiao, S. J. Chanock, S. H. Orkin, M. C. Dinauer (1993). Gene targeting of X chromosome-linked chronic granulomatous disease locus in a human myeloid leukemia cell line and rescue by expression of recombinant gp91phox. *Proc Natl Acad Sci U S A*, 90:9832-9836.
12. Miller, E. W., A. E. Albers, A. Pralle, E. Y. Isacoff, C. J. Chang (2005). Boronate-based fluorescent probes for imaging cellular hydrogen peroxide. *J Am Chem Soc*, 127:16652-16659.
13. Ishii, T. M., J. Maylie, J. P. Adelman (1997). Determinants of apamin and d-tubocurarine block in SK potassium channels. *J Biol Chem*, 272:23195-23200.
14. Lazzari, K. G., P. Proto, E. R. Simons (1990). Neutrophil hyperpolarization in response to a chemotactic peptide. *J Biol Chem*, 265:10959-10967.
15. Naccache, P. H., H. J. Showell, E. L. Becker, R. I. Sha'afi (1977). Transport of sodium, potassium, and calcium across rabbit polymorphonuclear leukocyte membranes. Effect of chemotactic factor. *J Cell Biol*, 73:428-444.
16. Schumann, M. A., T. Tanigaki, D. N. Heller, T. A. Raffin (1992). Ca(2+)-dependent and Ca(2+)-independent mechanisms modulate whole-cell cationic currents in human neutrophils. *Biochem Biophys Res Commun*, 185:531-538.
17. Blatz, A. L., K. L. Magleby (1986). Single apamin-blocked Ca-activated K+ channels of small conductance in cultured rat skeletal muscle. *Nature*, 323:718-720.

18. Syme, C. A., A. C. Gerlach, A. K. Singh, D. C. Devor (2000). Pharmacological activation of cloned intermediate- and small-conductance Ca(2+)-activated K(+) channels. *Am J Physiol Cell Physiol*, 278:C570-581.
19. Devor, D. C., A. K. Singh, R. A. Frizzell, R. J. Bridges (1996). Modulation of Cl- secretion by benzimidazolones. I. Direct activation of a Ca(2+)-dependent K+ channel. *Am J Physiol*, 271:L775-784.
20. Stocker, M. (2004). Ca(2+)-activated K+ channels: molecular determinants and function of the SK family. *Nat Rev Neurosci*, 5:758-770.
21. Thrasher, A. J., N. H. Keep, F. Wientjes, A. W. Segal (1994). Chronic granulomatous disease. *Biochim Biophys Acta*, 1227:1-24.
22. Liu, Y., G. Fiskum, D. Schubert (2002). Generation of reactive oxygen species by the mitochondrial electron transport chain. *J Neurochem*, 80:780-787.
23. Votyakova, T. V., I. J. Reynolds (2001). DeltaPsi(m)-Dependent and - independent production of reactive oxygen species by rat brain mitochondria. *J Neurochem*, 79:266-277.
24. Lieven, C. J., M. J. Hoegger, C. R. Schlieve, L. A. Levin (2006). Retinal ganglion cell axotomy induces an increase in intracellular superoxide anion. *Invest Ophthalmol Vis Sci*, 47:1477-1485.
25. Idziorek, T., J. Estaquier, F. De Bels, J. C. Ameisen (1995). YOPRO-1 permits cytofluorometric analysis of programmed cell death (apoptosis) without interfering with cell viability. *J Immunol Methods*, 185:249-258.
26. Kohler, M., B. Hirschberg, C. T. Bond, J. M. Kinzie, N. V. Marrion, J. Maylie, J. P. Adelman (1996). Small-conductance, calcium-activated potassium channels from mammalian brain. *Science*, 273:1709-1714.
27. Bond, C. T., P. S. Herson, T. Strassmaier, R. Hammond, R. Stackman, J. Maylie, J. P. Adelman (2004). Small conductance Ca2+-activated K+ channel knock-out mice reveal the identity of calcium-dependent afterhyperpolarization currents. *J Neurosci*, 24:5301-5306.
28. Uceda, G., A. R. Artalejo, M. G. Lopez, F. Abad, E. Neher, A. G. Garcia (1992). Ca(2+)-activated K+ channels modulate muscarinic secretion in cat chromaffin cells. *J Physiol*, 454:213-230.
29. Tamarina, N. A., Y. Wang, L. Mariotto, A. Kuznetsov, C. Bond, J. Adelman, L. H. Philipson (2003). Small-conductance calcium-activated K+ channels are expressed in pancreatic islets and regulate glucose responses. *Diabetes*, 52:2000-2006.
30. Nagayama, T., Y. Fukushima, M. Yoshida, M. Suzuki-Kusaba, H. Hisa, T. Kimura, S. Satoh (2000). Role of potassium channels in catecholamine secretion in the rat adrenal gland. *Am J Physiol Regul Integr Comp Physiol*, 279:R448-454.
31. Quesada, I., W. C. Chin, J. Steed, P. Campos-Bedolla, P. Verdugo (2001). Mouse mast cell secretory granules can function as intracellular ionic oscillators. *Biophys J*, 80:2133-2139.
32. Jager, H., J. P. Adelman, S. Grissmer (2000). SK2 encodes the apamin-sensitive Ca(2+)-activated K(+) channels in the human leukemic T cell line, Jurkat. *FEBS Lett*, 469:196-202.

33. Reeves, E. P., H. Lu, H. L. Jacobs, C. G. Messina, S. Bolsover, G. Gabella, E. O. Potma, A. Warley, J. Roes, A. W. Segal (2002). Killing activity of neutrophils is mediated through activation of proteases by K+ flux. *Nature*, 416:291-297.
34. Bassoe, C. F., N. Li, K. Ragheb, G. Lawler, J. Sturgis, J. P. Robinson (2003). Investigations of phagosomes, mitochondria, and acidic granules in human neutrophils using fluorescent probes. *Cytometry B Clin Cytom*, 51:21-29.
35. Goetzl, E. J., K. F. Austen (1974). Stimulation of human neutrophil leukocyte aerobic glucose metabolism by purified chemotactic factors. *J Clin Invest*, 53:591-599.
36. Fossati, G., D. A. Moulding, D. G. Spiller, R. J. Moots, M. R. White, S. W. Edwards (2003). The mitochondrial network of human neutrophils: role in chemotaxis, phagocytosis, respiratory burst activation, and commitment to apoptosis. *J Immunol*, 170:1964-1972.
37. Genestier, A. L., M. C. Michallet, G. Prevost, G. Bellot, L. Chalabreysse, S. Peyrol, F. Thivolet, J. Etienne, G. Lina, F. M. Vallette, F. Vandenesch, L. Genestier (2005). Staphylococcus aureus Panton-Valentine leukocidin directly targets mitochondria and induces Bax-independent apoptosis of human neutrophils. *J Clin Invest*, 115:3117-3127.
38. Scheel-Toellner, D., K. Wang, R. Craddock, P. R. Webb, H. M. McGettrick, L. K. Assi, N. Parkes, L. E. Clough, E. Gulbins, M. Salmon, J. M. Lord (2004). Reactive oxygen species limit neutrophil life span by activating death receptor signaling. *Blood*, 104:2557-2564.
39. Burlak, C., A. R. Whitney, D. J. Mead, T. Hackstadt, F. R. Deleo (2006). Maturation of Human Neutrophil Phagosomes Includes Incorporation of Molecular Chaperones and Endoplasmic Reticulum Quality Control Machinery. *Mol Cell Proteomics*, 5:620-634.
40. Saito, M., I. Hisatome, S. Nakajima, R. Sato (1995). Possible mechanism of oxygen radical production by human eosinophils mediated by K+ channel activation. *Eur J Pharmacol*, 291:217-219.
41. Saito, M., R. Sato, I. Hisatome, T. Narahashi (1996). RANTES and platelet-activating factor open Ca2+-activated K+ channels in eosinophils. *Faseb J*, 10:792-798.
42. Saito, M., R. Sato, N. M. Munoz, A. Herrnreiter, M. Oyaizu, H. Kasugai, T. Narahashi, A. R. Leff (1997). Association of granular exocytosis with Ca(2+)-activated K+ channels in human eosinophils. *Am J Physiol*, 273:L16-21.
43. Khanna, R., L. Roy, X. Zhu, L. C. Schlichter (2001). K+ channels and the microglial respiratory burst. *Am J Physiol Cell Physiol*, 280:C796-806.
44. Dale, T. J., J. E. Cryan, M. X. Chen, D. J. Trezise (2002). Partial apamin sensitivity of human small conductance Ca2+-activated K+ channels stably expressed in Chinese hamster ovary cells. *Naunyn Schmiedebergs Arch Pharmacol*, 366:470-477.
45. Jankowski, A., C. C. Scott, S. Grinstein (2002). Determinants of the phagosomal pH in neutrophils. *J Biol Chem*, 277:6059-6066.
46. Kaur, H., I. Fagerheim, M. Grootveld, A. Puppo, B. Halliwell (1988). Aromatic hydroxylation of phenylalanine as an assay for hydroxyl radicals: application to

activated human neutrophils and to the heme protein leghemoglobin. *Anal Biochem*, 172:360-367.

47. Chen, Y. R., C. L. Chen, L. Zhang, K. B. Green-Church, J. L. Zweier (2005). Superoxide generation from mitochondrial NADH dehydrogenase induces self-inactivation with specific protein radical formation. *J Biol Chem*, 280:37339-37348.
48. Baehner, R. L., D. G. Nathan (1967). Leukocyte oxidase: defective activity in chronic granulomatous disease. *Science*, 155:835-836.
49. Dinauer, M. C., S. H. Orkin, R. Brown, A. J. Jesaitis, C. A. Parkos (1987). The glycoprotein encoded by the X-linked chronic granulomatous disease locus is a component of the neutrophil cytochrome b complex. *Nature*, 327:717-720.
50. Reeves, E. P., M. Nagl, J. Godovac-Zimmermann, A. W. Segal (2003). Reassessment of the microbicidal activity of reactive oxygen species and hypochlorous acid with reference to the phagocytic vacuole of the neutrophil granulocyte. *J Med Microbiol*, 52:643-651.
51. Maianski, N. A., J. Geissler, S. M. Srinivasula, E. S. Alnemri, D. Roos, T. W. Kuijpers (2004). Functional characterization of mitochondria in neutrophils: a role restricted to apoptosis. *Cell Death Differ*, 11:143-153.
52. Turrens, J. F., A. Alexandre, A. L. Lehninger (1985). Ubisemiquinone is the electron donor for superoxide formation by complex III of heart mitochondria. *Arch Biochem Biophys*, 237:408-414.
53. Han, D., R. Canali, D. Rettori, N. Kaplowitz (2003). Effect of glutathione depletion on sites and topology of superoxide and hydrogen peroxide production in mitochondria. *Mol Pharmacol*, 64:1136-1144.
54. Turrens, J. F., A. Boveris (1980). Generation of superoxide anion by the NADH dehydrogenase of bovine heart mitochondria. *Biochem J*, 191:421-427.
55. Pelicano, H., L. Feng, Y. Zhou, J. S. Carew, E. O. Hileman, W. Plunkett, M. J. Keating, P. Huang (2003). Inhibition of mitochondrial respiration: a novel strategy to enhance drug-induced apoptosis in human leukemia cells by a reactive oxygen species-mediated mechanism. *J Biol Chem*, 278:37832-37839.
56. Li, N., K. Ragheb, G. Lawler, J. Sturgis, B. Rajwa, J. A. Melendez, J. P. Robinson (2003). Mitochondrial complex I inhibitor rotenone induces apoptosis through enhancing mitochondrial reactive oxygen species production. *J Biol Chem*, 278:8516-8525.
57. Krause, K. H., M. J. Welsh (1990). Voltage-dependent and Ca2(+)-activated ion channels in human neutrophils. *J Clin Invest*, 85:491-498.
58. Dallaporta, B., T. Hirsch, S. A. Susin, N. Zamzami, N. Larochette, C. Brenner, I. Marzo, G. Kroemer (1998). Potassium leakage during the apoptotic degradation phase. *J Immunol*, 160:5605-5615.
59. Hughes, F. M., Jr., C. D. Bortner, G. D. Purdy, J. A. Cidlowski (1997). Intracellular K+ suppresses the activation of apoptosis in lymphocytes. *J Biol Chem*, 272:30567-30576.
60. Yu, S. P., C. H. Yeh, S. L. Sensi, B. J. Gwag, L. M. Canzoniero, Z. S. Farhangrazi, H. S. Ying, M. Tian, L. L. Dugan, D. W. Choi (1997). Mediation of neuronal apoptosis by enhancement of outward potassium current. *Science*, 278:114-117.

61. Wang, H., Y. Zhang, L. Cao, H. Han, J. Wang, B. Yang, S. Nattel, Z. Wang (2002). HERG K+ channel, a regulator of tumor cell apoptosis and proliferation. *Cancer Res*, 62:4843-4848.
62. Krick, S., O. Platoshyn, M. Sweeney, H. Kim, J. X. Yuan (2001). Activation of K+ channels induces apoptosis in vascular smooth muscle cells. *Am J Physiol Cell Physiol*, 280:C970-979.
63. Lang, P. A., S. Kaiser, S. Myssina, T. Wieder, F. Lang, S. M. Huber (2003). Role of Ca2+-activated K+ channels in human erythrocyte apoptosis. *Am J Physiol Cell Physiol*, 285:C1553-1560.
64. Elliott, J. I., C. F. Higgins (2003). IKCa1 activity is required for cell shrinkage, phosphatidylserine translocation and death in T lymphocyte apoptosis. *EMBO Rep*, 4:189-194.
65. Storey, N. M., M. Gomez-Angelats, C. D. Bortner, D. L. Armstrong, J. A. Cidlowski (2003). Stimulation of Kv1.3 potassium channels by death receptors during apoptosis in Jurkat T lymphocytes. *J Biol Chem*, 278:33319-33326.
66. Kasahara, Y., K. Iwai, A. Yachie, K. Ohta, A. Konno, H. Seki, T. Miyawaki, N. Taniguchi (1997). Involvement of reactive oxygen intermediates in spontaneous and CD95 (Fas/APO-1)-mediated apoptosis of neutrophils. *Blood*, 89:1748-1753.
67. Varela, D., F. Simon, A. Riveros, F. Jorgensen, A. Stutzin (2004). NAD(P)H oxidase-derived H(2)O(2) signals chloride channel activation in cell volume regulation and cell proliferation. *J Biol Chem*, 279:13301-13304.
68. Adachi, Y., A. L. Kindzelskii, N. Ohno, T. Yadomae, H. R. Petty (1999). Amplitude and frequency modulation of metabolic signals in leukocytes: synergistic role of IFN-gamma in IL-6- and IL-2-mediated cell activation. *J Immunol*, 163:4367-4374.
69. van den Dobbelsteen, D. J., C. S. Nobel, J. Schlegel, I. A. Cotgreave, S. Orrenius, A. F. Slater (1996). Rapid and specific efflux of reduced glutathione during apoptosis induced by anti-Fas/APO-1 antibody. *J Biol Chem*, 271:15420-15427.
70. Gao, L., J. R. Broughman, T. Iwamoto, J. M. Tomich, C. J. Venglarik, H. J. Forman (2001). Synthetic chloride channel restores glutathione secretion in cystic fibrosis airway epithelia. *Am J Physiol Lung Cell Mol Physiol*, 281:L24-30.

Figure 1

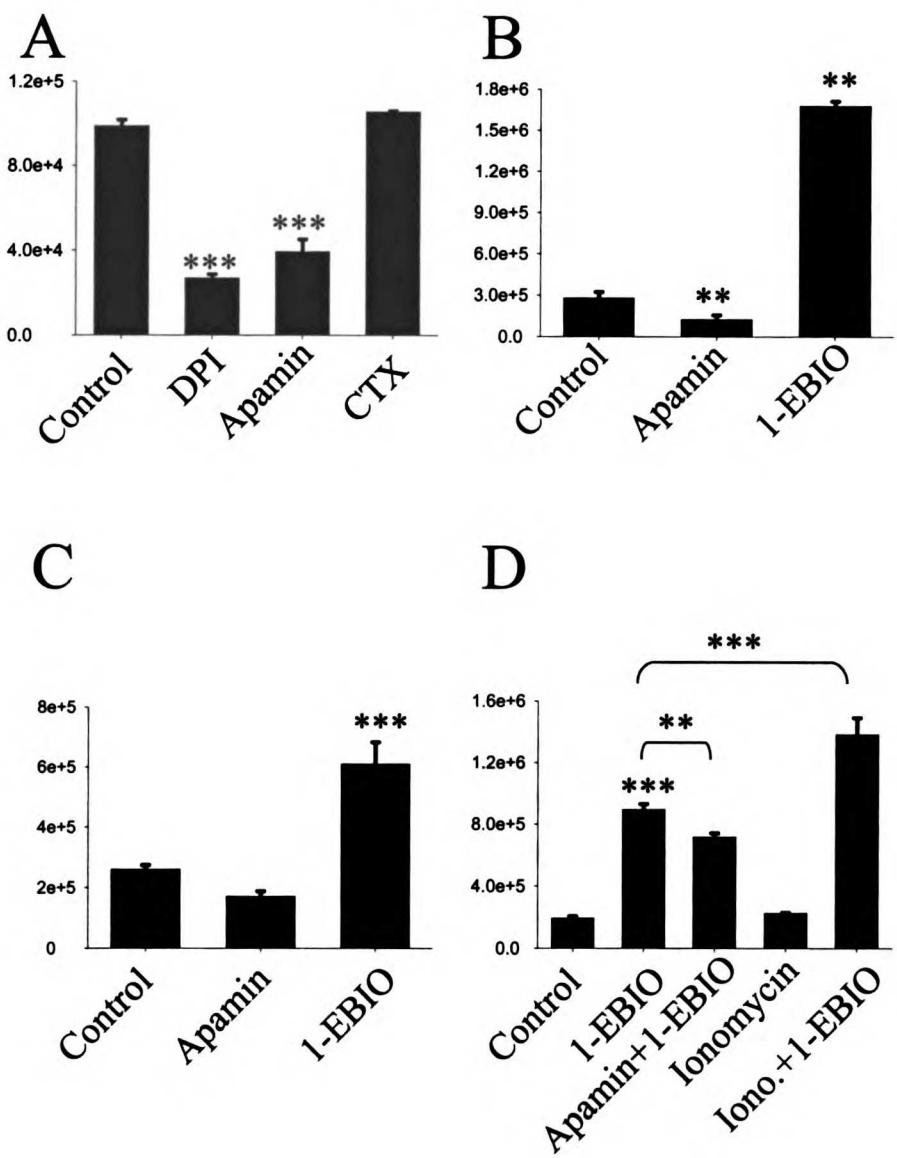

1. SK Blocker and Opener Affect PLB-985 ROS Production. A. Effects of NADPH Oxidase, SK, and BK/IK blockers on opsonized *S. aureus*-induced DHR 123 oxidation. B. SK/IK Opener1 EBIOEnhances ROS Production. C. Apamin and 1-EBIO effects on PF1 oxidation by H_2O_2. D. Apamin partially inhibits, ionomycin potentiates stimulation of ROS production by 1-EBIO. Arbitrary Units. **P<0.01, ***P<0.001.

Figure 2

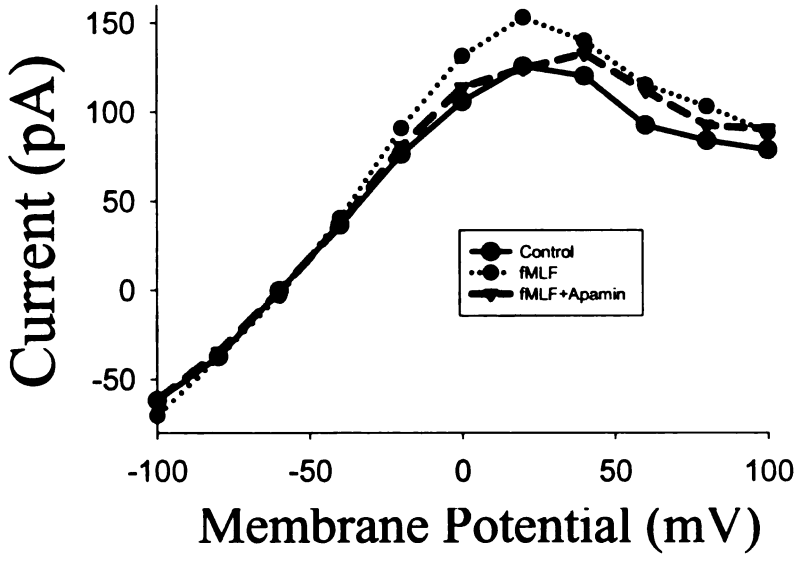

2. Whole Cell Electrophysiology of PLB-985 Cells. Representative example of fMLF-Stimulated (100 nM) outward current, which can be blocked by apamin (3 μM).

Figure 3

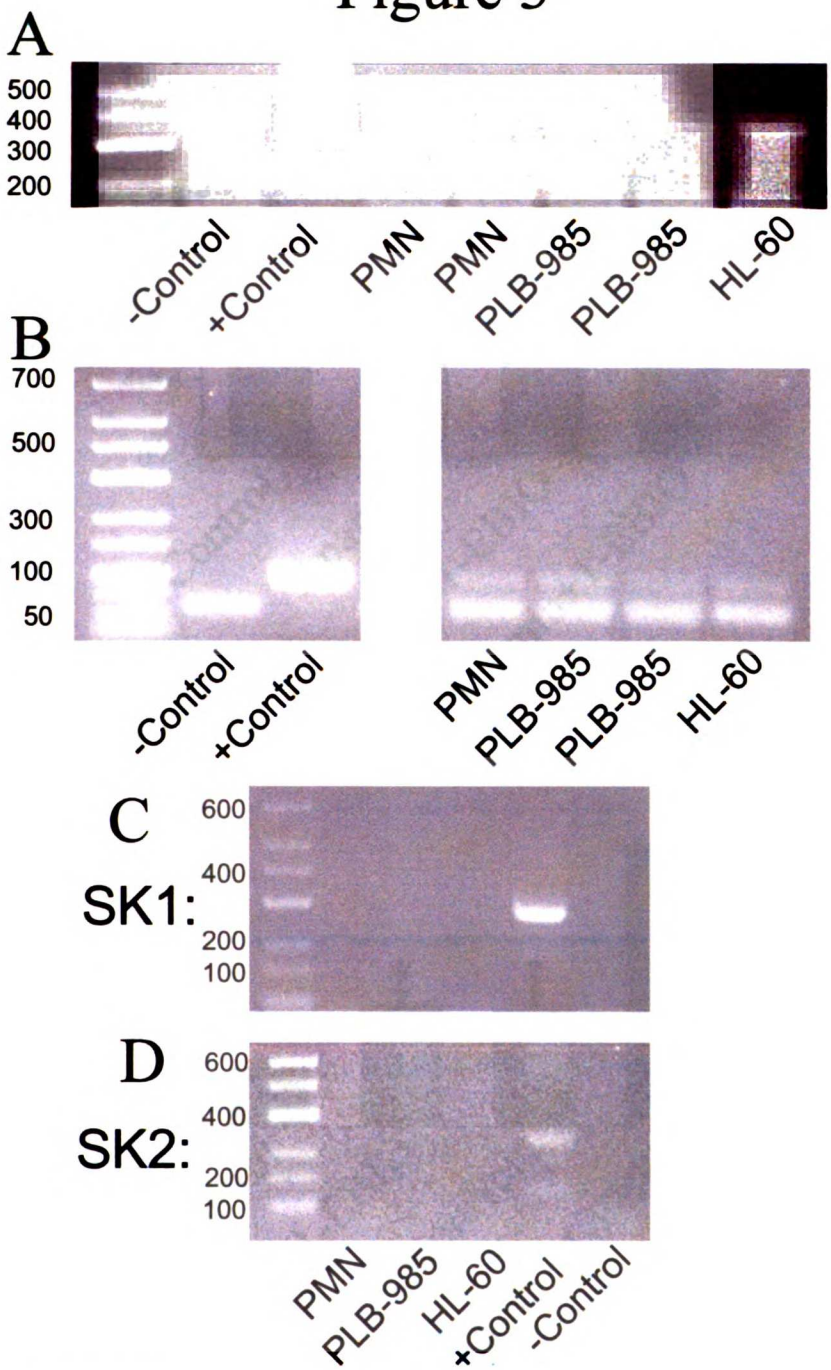

3. RT-PCR Analysis of RNA to Identify SK1, SK2, and SK3 Expression in Neutrophils and Neutrophil-Like Cells. Results are shown for two pairs of SK3-specific primers (A,B) and one pair of primers each for SK1 (C) and SK2 (D).

Figure 4

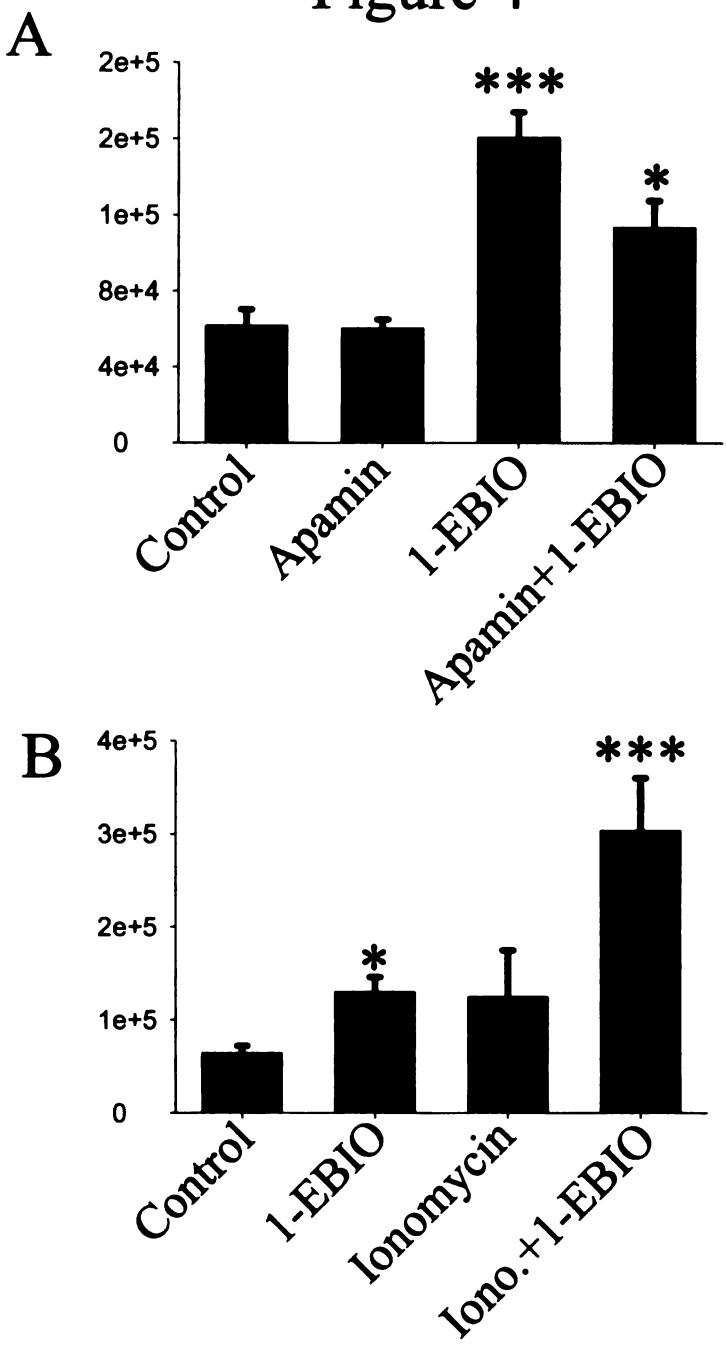

4. SK Blocker and Opener Effects on Superoxide Production. A. SK/IK Opener1-EBIO enhances DHE oxidation, partially inhibited by Apamin. B. Ionomycin increases stimulation of Superoxide production by 1-EBIO. *P<0.05, ***P<0.001.

Figure 5

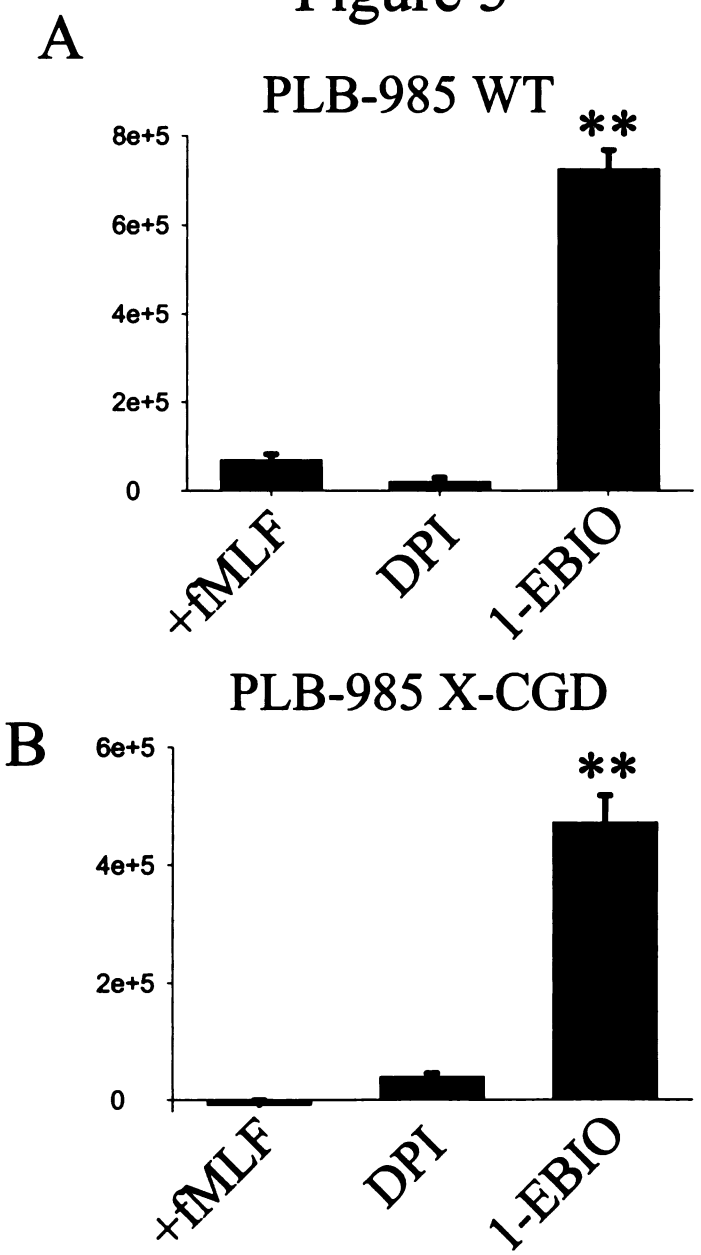

5. DHR 123 Oxidation by Wild-type and gp91*phox* knockout PLB-985 cells A. The NADPH oxidase inhibitor DPI decreases, while 1-EBIO increases fMLF-stimulated ROS production in PLB-985-WT cells. B. PLB-985-X-CGD cells lack fMLF-stimulated ROS production, but ROS production is still stimulated by 1-EBIO. Arbitrary Units. **P<0.01.

Figure 6

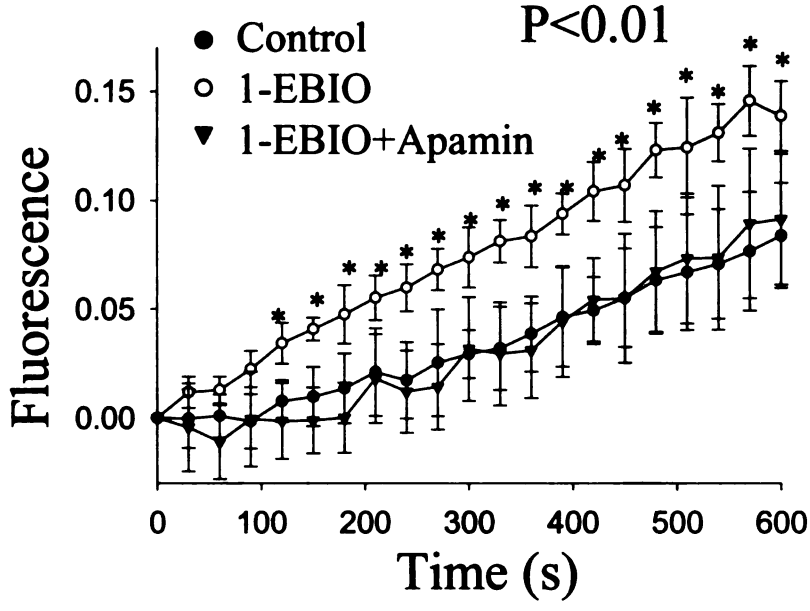

6. Effects of Apamin and 1-EBIO on Mitochondrial Superoxide Production Measured by MitoSOX oxidation. Differences between Control and 1-EBIO, and between Control and 1-EBIO+Apamin are statistically significant (P<0.01).

Figure 7

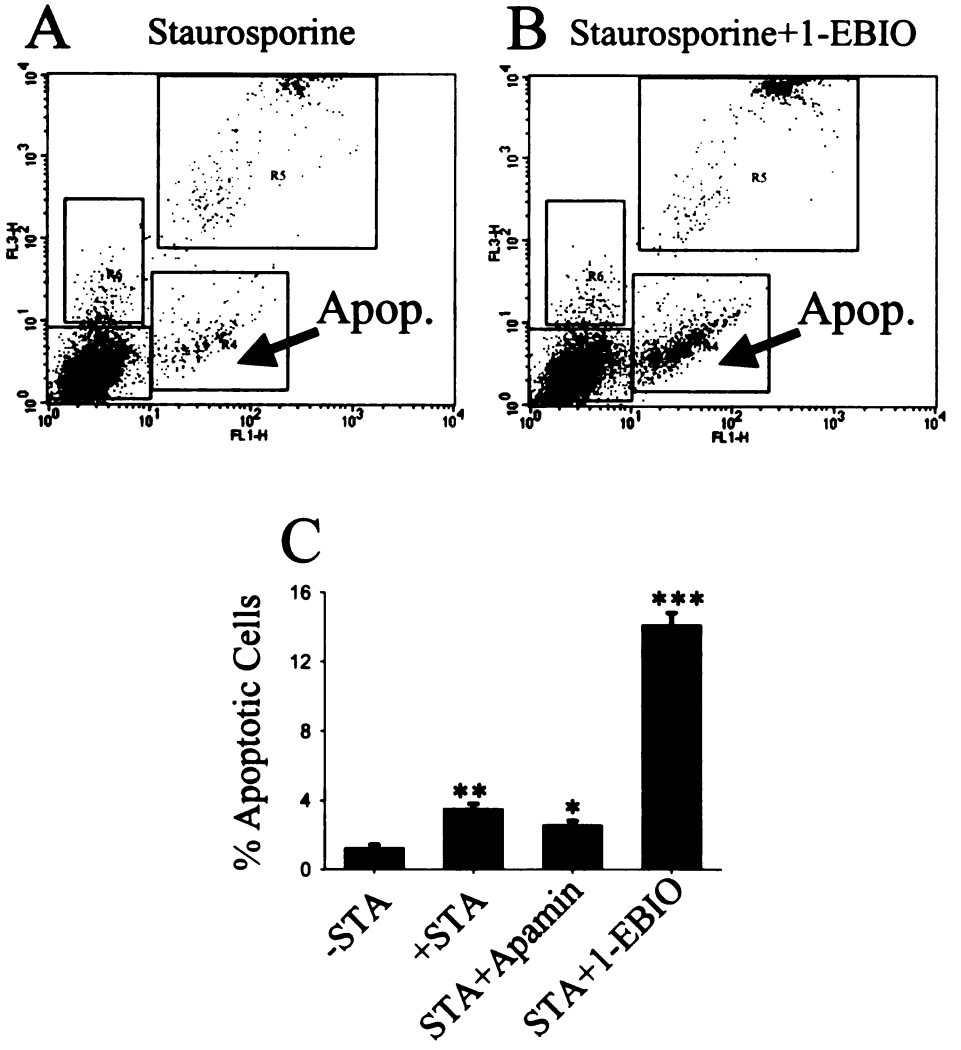

7. Effects of SK Drugs on PLB-985 Cell Apoptosis. FACS dot plots showing live (lower left box), apoptotic (lower right box), and necrotic cells after treatment with staurosporine (A) or 1-EBIO (B). C. Quantification of Effects of Apamin and 1-EBIO on STA-induced apoptosis. *P<0.05, **P<0.01, ***P<0.001.

Chapter 3

Microtubule Plus-end Tracking Proteins Target Gap Junction Proteins Directly from the Cell Interior to Adherens Junctions

Robin M. Shaw[1**], Alex J. Fay[2**], Yuh-Nung Jan[3], and Lily Y. Jan[3,*]

[1] Department of Medicine, University of California, San Francisco, CA 94143, USA

[2] Graduate Group in Biophysics, University of California, San Francisco, CA 94143, USA

[3] Howard Hughes Medical Institute and Departments of Physiology and Biochemistry, University of California, San Francisco, CA 94143, USA

** Equal contributor

* Correspondence:
Lily Y. Jan
Ph: 415-476-8752; Fax: 415-476-5774
gkw@itsa.ucsf.edu

SUMMARY

Gap junctions are intercellular channels that connect the cytoplasms of adjacent cells. For gap junctions to properly control organ formation and electrical synchronization in the heart and brain, connexin-based hemichannels must be correctly targeted to cell-cell borders. While it is generally accepted that gap junctions form via lateral diffusion of hemichannels following microtubule-mediated delivery to the plasma membrane, we provide evidence for direct targeting of hemichannels to cell-cell junctions through a pathway dependent on microtubule dynamics, the adherens junction proteins N-cadherin and β-catenin, the microtubule plus-end tracking protein (+TIP) EB1, and its interacting protein p150(Glued). Based on siRNA knockdown studies, live cell imaging, and recovery of fluorescence after photobleaching (FRAP) experiments, we propose that preferential tethering of microtubule plus-ends at the adherens junction promotes delivery of connexin hemichannels directly to the cell-cell border.

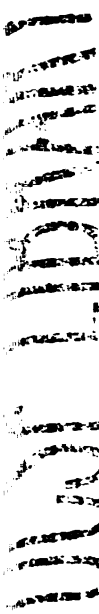

RUNNING TITLE:

Microtubule +TIPs target Cx43 to adherens junctions

INTRODUCTION

Gap junctions are formed by the serial coupling of hemichannels of adjacent cells, and allow direct sharing of ions and small cytoplasmic molecules between cells. They are important for organ formation, cardiac action potential propagation, distribution of small molecules and ions among hepatocytes or glial cells, synchronization of neuronal circuits by electrical synapses, and sharing of antigenic peptides between virally-infected cells and professional antigen-presenting cells (Bennett and Zukin, 2004; Cruikshank et al., 2005; Gallagher and Benfey, 2005; Giepmans, 2004; Heath and Carbone, 2005; Rudy and Shaw, 1997; Sohl et al., 2005). It is important to understand how the hemichannels are brought to the cell-cell border for gap junction formation, since the development and physiological functions of many tissues depend on proper placement of gap junctions.

Extensive studies of gap junctions have delineated their molecular composition and the consequences of abnormal gap junction formation. Each hemichannel is a hexamer of connexin protein, the most common isotype being Connexin43 (Cx43). Gap junctions reside at cell-cell borders, where their density is of critical importance. In the heart, for example, gap junctions are concentrated at the intercalated disc joining the ends of cardiomyocytes, where they ensure propagation of action potentials (Gros and Jongsma, 1996; Shaw and Rudy, 1997). Altered Cx43 gap junction distribution in cardiomyocytes following cardiac ischemia contributes to the pathogenesis of malignant ischemic arrhythmias (Kaprielian et al., 1998; Kleber et al., 1987; Peters et al., 1997; Shaw and Rudy, 1995; Shaw and Rudy, 1997). Preventing or reversing this process offers a strategy to repair damaged heart (Abraham et al., 2005; Menasche et al., 2003;

Reinecke et al., 2004). Understanding the molecular mechanism of gap junction localization at the cell-cell border, therefore, is important not only for addressing the basic cell biological question of gap junction formation, but also for the development of treatments for life-threatening diseases.

A model for gap junction formation has emerged from biochemical and cell biological studies over the past decade. The half-life of Cx43 protein is between one and three hours (Beardslee et al., 1998; Darrow et al., 1995; Laird et al., 1991), indicating that gap junction trafficking is a dynamic process. Gap junction hemichannels are packaged in vesicles that emerge from the Golgi and reach the cortical membrane via microtubules, even for isolated cells not in contact with other cells (Jordan et al., 1999; Lauf et al., 2002). The point of insertion can be anywhere on the membrane surface (Jordan et al., 1999), and clusters of gap junctions known as plaques form at cell-cell borders. FRAP studies of cortical hemichannels and plaque dynamics show that connexin hemichannels can float freely within the cortical membrane (Lauf et al., 2002). Over a time course of tens of minutes or hours, newer hemichannels are evident first at the plaque perimeter and later on throughout the plaque (Gaietta et al., 2002; Lauf et al., 2002). Based on these observations, the commonly held view of gap junction plaque formation is that, after their microtubule-mediated delivery to the cortical membrane, hemichannels diffuse laterally within the membrane to cell-cell border regions. In this model, hemichannels that coalesce at the periphery of the plaques then move inwards, and those reaching the center of the plaque become internalized for degradation as annular gap junctions (Laird, 2005; Segretain and Falk, 2004).

The current model is the simplest scenario that could account for the experiments reported thus far, but it does not explain how plaques occur at specific locations of the cell membrane. While junctional proteins such as ZO-1 may retain connexins (Giepmans and Moolenaar, 1998), few other connexin-binding proteins have been identified. In multiple tissues, gap junctions colocalize with adherens junctions formed by cadherins, including at the cardiac intercalated disc. The adherens junctions are assembled at the intercalated discs prior to the establishment of a Cx43 gap junction plaque (Angst et al., 1997; Kostin et al., 1999). And mislocalized Cx43 plaques in ischemic myocardium are associated with similarly mislocalized adherens junctions (Matsushita et al., 1999). The importance of cadherins in gap junction formation is underscored by the finding that transfection of E-cadherin into gap junction-incompetent cells allows the transfected cells to form functional gap junctions (Mege et al., 1988). Moreover, N-cadherin knockout mice cannot form gap junctions (Luo and Radice, 2003), and conditional knockout of N-cadherin in the heart causes poor expression and mislocalization of gap junctions, leading to arrhythmogenic death (Li et al., 2005).

Since Cx43-laden microtubules must interact with the plasma membrane to deliver the hemichannels and cadherin-mediated signaling is implicated in microtubule regulation (Jamora and Fuchs, 2002), we wondered whether plaque formation involves microtubule interaction with the adherens junction. We looked into the possible involvement of the microtubule plus-end tracking proteins (+TIPs), because they control microtubule dynamics and could be captured by membrane-associated proteins (Akhmanova and Hoogenraad, 2005; Mimori-Kiyosue et al., 2005). Among the +TIPs, the dimeric EB1 associates directly with the plus ends of microtubules, and has dual

binding sites for a number of proteins, including p150(Glued), a component of the dynein/dynactin complex. The dynein/dynactin complex, in turn, has been implicated in tethering microtubules at adherens junctions (Chausovsky et al., 2000; Ligon et al., 2001).

In this study, we analyzed plaques formed by fluorescently tagged Cx43 in HeLa cells that do not express endogenous Cx43. Our FRAP studies revealed that, within a few minutes following the photobleaching of a plaque and its surrounding area, there was rapid replenishment of fluorescent Cx43 within the plaque but not in the bleached surrounding area. In addition, this recovery was sensitive to reagents that alter microtubule dynamics. Time-lapse imaging of live cells expressing fluorescently tagged EB1 and Cx43 further showed that microtubule plus-ends approached the plaque more frequently than the rest of the cortical membrane and remained at the plaque for longer periods of time. Moreover, siRNA knockdown of EB1, its binding partner p150(glued), and the adherens junction protein β-catenin, interfered with gap junction plaque formation. Finally, plaque formation was also disrupted by the application of peptides that compromise homophilic cadherin interactions at the adherens junction. Thus, besides lateral diffusion of Cx43 on the cell membrane, mammalian cells use +TIPs for targeted delivery of Cx43 to form gap junction plaques that are spatially coincident with adherens junctions, a mechanism that could restrict intercellular communication to cells of the same tissue type.

Results

Microtubules Extend Directly to Gap Junction Plaques at the Cell-Cell Border

We began by observing HeLa cells transiently transfected with a construct containing connexin43 tagged with yellow fluorescent protein (Cx43-YFP). In isolated cells, Cx43-YFP was concentrated in the perinuclear Golgi, but was translocated to the cell-cell border when two cells were in contact. Imaging isolated cells with low levels of Cx43-YFP expression indicated that Cx43-YFP is localized to microtubules, consistent with the documented role of microtubules in transporting hemichannel-containing vesicles to the cortical membrane (Giepmans et al., 2001; Lauf et al., 2002) (Figure 1A). To avoid artifacts of microtubule morphology due to fixation, we used deconvolution software to resolve the distribution of GFP-□-tubulin and Cx43-RFP in live HeLa cells (Figure 1B). There was a strong correlation between cortical microtubule ends and Cx43 plaques. Within sparsely populated plaques, it is possible to resolve individual microtubules and their orientation and location relative to Cx43 distribution. In such plaques, the regions of highest Cx43 intensity directly overlayed with the tips of microtubules contacting the cortical membrane (Figures 1C, 1D).

Microtubules Allow Rapid Connexin Delivery to Gap Junction Plaques

Having observed a correlation between the ends of microtubules and gap junction plaques (Figure 1), we asked if microtubules might contribute to directed delivery of

connexin to gap junction plaques. After transfecting HeLa cells with Cx43-YFP, we used a confocal microscope in FRAP studies to follow Cx43-YFP dynamics in live cells. Entire plaques and their surrounding areas were subjected to fluorescence photobleaching, and the recovery of fluorescence was monitored every 20 s for five minutes, revealing rapid repopulation of the plaque in its original geometry. Plaque reappearance was inhibited by 100 μM nocodazole, which depolymerizes microtubules, and 10 μM Taxol, which stabilizes microtubules but prevents growth at the plus end. Because the cell pairs showed a range of plaque geometries, we performed the bleaching experiments in two different ways: by bleaching and recording in the horizontal XY plane for horizontal plaques (data not shown) and by bleaching in the horizontal plane and recording in the vertical plane for vertically aligned plaques (Figure 2A). There were no significant differences in recovery kinetics between these two FRAP techniques. Pooled data from both revealed rapid plaque repopulation, while regions surrounding the plaque acquired much lower levels of fluorescence (Figure 2B), suggesting direct delivery of connexin to the plaque region by a process dependent on microtubule dynamics.

To quantify the efficiency of plaque formation, we developed an assay with fixed cells to compare the concentration of cortical connexin at the cell-cell border under different conditions. HeLa cells transfected with Cx43-YFP were plated on coverslips and allowed to form plaques over 18-24 hrs. Cells were then treated with nocodazole (30 min) or Taxol (2 hrs), washed, and fixed before imaging by fluorescence microscopy. Isolated pairs of Cx43-YFP expressing cells were identified (Figure 3A), and the percent of the cell-cell border with cortical connexin plaques was recorded (Figure 3B), revealing

a marked reduction in the concentration of Cx43 at the cell-cell border after treatment with nocodazole or Taxol.

Preferential and prolonged association of the microtubule plus ends with plaques at the cell-cell border

To test whether microtubule plus ends preferentially interact with the cortical membrane in the vicinity of connexin plaques, we co-transfected HeLa cells with Cx43-RFP and fluorescently tagged EB1, a marker for rapidly growing microtubule plus-ends, and monitored the frequency and duration of the appearance of microtubule plus-ends at different regions of the cell cortex (Figure 4A). By comparing time series of EB1 dynamics at Cx43 plaques, at regions of cell-cell border without Cx43 plaques, or at cell edges not in contact with other cells (Figure 4B, Supplemental Data), we found that EB1-capped microtubules grew towards the connexin plaque three times more frequently than their approach to the cortical membrane not in contact with other cells, and that each microtubule lasted on average 3.5 times longer when it was within 2 μm of a plaque (Figure 4C). Microtubule plus-end orientation (frequency of cortical approaches) and stabilization (duration of appearance near the cortex) were significantly greater at plaques than non-plaque regions of the cortical membrane (Figure 4C). The higher frequency and longer duration of connexin-laden microtubules reaching the plaque (Figure 4) may account for the rapid repopulation of plaques after photobleaching (Figure 2).

EB1 siRNA Knockdown Disrupts Gap Junction Plaque Formation

Next, we asked whether Cx43 plaque formation requires specific proteins that interact with the microtubule plus ends. Because Taxol can dissociate EB1 from microtubule plus ends (Morrison et al., 1998), we tested the involvement of EB1 in plaque formation by exposing HeLa cells to EB1 siRNA for 24 hours before transfection with Cx43-YFP. Knockdown of EB1 protein caused a substantial reduction of connexin plaque formation at the cell-cell border (Figures 4D and 5C). Taken together with our finding of a concentration of EB1 comets near the plaque (Figure 4C), the dependence of plaque formation on endogenous EB1 suggests that EB1 at the microtubule plus ends may interact with proteins at the cell-cell border and enhance targeted delivery of Cx43.

EB1-interacting protein p150(Glued) and β-catenin are required for Cx43 Delivery to the Plaque

The cadherin-based adherens junction (AJ) is a highly efficient "glue" that binds cells together, and may also regulate the microtubule cytoskeleton (Chausovsky et al., 2000; Waterman-Storer et al., 2000). Moreover, β-catenin, which is the cytoplasmic binding partner of cadherin, binds dynein (Ligon et al., 2001). The dynein/dynactin complex is a potential cortical anchor of microtubules (Fuchs and Karakesisoglou, 2001), since p150(Glued) in the dynactin complex has a binding domain for EB1 (Askham et al., 2002; Hayashi et al., 2005). Therefore, we tested for the involvement of p150(Glued) and β-catenin in forming gap junction plaques.

Immunocytochemistry was performed on HeLa cells expressing Cx43-YFP with or without co-expression of p150(Glued) siRNA (Figure 5A). In the control cells,

p150(Glued) was present in a cytoplasmic pool and was also found at the cell-cell border, near the plaques formed by Cx43-YFP. Furthermore, siRNA knockdown of p150(Glued) greatly decreased Cx43-YFP accumulation at the cortical membrane of the cell-cell border (Figure 5A, bottom row, and Figure 5C). These findings are consistent with the role of p150(Glued)-containing dynein/dynactin in anchoring microtubules at the cell-cell border (Dujardin and Vallee, 2002; Koonce and Samso, 2004). Dynein/dynactin may thus help Cx43-containing vesicles on microtubules to reach the cortex and offload connexin to the cortical membrane at the cell-cell border.

If p150(Glued) connects the microtubule plus-end to the adherens junction, β-catenin is likely to constitute part of the cortical anchor, given that both β-catenin and the p150(Glued)-containing dynactin complex bind dynein. Indeed, immunocytochemistry of HeLa cells transfected with Cx43-YFP, with or without coexpression of β-catenin siRNA (Figure 5B), revealed that not only was Cx43-YFP colocalized with β-catenin, but siRNA knockdown of β-catenin also significantly reduced plaque formation (Figures 5B and 5C).

We then examined the distribution of endogenous p150(Glued), β-catenin and Cx43 in adult ventricular cardiomyocytes, and found that they colocalized at the intercalated discs. Colocalization of cardiac Cx43 and β-catenin (Figure 5D) is consistent with the observation that the intercalated disc is rich in both gap junctions and adherens junctions. The colocalization of p150(Glued) and Cx43 at the intercalated disc, both in isolated cardiomyocytes and at intact cell-cell borders of isolated pairs (Figure 5E), indicates that p150(Glued) is poised in native heart cells to connect cadherins with microtubule plus ends for Cx43 delivery.

Homophilic cadherin interactions are required for plaque formation

Having found that EB1, p150(Glued), and β-catenin are crucial for targeting Cx43 to the cell-cell border, we wondered whether plaque formation also depends on cadherin, which binds β-catenin via its cytoplamic domain and engages in homophilic interactions via its extracellular domain. In order to test if functional N-cadherin on the cell membrane contributes to the formation of gap junction plaques, we applied a peptide that blocks homophilic intercellular N-cadherin interactions (Frenzel and Johnson, 1996) to HeLa cells already transfected with Cx43-YFP and adherent on coverslips. This treatment disrupted most cell-cell contacts, although isolated cell pairs could still be found (Figure 6A). Cells were fixed 24 hr after exposure to the peptides, and the cortical connexin at the cell-cell border was quantified for isolated cell pairs (Figure 6B), revealing that N-cadherin blocking peptides caused a major reduction of connexin deposition at the cell-cell border. Another way to disrupt cadherin-mediated adherens junction formation is to induce actin depolymerization (Ko et al., 2001). We found that actin depolymerization agents also reduced Cx43 plaque formation (not shown). Taken together, these observations suggest that homophilic cadherin interactions transmit the signal of cell-cell contact to induce targeted Cx43 delivery.

DISCUSSION

It is important to characterize gap junction formation and maintenence at the cell biological level, because a mechanistic understanding of this process will inform studies

of tissue organization and cell migration during development, electrical coupling between excitable cells such as neurons and cardiomyocytes, and other intercellular communications that are critical to the renal, hepatic, immune, cardiovascular, reproductive and nervous systems. In this study we found that dynamic microtubules preferentially approach cortical membrane regions containing gap junctions (Figures 1 and 4). Moreover, plaque formation at the cell-cell border depends on the +TIP EB1, p150(Glued) and β-catenin (Figures 4D and 5) as well as homophilic interaction between cadherins (Figure 6), raising the intriguing possibility that preferential attachment of microtubules to adherens junctions results in targeted delivery of connexin directly to the cell-cell border (Figure 7). This novel mechanism could account for the fast delivery of fluorescent Cx43 to plaques in our FRAP experiments and the dependence of this process on microtubule dynamics (Figures 2, 3). Below, we discuss how our findings may be reconciled with earlier studies which argue that gap junction proteins first reach the cell membrane uniformly via microtubule-mediated transport and then diffuse laterally to the cell-cell border to form plaques. We then consider the implications of the novel finding that connexins are directly targeted to the cell-cell border.

Microtubule Delivery of Gap Junction Proteins Directly to Plaques at Cell-cell Border

Although we found that microtubules are uniformly laden with connexin (Figure 1A), most microtubules do not reach the cellular cortex. However, regions containing gap junction plaques always have at least one associated microtubule (Figure 1B), and these regions appear to interact with EB1-capped microtubules more frequently and for a

greater duration than other regions of the cell cortex (Figure 4C). These observations raise the possibility of targeted, microtubule-mediated, delivery of connexin.

If microtubules deliver Cx43 directly to the plaques, fluorescent Cx43 would repopulate bleached plaques with a distribution that mimics the pre-bleach plaque morphology, rather than appearing first at the plaque perimeter. Indeed, our FRAP studies revealed a fast repopulation (time constant of about 2 min) that restored the original plaque morphology (Figure 2). Moreover, microtubule disruptors nocodazole and Taxol worked immediately in the post-bleach period to retard recovery of the plaque, indicating that the fast repopulation of a plaque involves microtubule-mediated transport from the cell interior, rather than simply lateral diffusion from unbleached cell membrane. As nocodazole and Taxol do not promote endocytosis (Hamm-Alvarez et al., 1996), it is also unlikely that selective retention or increased endocytosis accounts for the differences in recovery rates.

How might our findings be reconciled with experiments that led to the lateral diffusion model of gap junction plaque formation? Previous studies have documented fusion between Cx43-containing vesicles and the plasma membrane of isolated cells, and the presence and mobility of tagged Cx43 on the non-junctional surface of HeLa cells (Jordan et al., 1999; Lauf et al., 2002). However, gap junction delivery to the plasma membrane, even in the lateral diffusion model, depends not only on the potential for Cx43 hemichannels to arrive at non-contact regions (Jordan et al., 1999; Lauf et al., 2002), but also on the relative frequency of microtubule approaches to the cell-cell border versus other regions of the plasma membrane (Figure 4C). Taken together with the colocalization of Cx43 plaques with β-catenin (Figure 5B,D), studies to date are

consistent with microtubule-based transport that delivers connexin to the adherens junction to a greater extent than to the rest of the cell membrane.

Plaque repopulation has also been investigated using both FRAP and successive labeling of tetracysteine-tagged Cx43 with different fluorophores (Gaietta et al., 2002; Lauf et al., 2002). In the FRAP studies, thirty minutes to several hours after bleaching a portion of the plaque, YFP-tagged Cx43 was observed to accumulate at plaque edges (Lauf et al., 2002). The time resolution and the low fluorescence sensitivity necessitated by the imaging of the remaining unbleached plaque in this study would have precluded the detection of rapid plaque repopulation within a few minutes (Figure 2). In the tetracysteine labeling studies (Gaietta et al., 2002), newer Cx43 appears at the perimeter of the plaque when examined 4-8 hours after the initial Cx43 labeling, though there appear to be low levels of newer Cx43 within the central "old" plaques. Given that gap junctions are internalized at the center of a plaque within several hours (Laird, 2005), it seems likely that the size of the plaque is maintained by the formation of new plaques as membranes at the plaque perimeter come into close apposition. The bright rim of fluorescent Cx43 observed in the earlier studies could, under this scenario, represent new plaques formed entirely by freshly delivered Cx43.

It has never been directly shown that tagged Cx43 from non-border regions of the cell membrane makes its way to existing plaque, though lateral diffusion most likely accounts for the residual recovery after photobleaching following nocodazole treatment in previous studies (Lauf et al., 2002; Thomas et al., 2005) and in ours. In our FRAP studies, we bleached the entire plaque and observed repopulation at 20 s intervals, revealing a rapid, microtubule-dependent repopulation of the original plaque (Figure 2).

We further showed that homophilic cadherin-cadherin interaction is important for gap junction formation, using peptides that block the extracellular domain of cadherin (Williams et al., 2000). The peptide, unlike cadherin knockdown with siRNA, prevents homophilic cadherin interactions without interfering with cadherin placement on the cell surface. It thus appears that microtubule-mediated direct targeting of connexin to adherens junctions contributes significantly to gap junction formation. These findings are consistent with previous reports of calcium dependence of cell-cell communication (Davidson et al., 1984; Loewenstein, 1967), attributed to an adhesion event and the cadherin family of proteins (Meyer et al., 1992; Musil and Goodenough, 1990; Takeichi, 1990). In agreement with reports that gap junction plaque formation is preceded by cell-cell contact and homophilic cadherin-cadherin interaction (Angst et al., 1997; Hertig et al., 1996; Kostin et al., 1999), our results support a model for targeted Cx43 delivery involving more frequent and longer lasting microtubule attachment to the adherens junction. This mechanism of plaque localization at adherens junctions places cell-cell communication channels precisely at the locations of cell-cell contact, though it does not preclude microtubule-mediated transport of connexin to non-border regions of the plasma membrane generally, or lateral diffusion of connexin within the cell membrane.

Other protein interactions of potential relevance include a recently reported interdependence between Cx43 and N-cadherin surface expression (Wei et al., 2005). This phenomenon, however, does not appear to affect adherens junction formation between HeLa cells lacking endogenous connexin. The ability of Cx43 to bind microtubules (Giepmans et al., 2001) could also contribute to microtubule interactions at

plaques, perhaps after their capture via cadherin-associated proteins and +TIPs, as discussed below.

Microtubule +TIP involvement in Gap Junction Plaque Formation

Our FRAP studies revealed that nocodazole and Taxol both cause disruption of the fast repopulation of Cx43 plaques (Figure 2). While nocodazole depolymerizes microtubules, Taxol stabilizes them, but disrupts their interactions with EB1 (Nakata and Hirokawa, 2003), which normally associates with rapidly growing microtubule plus ends (Schuyler and Pellman, 2001). We found that EB1-capped microtubules interact more frequently, and for a longer period of time, at plaques than at non-plaque plasma membrane (Figure 4C), and that EB1 knockdown decreases plaque formation at the cell-cell border (Figures 4D and 5C), thereby implicating EB1 as a major player in gap junction formation.

How might the plus end binding protein EB1 facilitate connexin delivery? The C-terminus of EB1 binds the p150(glued) subunit of the dynein/dynactin complex (Askham et al., 2002; Hayashi et al., 2005). Moreover, dynein/dynactin localizes with adherens junctions at cell-cell contact points through direct binding with β-catenin (Ligon et al., 2001). In this manner, dynein/dynactin may serve as an anchor for microtubules at the adherens junction. We found that knockdown of p150(Glued) or β-catenin disrupts the formation of gap junction plaques (Figure 5). While it is possible that targeted connexin delivery involves other cytoskeletal elements, +TIPs, and cortical proteins, this study identifies some key components of functional importance: the microtubule plus end binding protein EB1, the EB1-binding protein p150(Glued) as part of the dynein/dynactin

complex that could tether microtubules to the adherens junction, and β-catenin as the cytoplasmic enforcer of homophilic cadherin-cadherin interaction. Most likely, actin also acts as an important initial sensor of cell-cell interaction and guides the localization of adherens junctions (Drees et al., 2005), with assistance from Rho-GTPases (Noren et al., 2001). It will be interesting to determine how other proteins associated with the cytoskeleton or cell-cell junctions may contribute to targeted delivery of gap junction proteins.

Implications for Developmental Biology and Cancer

The proposed model for connexin trafficking suggests a mechanism for membrane protein localization at specific regions of the plasma membrane, and a pathway of particular interest in developmental biology. Cadherin-cadherin interactions are known to affect cell sorting during tissue development, based on preferential adhesion between cells expressing the same cadherin type(s) or similar levels of cadherin (Wheelock and Johnson, 2003). Our findings suggest that connexin reaches the adherens junction via direct, microtubule-mediated delivery, so that gap junctions may form preferentially between cell types expressing the same type of cadherin. Mutations in Cx43 are associated with deafness, cataracts, germ cell development defects, oculodentodigital dysplasia and cardiac outflow abnormalities (Wei et al., 2004). It would be interesting to explore the potential involvement of microtubule-mediated Cx43 delivery to adherens junctions in these developmental processes and pathological conditions.

Cancer cells tend to lose gap junction communication normally maintained between non-malignant cells and, once they invade other tissues, generally form gap junctions only with other cancer cells. Just as loss of E-cadherin or upregulation of N-cadherin can lead to tumor invasiveness (Mareel and Leroy, 2003), both gain and loss of connexin expression are associated with cancers. Cx43 expression is down-regulated in a variety of cancers, including prostate, lung, bladder, and cervical cancers, as well as gliomas and melanomas (Mesnil, 2002). Reduced gap junction coupling may help cells to complete malignant transformation by limiting the spread of Ca^{2+}-mediated apoptosis (Krutovskikh, 2002), while overexpression of Cx43 may lead to increased invasiveness of human glioblastomas (Oliveira et al., 2005). At present, there are few data linking cadherin to Cx43 in malignant cells. Testing for a correlation between Cx43 targeting and cadherin-based adherens junctions may be a first step towards developing strategies to limit tumor growth and metastasis.

Implications for Channel Trafficking and Cardiac Disease

Cardiac excitation is an iterative process, whereby inward current depolarizes the plasma membrane of a cardiomyocyte and initiates an action potential, which, in turn, drives a depolarizing current that spreads to adjacent cardiomyocytes through gap junctions. The flow of current for proper cardiac action potential propagation requires that electrical coupling through gap junctions be both robust and oriented along the long axis of cardiac fibers. Decreased or disorganized gap junction coupling due to myocardial ischemia leads to ventricular arrhythmias of sudden cardiac death (330,000 annual U.S. cases) (Peters et al., 1997; Thom et al., 2006) and contributes to the

pathogenesis of congestive heart failure (550,000 new U.S. cases and 53,000 deaths annually) (Kaprielian et al., 1998; Thom et al., 2006; Yamada et al., 2003). In addition, disorganization of gap junctions in ischemic myocardium is preceded by disorganized adherens junctions (Matsushita et al., 1999). Our model for +TIPs-mediated gap junction trafficking suggests that adherens junction disruption contributes directly to the rearrangement of gap junction distribution. Furthermore, we provide a mechanism for gap junction localization that will likely apply to the subcellular targeting of other membrane proteins.

EXPERIMENTAL PROCEDURES

Cell Culture and Transfection

HeLa cells were cultured at 37°C and 5% CO_2 in MEM Eagle's Medium with Earle's BSS, supplemented with 10% Fetal Bovine Serum, Penicillin/Streptomycin, and Non-Essential Amino Acids (UCSF Cell Culture Facility). Cells were transfected with Cx43 in pEYFP (Jordan et al., 1999) (courtesy of Dale Laird) using FuGene 6 (Roche, Indianapolis) according to the manufacturer's instructions. Cells were cultured for 18-48 hours before use in live-cell or fixed cell imaging. For transfection of siRNA, either FuGene 6 or siRNA X-tremeGene (Roche, Indianapolis) was used with pooled siRNA (Dharmacon, Lafayette, CO), added to HeLa cells 24 hrs prior to transfection with Cx43-YFP.

Immunostaining and Imaging of Fixed Cells

Cells were cultured on 12 mm coverslips (Warner Instrument Corp., Hamden, CT) pre-coated with bovine fibronectin (50 □g/ml) and transfected. Taxol (10 μM) and nocodazole (100 μM) (Sigma-Aldrich) were applied for 2 hr and 30 min, respectively, prior to fixation. N-Cadherin peptide N-Ac-INPISGQ-NH_2 (WILLIAMS ET AL., 2000) (10 mM, Anaspec, San Jose, CA) was applied shortly after transfection. Cells were fixed with methanol (-20°C) for 5 min, permeabilized with 0.2% Triton X-100 in PBS, and blocked in PBS + 0.1% Triton X-100 + 5% goat serum or donkey serum (Jackson ImmunoResearch Laboratories, Inc., West Grove, PA). Primary antibodies were diluted into PBS + 0.1% Triton X-100 + 2% serum and incubated at room temperature for 1 hr at the following dilutions: mouse anti-β-catenin (1:500, Santa Cruz Biotechnology, Santa Cruz, CA), mouse anti N-Cadherin (1:500, BD Transduction Laboratories, San Jose, CA), mouse anti-α-tubulin (1:1000, Sigma-Aldrich, St. Louis, MO), mouse anti-EB1 (1:1000, BD Transduction Laboratories), mouse anti-p150(glued) (1:100, BD Transduction Laboratories), rabbit anti-connexin 43 (1:400, Sigma-Aldrich). Coverslips were washed in PBS, followed by incubation with goat or donkey anti-mouse and anti-rabbit secondary antibodies, conjugated to Alexa 488, Cy3 or Cy5 (Jackson ImmunoResearch Laboratories, 1:1000 or 1:500 dilution in PBS + 0.1 % Triton X-100 + 2 % serum) with 1 μg/ml Hoechst 33342 (Invitrogen, Carlsbad, CA) for 1 hr at room temperature. Cells were mounted on to microscope slides with GelMount aqueous mounting medium (Biomeda Corp., Foster City, CA). Fixed cells were imaged with either a Nikon E800 epifluorescence microscope equipped with a Spot charge-coupled device digital camera and software (Diagnostic Instruments) or a Nikon TE2000-U

inverted fluorescence microscope with Photometrics Coolsnap HQ CCD camera and MetaVue software (Molecular Devices, Sunnyvale, CA).

Live Cell FRAP Imaging

For live-cell imaging, cells were cultured and transfected on 18 mm coverslips (Fisher, Hampton, NH) pre-coated with fibronectin. Prior to imaging, coverslips were transferred to a custom-made, temperature-controlled, closed chamber stage (Brook Industries, Lake Villa, IL), and maintained in Hanks' BSS + 5 % Fetal Bovine Serum (UCSF Cell Culture Facility) at 37°C. Plaques were identified at the border between two cells and pre-bleach images in the XYplane and along the Z-axis (stack of line scans every 0.4 μm) were recorded, followed by bleaching for 40 seconds in the XY plane and acquisition of a new Z-plane image every 20 s for 5 min. Taxol and nocodazole (Sigma-Aldrich) were diluted in DMSO and used at 10 μM and 100 μM, respectively. Images were collected on a Zeiss LSM Laser Confocal microscope with a 63x objective, and analyzed with MetaVue software (Molecular Devices, Sunnyvale, CA).

Quantification of Connexin Plaque at Cell-Cell Border

Approximately 20 cell pairs, in robust contact with each other but not touching other cells, were identified for each condition. Exposure time was fixed for each fluorophore. With Metavue software, the common border was outlined in each cell pair, and the percentage of Cx43-YFP plaque was calculated by dividing the number of pixels over a pre-set intensity threshold by the number of pixels in the border. Percentage of cortical connexin at the border was compared among various conditions and evaluated for statistical significance by one-tailed Student's t-test.

Imaging of Microtubule Plus-End Dynamics

HeLa cells plated on fibronectin-coated coverslips were co-transfected with Cx43-mRFP and GFP-EB1 and allowed to express the fusion constructs for 16-20 hrs before imaging. Cells were placed in a custom-built, temperature-controlled chamber and maintained at 35°C throughout the course of the experiment. Cx43 plaques were identified at the border between two cells, and the dynamics of GFP-EB1 fluorescence imaged using a Nikon TE2000-U inverted fluorescence microscope with Photometrics Coolsnap HQ CCD camera and MetaVue software. Images were captured every 2-5 s for 3-4 min with a 100x objective. The time series were then analyzed by drawing a semicircle of 2 μm, with the flat side against the cell-cell border or a non-border edge of the cell, and counting the number of plus-ends that appeared in the semicircle per minute and the duration of each plus-end. These data were then pooled and evaluated for statistical significance by one-tailed Student's t-test.

Preparation of Isolated Cardiomyocytes

Rat ventricular myocytes were isolated from adult SD rats (200 to 300 g, Charles River) after dissociation with collagenase type 2 (Worthington, Lakewood, NJ), with previously described methods (Hu et al., 2003). Attachment to coverslips, fixation, and immunostaining followed the same protocols as those used for HeLa cells (above).

ACKNOWLEDGEMENTS

We are grateful to Dr. Dale Laird (Ontario) for the Cx43-YFP construct, Dr. Bert Vogelstein (Johns Hopkins) for the GFP-EB1 construct, and to Dr. Xiang Qian (Jan Lab) for technical assistance with cardiomyocytes, and to other members of the Jan Lab for comments on this manuscript. This work was supported by National Institutes of Health Grants NIMH 63981 (LYJ), NHLBI 075449 (RMS), and American Heart Association Grant 0475022N (RMS). Y.-N.J. and L.Y.J. are Howard Hughes Medical Institute Investigators.

FIGURE LEGENDS

Figure 1. Microtubules are Associated with Cx43 Plaques at the Cell-Cell Border.

(A) Confocal image (100X) of a fixed isolated HeLa cell transfected with Cx43-YFP (green) and stained with antibody to α-tubulin (red), selected for low Cx43-YFP expression to visualize its distribution on microtubules.

(B) Deconvolution of live cell images of HeLa cells transfected with □-tubulin-GFP (green) and Cx43-RFP (red).

(C) Enlargement of cell-cell border region from (B), right cell on top.

(D) Manually traced composite cell-cell border region of a deconvolved 1.5 □m stack of images (consisting of fifteen 100 nm planes). Microtubules of right cell (red), microtubules of left cell (blue), Cx43 plaques (green).

Figure 2. Cx43 Plaques are Repopulated in a Microtubule-dependent Manner.

(A) FRAP procedure and plaque repopulation with Cx43-YFP in the presence and absence of nocodazole and Taxol.

(B) Recovery of fluorescence quantified and averaged for images viewed at either the XY or XZ plane. Filled symbols, recovery within plaques; open symbols, recovery in surrounding non-plaque regions.

Figure 3. Microtubule Disruptors Limit Plaque Formation.

(A) HeLa cells transfected with Cx43-YFP (green) immunostained with anti-□-tubulin (red) and Hoechst 33342 nuclear stain (blue).

(B) Quantification of nocodazole and Taxol effects on Cx43 plaque formation at cell-cell borders (* $P < 0.001$).

Figure 4. Cortical EB1 dynamics are different at Cx43 Plaques.

(A) Live HeLa cells transfected with Cx43-RFP (green) and GFP-EB1 (black). A growing plaque is chosen (left side of bottom cell) and 2 μm radius semicircular regions drawn at the plaque and two regions of non-plaque cortical membrane (red semicircles, bottom panel).

(B) EB1 dynamics within each semicircular region.

(C) Quantification of EB1 events at Cx43 plaques (n=17 cells), at cell-cell borders without plaque (n=13 cells), and at non-contacting cell edges (n=17 cells). (* $P < 0.001$, ** $P < 0.0001$)

(D) HeLa cells transfected with Cx43-YFP with (bottom row) and without (top row) exposure to EB1 siRNA (quantification in Figure 5C).

Figure 5. Plaque formation Depends on p150(Glued) and β-catenin.

(A) p150(Glued) (red) immunostaining in HeLa cells expressing Cx43-YFP (green) without and with siRNA knockdown.

(B) β-catenin (red) immunostaining in HeLa cells expressing Cx43-YFP (green) without and with siRNA knockdown.

(C) Quantification of Cx43 plaque (percent of cell-cell border) after siRNA knockdown of EB1 (n=17), p150(Glued) (n=19), and β-catenin (n=20). * $P<0.0001$.

(D) β-catenin and Cx43 co-localization at the two intercalated discs (ID) of a single binucleated (N) adult rat cardiomyocyte.

(E) p150(Glued) and Cx43 co-localization at the ID of adult rat cardiomyocyte.

Figure 6. Gap Junction Plaques Depend on Homophilic Cadherin Interactions.

(A) Immunostaining of Cx43-YFP-transfected (green) control cells (first row) and cells exposed to cadherin blocking peptides (second row). Nuclei (blue) and N-cadherin (red).

(B) Quantification of Cx43 plaques (percent at the cell-cell border) for control cell pairs (n=27), and cell pairs exposed to N-cadherin blocking peptide (n=25). * $P<0.0001$.

FIGURE 7. MODEL OF DIRECTED CX43 TARGETING TO ADHERENS JUNCTIONS

(A) Proposed paradigm for gap junction plaque formation is based on localized cortical capture of microtubules.

(B) Cortical capture involves interaction between the plus end binding protein EB1 and p150(Glued) of the dynein/dynactin complex, which in turn attaches to N-cadherin via β-catenin, resulting in focal delivery of Cx43 hemichannels directly to plaques at the cell-cell border.

Figure S1. EB1 Dynamics at Developing Plaque.

Movie of GFP-EB1 (black) imaged at same region of cell-cell border from Figure 4. Movie consists of 50 frames captured at 3 second intervals (3 minutes imaging time).

Playback is 30x faster. Still frame on right is Cx-RFP (green) signal provided for reference. Scale bar is 4 □m.

REFERENCES

Abraham, M. R., Henrikson, C. A., Tung, L., Chang, M. G., Aon, M., Xue, T., Li, R. A., B, O. R., and Marban, E. (2005). Antiarrhythmic engineering of skeletal myoblasts for cardiac transplantation. Circ Res *97*, 159-167.

Akhmanova, A., and Hoogenraad, C. C. (2005). Microtubule plus-end-tracking proteins: mechanisms and functions. Curr Opin Cell Biol *17*, 47-54.

Angst, B. D., Khan, L. U., Severs, N. J., Whitely, K., Rothery, S., Thompson, R. P., Magee, A. I., and Gourdie, R. G. (1997). Dissociated spatial patterning of gap junctions and cell adhesion junctions during postnatal differentiation of ventricular myocardium. Circ Res *80*, 88-94.

Askham, J. M., Vaughan, K. T., Goodson, H. V., and Morrison, E. E. (2002). Evidence that an interaction between EB1 and p150(Glued) is required for the formation and maintenance of a radial microtubule array anchored at the centrosome. Mol Biol Cell *13*, 3627-3645.

Beardslee, M. A., Laing, J. G., Beyer, E. C., and Saffitz, J. E. (1998). Rapid turnover of connexin43 in the adult rat heart. Circ Res *83*, 629-635.

Bennett, M. V., and Zukin, R. S. (2004). Electrical coupling and neuronal synchronization in the Mammalian brain. Neuron *41*, 495-511.

Chausovsky, A., Bershadsky, A. D., and Borisy, G. G. (2000). Cadherin-mediated regulation of microtubule dynamics. Nat Cell Biol *2*, 797-804.

Cruikshank, S. J., Landisman, C. E., Mancilla, J. G., and Connors, B. W. (2005). Connexon connexions in the thalamocortical system. Prog Brain Res *149*, 41-57.

Darrow, B. J., Laing, J. G., Lampe, P. D., Saffitz, J. E., and Beyer, E. C. (1995). Expression of multiple connexins in cultured neonatal rat ventricular myocytes. Circ Res *76*, 381-387.

Davidson, J. S., Baumgarten, I. M., and Harley, E. H. (1984). Effects of extracellular calcium and magnesium on junctional intercellular communication in human fibroblasts. Exp Cell Res *155*, 406-412.

Drees, F., Pokutta, S., Yamada, S., Nelson, W. J., and Weis, W. I. (2005). Alpha-catenin is a molecular switch that binds E-cadherin-beta-catenin and regulates actin-filament assembly. Cell *123*, 903-915.

Dujardin, D. L., and Vallee, R. B. (2002). Dynein at the cortex. Curr Opin Cell Biol *14*, 44-49.

Frenzel, E. M., and Johnson, R. G. (1996). Gap junction formation between cultured embryonic lens cells is inhibited by antibody to N-cadherin. Dev Biol *179*, 1-16.

Fuchs, E., and Karakesisoglou, I. (2001). Bridging cytoskeletal intersections. Genes Dev *15*, 1-14.

Gaietta, G., Deerinck, T. J., Adams, S. R., Bouwer, J., Tour, O., Laird, D. W., Sosinsky, G. E., Tsien, R. Y., and Ellisman, M. H. (2002). Multicolor and electron microscopic imaging of connexin trafficking. Science *296*, 503-507.

Gallagher, K. L., and Benfey, P. N. (2005). Not just another hole in the wall: understanding intercellular protein trafficking. Genes Dev *19*, 189-195.

Giepmans, B. N. (2004). Gap junctions and connexin-interacting proteins. Cardiovasc Res *62*, 233-245.

Giepmans, B. N., and Moolenaar, W. H. (1998). The gap junction protein connexin43 interacts with the second PDZ domain of the zona occludens-1 protein. Curr Biol *8*, 931-934.

Giepmans, B. N., Verlaan, I., Hengeveld, T., Janssen, H., Calafat, J., Falk, M. M., and Moolenaar, W. H. (2001). Gap junction protein connexin-43 interacts directly with microtubules. Curr Biol *11*, 1364-1368.

Gros, D. B., and Jongsma, H. J. (1996). Connexins in mammalian heart function. Bioessays *18*, 719-730.

Hamm-Alvarez, S. F., Sonee, M., Loran-Goss, K., and Shen, W. C. (1996). Paclitaxel and nocodazole differentially alter endocytosis in cultured cells. Pharm Res *13*, 1647-1656.

Hayashi, I., Wilde, A., Mal, T. K., and Ikura, M. (2005). Structural Basis for the Activation of Microtubule Assembly by the EB1 and p150(Glued) Complex. Mol Cell *19*, 449-460.

Heath, W. R., and Carbone, F. R. (2005). Coupling and cross-presentation. Nature *434*, 27-28.

Hertig, C. M., Butz, S., Koch, S., Eppenberger-Eberhardt, M., Kemler, R., and Eppenberger, H. M. (1996). N-cadherin in adult rat cardiomyocytes in culture. II. Spatio-temporal appearance of proteins involved in cell-cell contact and communication. Formation of two distinct N-cadherin/catenin complexes. J Cell Sci *109 (Pt 1)*, 11-20.

Hu, K., Huang, C. S., Jan, Y. N., and Jan, L. Y. (2003). ATP-sensitive potassium channel traffic regulation by adenosine and protein kinase C. Neuron *38*, 417-432.

Jamora, C., and Fuchs, E. (2002). Intercellular adhesion, signalling and the cytoskeleton. Nat Cell Biol *4*, E101-108.

Jordan, K., Solan, J. L., Dominguez, M., Sia, M., Hand, A., Lampe, P. D., and Laird, D. W. (1999). Trafficking, assembly, and function of a connexin43-green fluorescent protein chimera in live mammalian cells. Mol Biol Cell *10*, 2033-2050.

Kaprielian, R. R., Gunning, M., Dupont, E., Sheppard, M. N., Rothery, S. M., Underwood, R., Pennell, D. J., Fox, K., Pepper, J., Poole-Wilson, P. A., and Severs, N. J. (1998). Downregulation of immunodetectable connexin43 and decreased gap junction size in the pathogenesis of chronic hibernation in the human left ventricle. Circulation *97*, 651-660.

Kleber, A. G., Riegger, C. B., and Janse, M. J. (1987). Electrical uncoupling and increase of extracellular resistance after induction of ischemia in isolated, arterially perfused rabbit papillary muscle. Circ Res *61*, 271-279.

Ko, K. S., Arora, P. D., Bhide, V., Chen, A., and McCulloch, C. A. (2001). Cell-cell adhesion in human fibroblasts requires calcium signaling. J Cell Sci *114*, 1155-1167.

Koonce, M. P., and Samso, M. (2004). Of rings and levers: the dynein motor comes of age. Trends Cell Biol *14*, 612-619.

Kostin, S., Hein, S., Bauer, E. P., and Schaper, J. (1999). Spatiotemporal development and distribution of intercellular junctions in adult rat cardiomyocytes in culture. Circ Res *85*, 154-167.

Krutovskikh, V. (2002). Implication of direct host-tumor intercellular interactions in non-immune host resistance to neoplastic growth. Semin Cancer Biol *12*, 267-276.

Laird, D. W. (2005). Connexin phosphorylation as a regulatory event linked to gap junction internalization and degradation. Biochim Biophys Acta *1711*, 172-182.

Laird, D. W., Puranam, K. L., and Revel, J. P. (1991). Turnover and phosphorylation dynamics of connexin43 gap junction protein in cultured cardiac myocytes. Biochem J *273(Pt 1)*, 67-72.

Lauf, U., Giepmans, B. N., Lopez, P., Braconnot, S., Chen, S. C., and Falk, M. M. (2002). Dynamic trafficking and delivery of connexons to the plasma membrane and accretion to gap junctions in living cells. Proc Natl Acad Sci U S A *99*, 10446-10451.

Li, J., Patel, V. V., Kostetskii, I., Xiong, Y., Chu, A. F., Jacobson, J. T., Yu, C., Morley, G. E., Molkentin, J. D., and Radice, G. L. (2005). Cardiac-specific loss of N-cadherin leads to alteration in connexins with conduction slowing and arrhythmogenesis. Circ Res *97*, 474-481.

Ligon, L. A., Karki, S., Tokito, M., and Holzbaur, E. L. (2001). Dynein binds to beta-catenin and may tether microtubules at adherens junctions. Nat Cell Biol *3*, 913-917.

Loewenstein, W. R. (1967). On the genesis of cellular communication. Dev Biol *15*, 503-520.

Luo, Y., and Radice, G. L. (2003). Cadherin-mediated adhesion is essential for myofibril continuity across the plasma membrane but not for assembly of the contractile apparatus. J Cell Sci *116*, 1471-1479.

Mareel, M., and Leroy, A. (2003). Clinical, cellular, and molecular aspects of cancer invasion. Physiol Rev *83*, 337-376.

Matsushita, T., Oyamada, M., Fujimoto, K., Yasuda, Y., Masuda, S., Wada, Y., Oka, T., and Takamatsu, T. (1999). Remodeling of cell-cell and cell-extracellular matrix interactions at the border zone of rat myocardial infarcts. Circ Res *85*, 1046-1055.

Mege, R. M., Matsuzaki, F., Gallin, W. J., Goldberg, J. I., Cunningham, B. A., and Edelman, G. M. (1988). Construction of epithelioid sheets by transfection of mouse sarcoma cells with cDNAs for chicken cell adhesion molecules. Proc Natl Acad Sci U S A *85*, 7274-7278.

Menasche, P., Hagege, A. A., Vilquin, J. T., Desnos, M., Abergel, E., Pouzet, B., Bel, A., Sarateanu, S., Scorsin, M., Schwartz, K., *et al.* (2003). Autologous skeletal myoblast transplantation for severe postinfarction left ventricular dysfunction. J Am Coll Cardiol *41*, 1078-1083.

Mesnil, M. (2002). Connexins and cancer. Biol Cell *94*, 493-500.

Meyer, R. A., Laird, D. W., Revel, J. P., and Johnson, R. G. (1992). Inhibition of gap junction and adherens junction assembly by connexin and A-CAM antibodies. J Cell Biol *119*, 179-189.

Mimori-Kiyosue, Y., Grigoriev, I., Lansbergen, G., Sasaki, H., Matsui, C., Severin, F., Galjart, N., Grosveld, F., Vorobjev, I., Tsukita, S., and Akhmanova, A. (2005). CLASP1 and CLASP2 bind to EB1 and regulate microtubule plus-end dynamics at the cell cortex. J Cell Biol *168*, 141-153.

Morrison, E. E., Wardleworth, B. N., Askham, J. M., Markham, A. F., and Meredith, D. M. (1998). EB1, a protein which interacts with the APC tumour suppressor, is associated with the microtubule cytoskeleton throughout the cell cycle. Oncogene *17*, 3471-3477.

Musil, L. S., and Goodenough, D. A. (1990). Gap junctional intercellular communication and the regulation of connexin expression and function. Curr Opin Cell Biol *2*, 875-880.

Nakata, T., and Hirokawa, N. (2003). Microtubules provide directional cues for polarized axonal transport through interaction with kinesin motor head. J Cell Biol *162*, 1045-1055.

Noren, N. K., Niessen, C. M., Gumbiner, B. M., and Burridge, K. (2001). Cadherin engagement regulates Rho family GTPases. J Biol Chem *276*, 33305-33308.

Oliveira, R., Christov, C., Guillamo, J. S., Debouard, S., Palfi, S., Venance, L., Tardy, M., and Peschanski, M. (2005). Contribution of gap junctional communication between tumor cells and astroglia to the invasion of the brain parenchyma by human glioblastomas. BMC Cell Biol *6*, 7.

Peters, N. S., Coromilas, J., Severs, N. J., and Wit, A. L. (1997). Disturbed connexin43 gap junction distribution correlates with the location of reentrant circuits in the epicardial border zone of healing canine infarcts that cause ventricular tachycardia. Circulation *95*, 988-996.

Reinecke, H., Minami, E., Virag, J. I., and Murry, C. E. (2004). Gene transfer of connexin43 into skeletal muscle. Hum Gene Ther *15*, 627-636.

Rudy, Y., and Shaw, R. M. (1997). Cardiac excitation: an interactive process of ion channels and gap junctions. Adv Exp Med Biol *430*, 269-279.

Schuyler, S. C., and Pellman, D. (2001). Search, capture and signal: games microtubules and centrosomes play. J Cell Sci *114*, 247-255.

Segretain, D., and Falk, M. M. (2004). Regulation of connexin biosynthesis, assembly, gap junction formation, and removal. Biochim Biophys Acta *1662*, 3-21.

Shaw, R. M., and Rudy, Y. (1995). The vulnerable window for unidirectional block in cardiac tissue: characterization and dependence on membrane excitability and intercellular coupling. J Cardiovasc Electrophysiol *6*, 115-131.

Shaw, R. M., and Rudy, Y. (1997). Ionic mechanisms of propagation in cardiac tissue. Roles of the sodium and L-type calcium currents during reduced excitability and decreased gap junction coupling. Circ Res *81*, 727-741.

Sohl, G., Maxeiner, S., and Willecke, K. (2005). Expression and functions of neuronal gap junctions. Nat Rev Neurosci *6*, 191-200.

Takeichi, M. (1990). Cadherins: a molecular family important in selective cell-cell adhesion. Annu Rev Biochem *59*, 237-252.

Thom, T., Haase, N., Rosamond, W., Howard, V. J., Rumsfeld, J., Manolio, T., Zheng, Z. J., Flegal, K., O'Donnell, C., Kittner, S., *et al.* (2006). Heart Disease and Stroke Statistics--2006 Update. A Report From the American Heart Association Statistics Committee and Stroke Statistics Subcommittee. Circulation.

Thomas, T., Jordan, K., Simek, J., Shao, Q., Jedeszko, C., Walton, P., and Laird, D. W. (2005). Mechanisms of Cx43 and Cx26 transport to the plasma membrane and gap junction regeneration. J Cell Sci *118*, 4451-4462.

Waterman-Storer, C. M., Salmon, W. C., and Salmon, E. D. (2000). Feedback interactions between cell-cell adherens junctions and cytoskeletal dynamics in newt lung epithelial cells. Mol Biol Cell *11*, 2471-2483.

Wei, C. J., Francis, R., Xu, X., and Lo, C. W. (2005). Connexin43 associated with an N-cadherin-containing multiprotein complex is required for gap junction formation in NIH3T3 cells. J Biol Chem *280*, 19925-19936.

Wei, C. J., Xu, X., and Lo, C. W. (2004). Connexins and cell signaling in development and disease. Annu Rev Cell Dev Biol *20*, 811-838.

Wheelock, M. J., and Johnson, K. R. (2003). Cadherins as modulators of cellular phenotype. Annu Rev Cell Dev Biol *19*, 207-235.

Williams, E. J., Williams, G., Gour, B., Blaschuk, O., and Doherty, P. (2000). INP, a novel N-cadherin antagonist targeted to the amino acids that flank the HAV motif. Mol Cell Neurosci *15*, 456-464.

Yamada, K. A., Rogers, J. G., Sundset, R., Steinberg, T. H., and Saffitz, J. E. (2003). Up-regulation of connexin45 in heart failure. J Cardiovasc Electrophysiol *14*, 1205-1212.

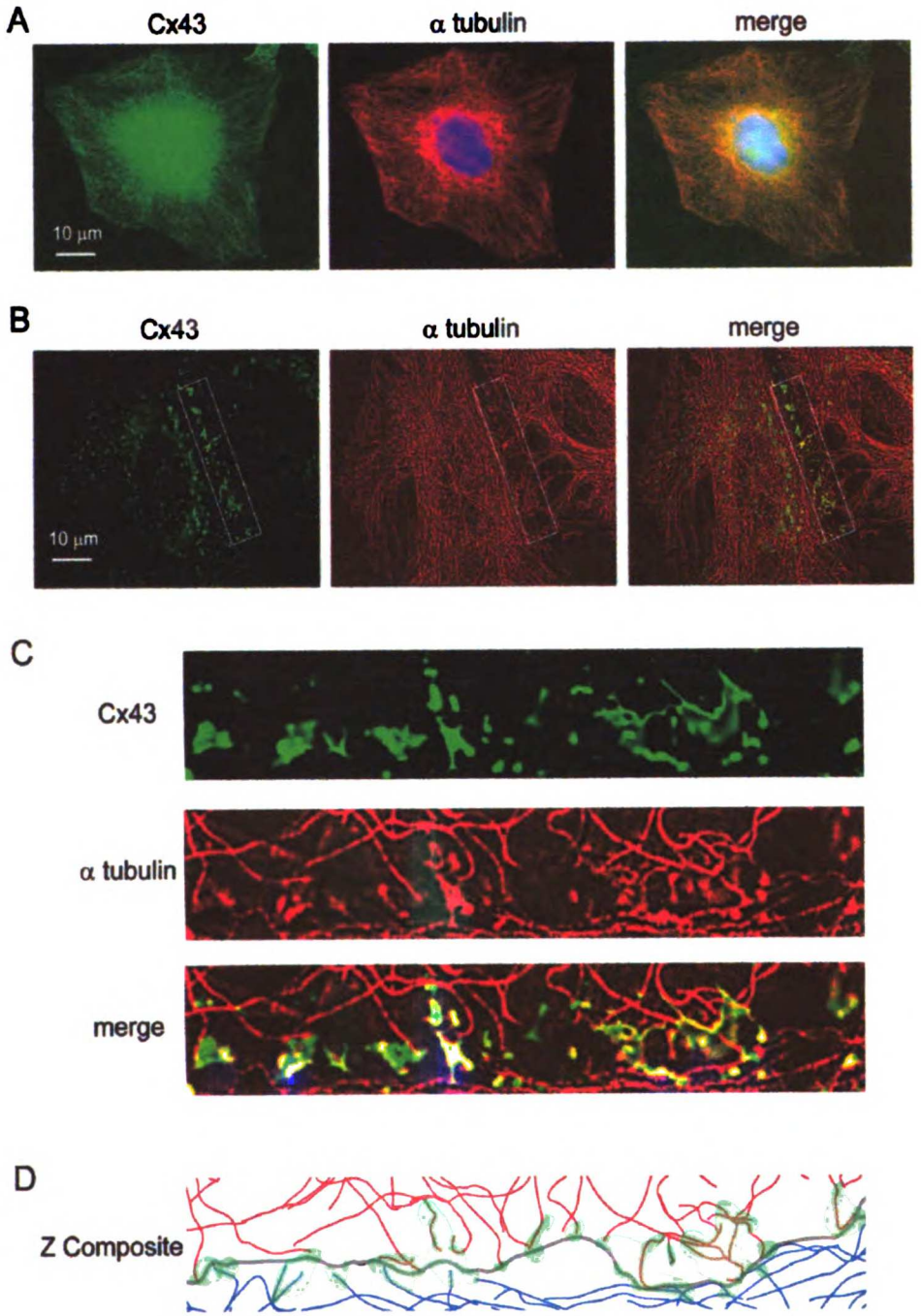
A
Cx43
α tubulin
merge
10 μm
B
Cx43
α tubulin
merge
10 μm
C
Cx43
α tubulin
merge
D
Z Composite

Figure 1

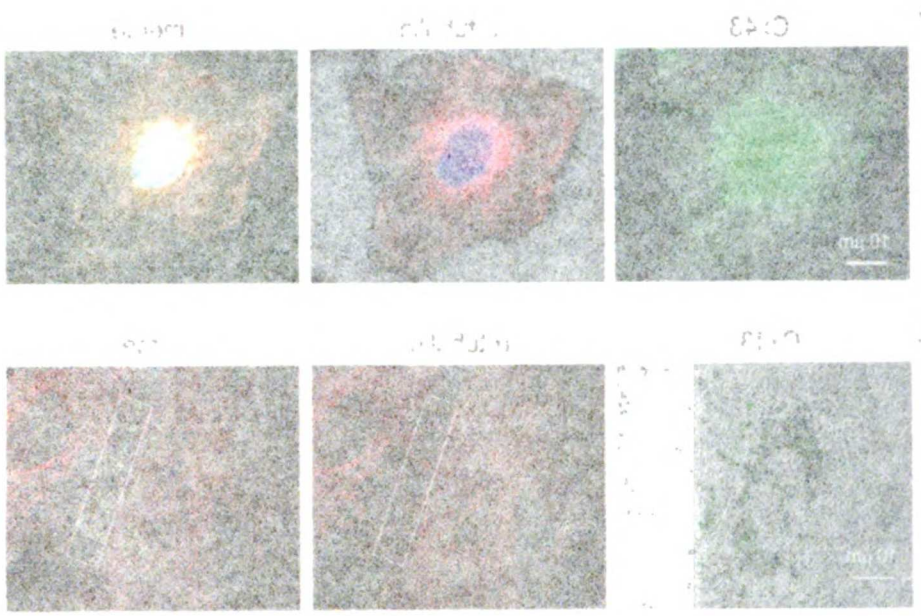

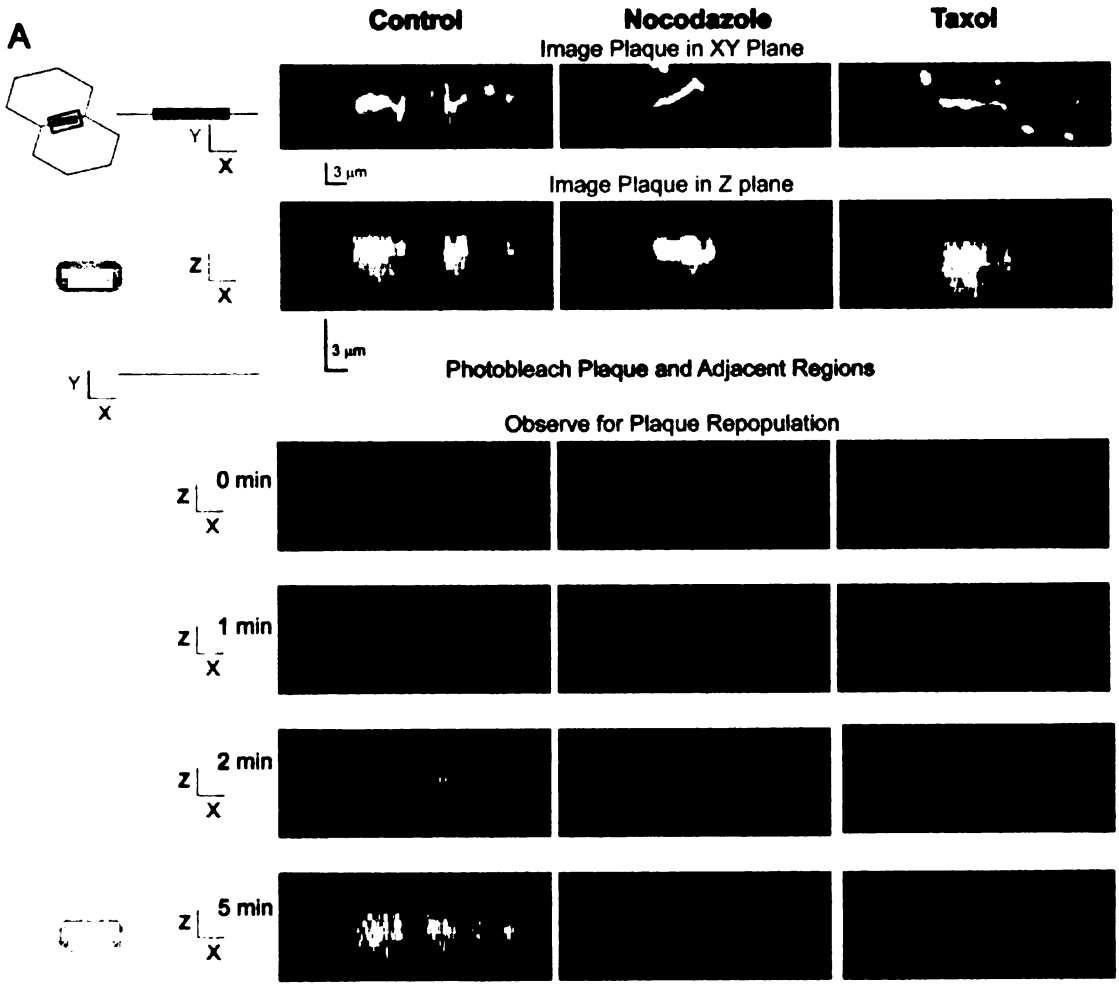
A
Control
Nocodazole
Taxol
Image Plaque in XY Plane
Y
X
3 µm
Image Plaque in Z plane
Z
X
3 µm
Photobleach Plaque and Adjacent Regions
Y
X
Observe for Plaque Repopulation
Z
X
0 min
1 min
2 min
5 min

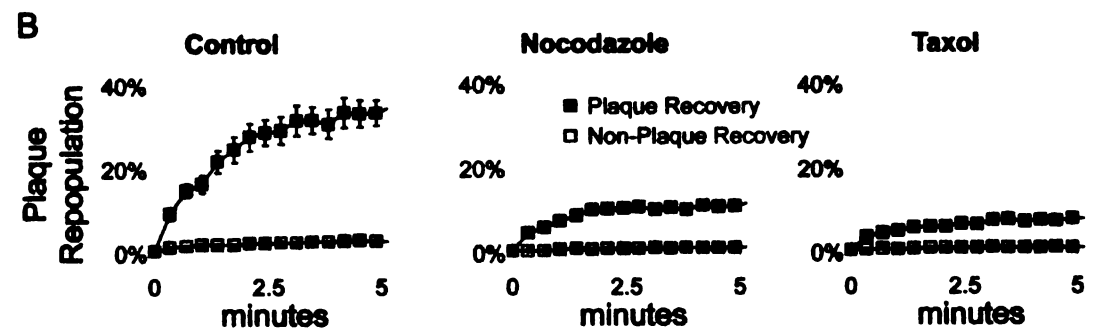
B
Control
Nocodazole
Taxol
Plaque Repopulation
40%
20%
0%
0
2.5
5
minutes
Plaque Recovery
Non-Plaque Recovery

Figure 2

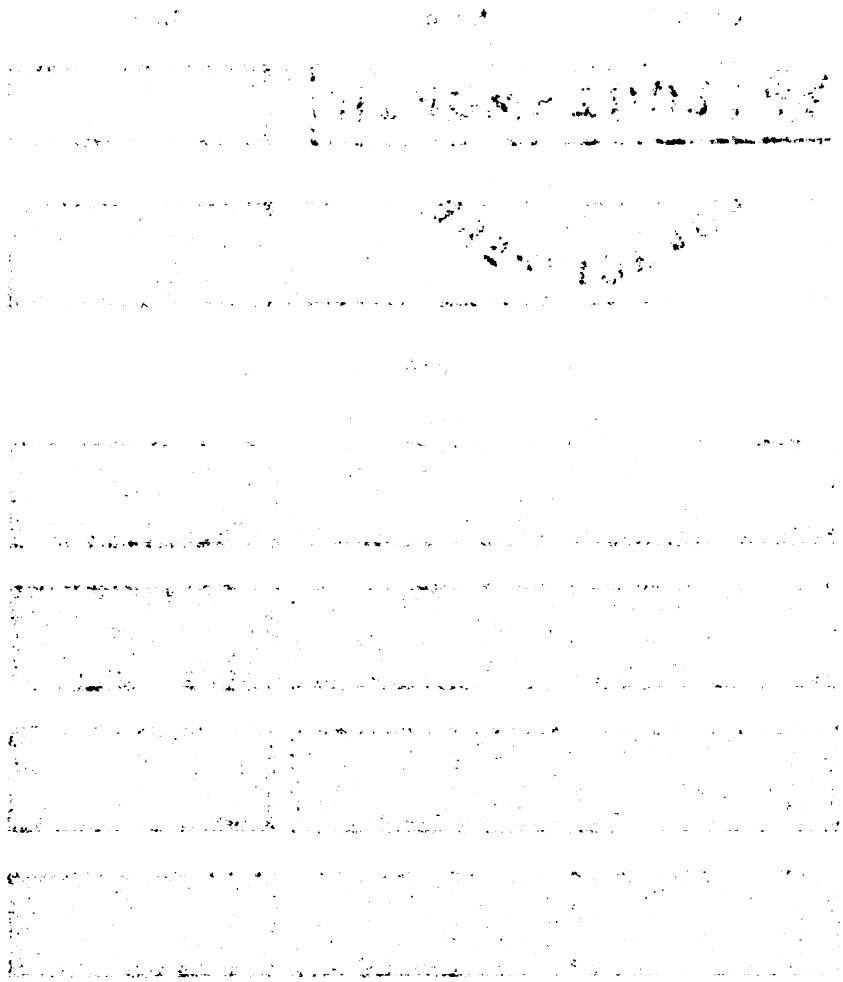

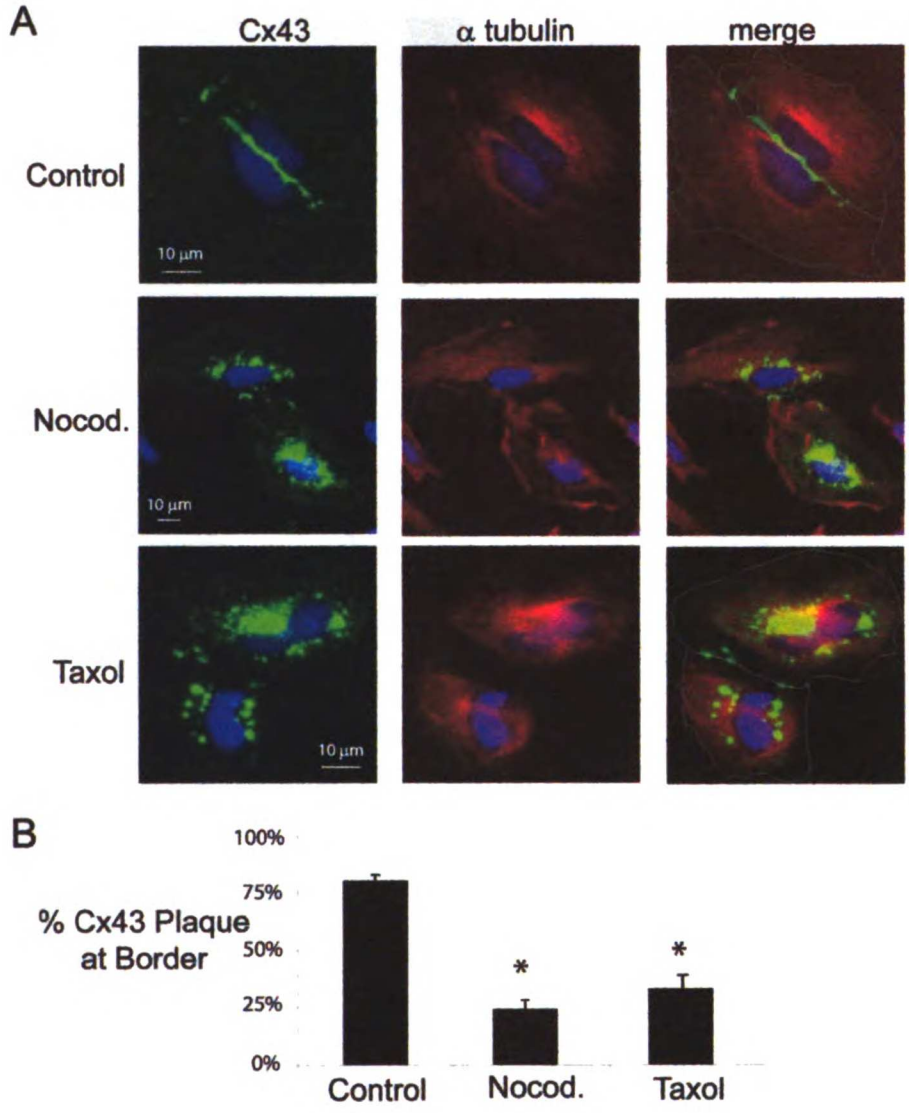
A
Cx43
α tubulin
merge
Control
Nocod.
Taxol
10 μm
10 μm
10 μm
B
% Cx43 Plaque at Border
100%
75%
50%
25%
0%
*
*
Control
Nocod.
Taxol

Figure 3

A
Cx43
α tubulin
merge
Control
Nocod.
Taxol
10 μm
B
% Cx43 Plaque
at border
Control
Noco-d.
Taxol

Figure 3

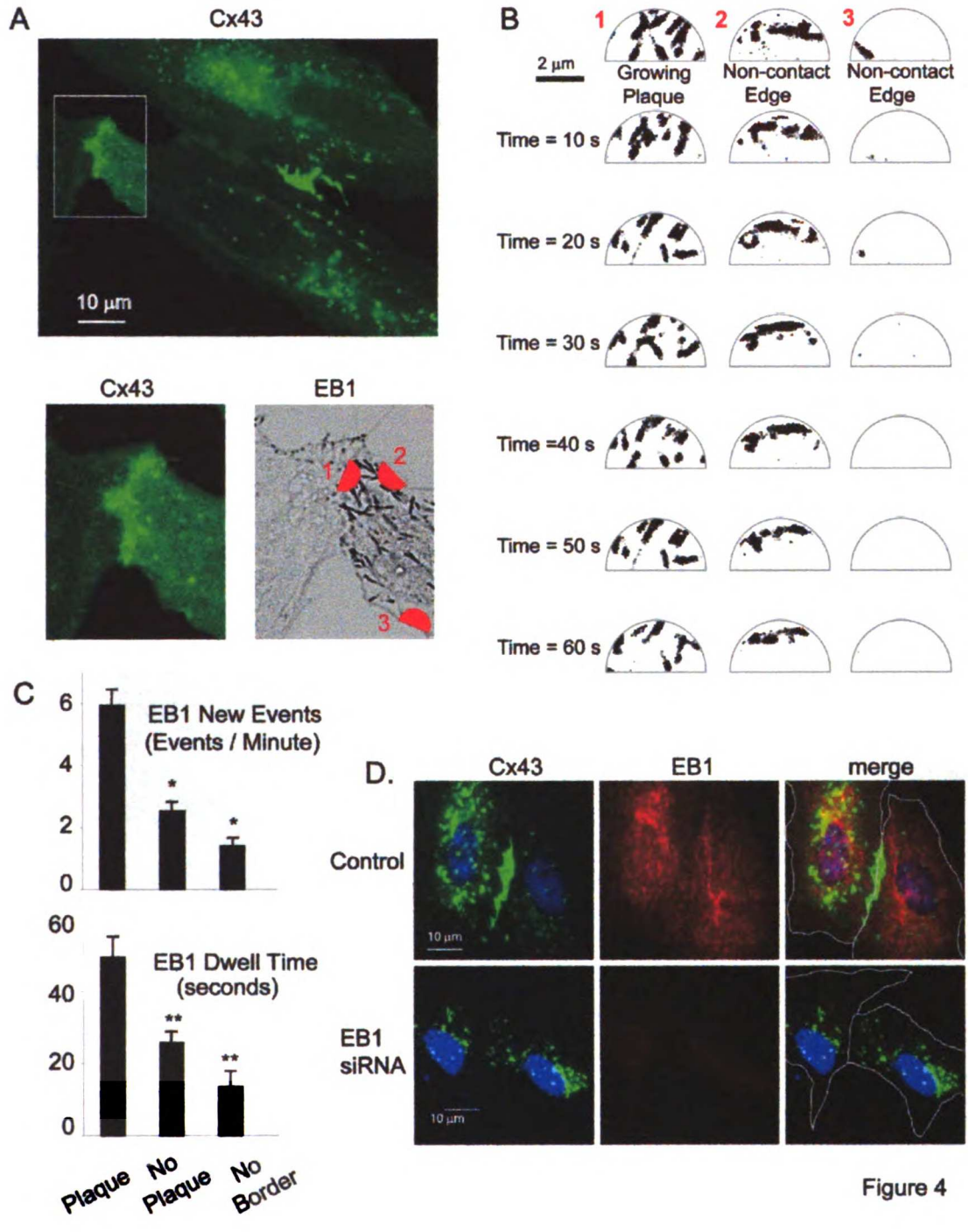
A
Cx43
10 µm
Cx43
EB1
1
2
3
B
1
2
3
2 µm
Growing Plaque
Non-contact Edge
Non-contact Edge
Time = 10 s
Time = 20 s
Time = 30 s
Time =40 s
Time = 50 s
Time = 60 s
C
EB1 New Events (Events / Minute)
6
4
2
0
*
*
60
40
20
0
EB1 Dwell Time (seconds)
**
**
Plaque
No Plaque
No Border
D.
Cx43
EB1
merge
Control
EB1 siRNA
10 µm
10 µm

Figure 4

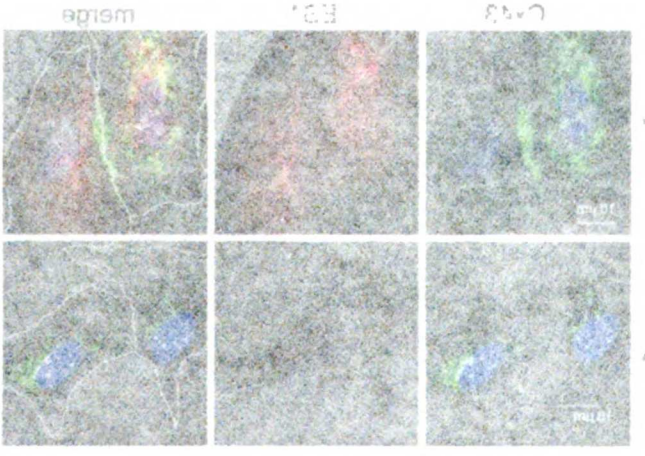
merge
EB3
Cav3
10 µm

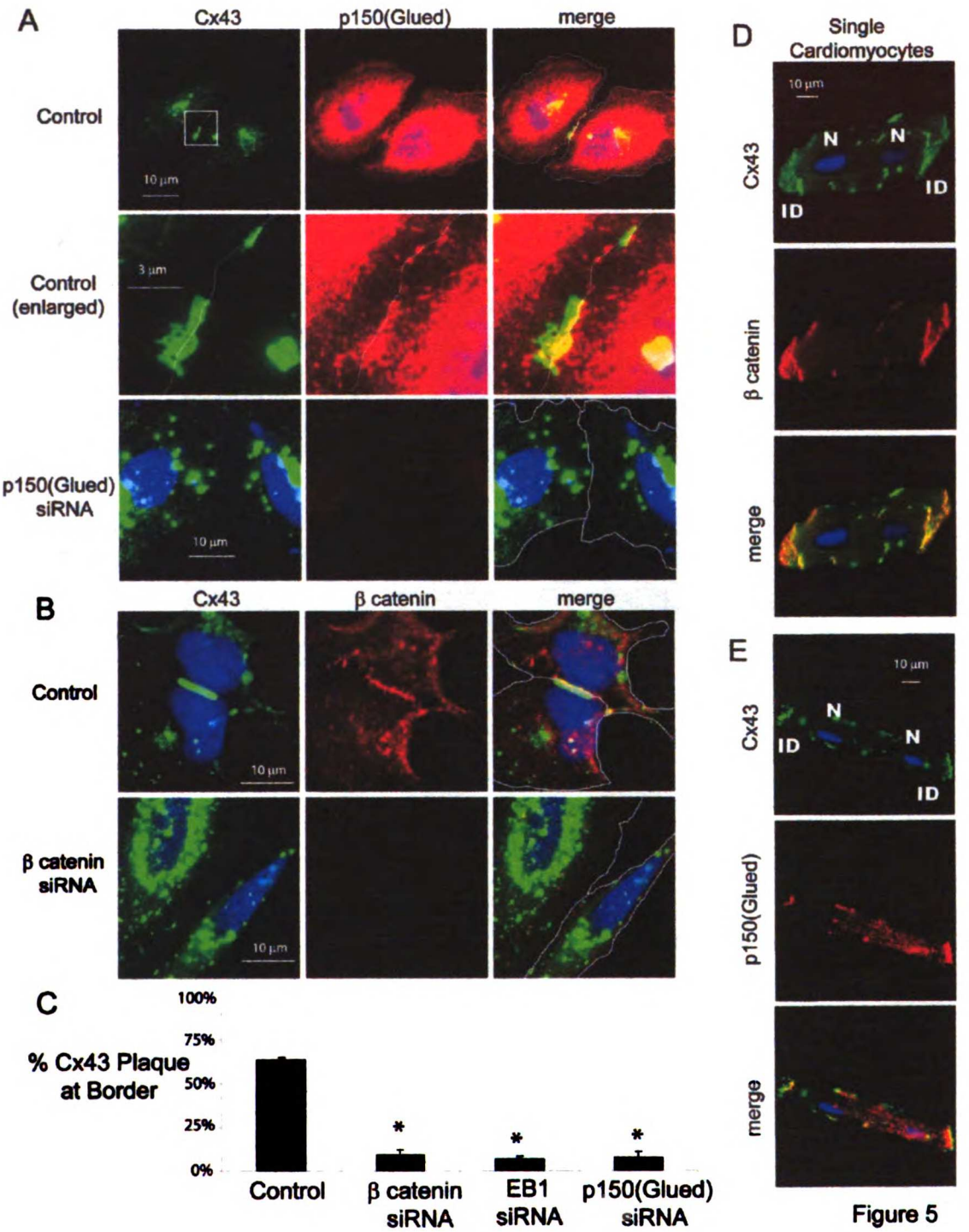
A
Cx43
p150(Glued)
merge
Control
10 μm
Control (enlarged)
3 μm
p150(Glued) siRNA
10 μm
B
Cx43
β catenin
merge
Control
10 μm
β catenin siRNA
10 μm
C
% Cx43 Plaque at Border
100%
75%
50%
25%
0%
*
*
*
Control
β catenin siRNA
EB1 siRNA
p150(Glued) siRNA
D
Single Cardiomyocytes
10 μm
Cx43
N
N
ID
ID
β catenin
merge
E
10 μm
Cx43
N
ID
N
ID
p150(Glued)
merge

Figure 5

merge
p150(Glued)
Cardiomyocytes
N
N
1D
1D
siRNA
siRNA
siRNA
Control
β catenin
EB1
p150(Glued)

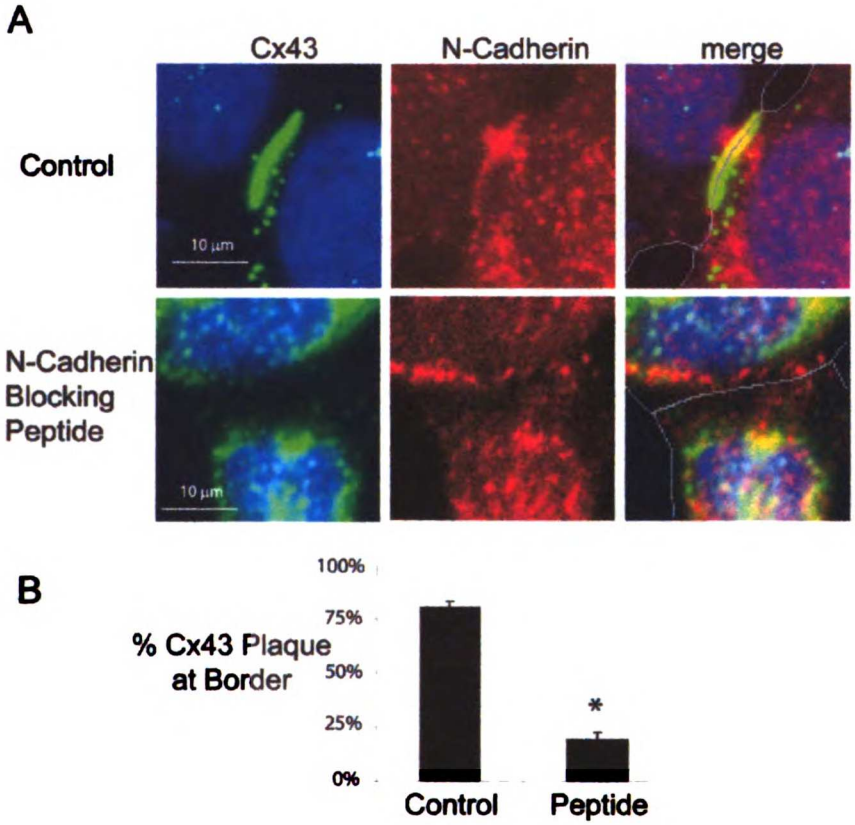
A
Cx43
N-Cadherin
merge
Control
10 μm
N-Cadherin
Blocking
Peptide
10 μm
B
% Cx43 Plaque
at Border
100%
75%
50%
25%
0%
*
Control
Peptide

Figure 6

A
Cx43
merge
Control
10 µm
10 µm
B

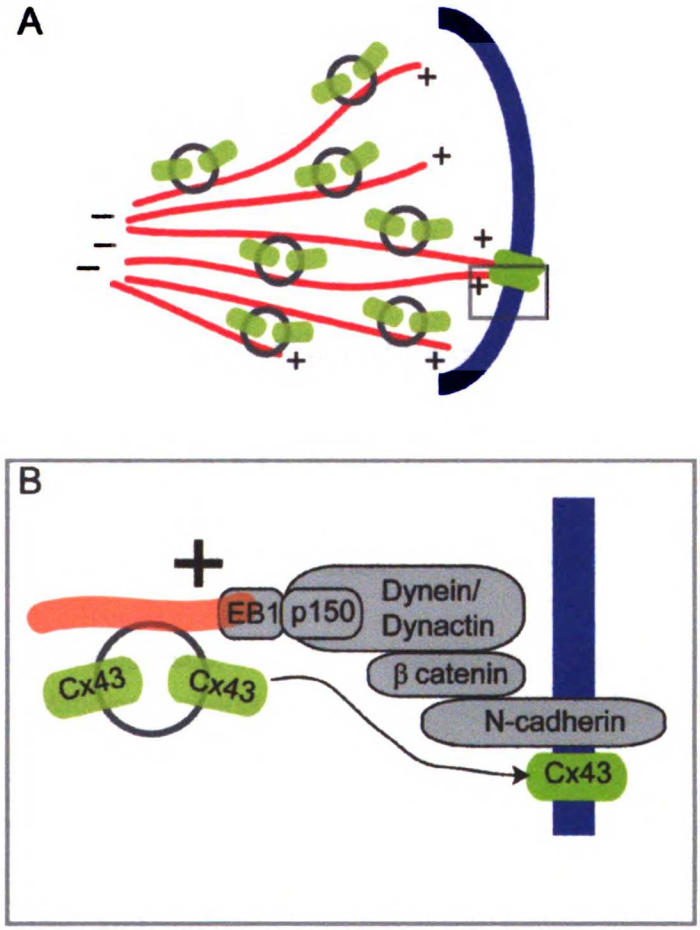
A
B
EB1
p150
Dynein/
Dynactin
β catenin
N-cadherin
Cx43
Cx43
Cx43

Figure 7

Figure 7

Chapter 4

Gap Junctions Mediate Internuclear Transport

Alex J. Fay[1**], Robin M. Shaw[2**], Yuh-Nung Jan[3], and Lily Y. Jan[3]

[1] Graduate Group in Biophysics, University of California, San Francisco, CA 94143, USA

[2] Department of Medicine, University of California, San Francisco, CA 94143, USA

[3] Howard Hughes Medical Institute and Departments of Physiology and Biochemistry, University of California, San Francisco, CA 94143, USA

** Equal contributor

Gap junctions are channels that span the plasma membranes of adjacent cells and allow for the intercellular exchange of cytosolic molecules of approximately 1 kDa or smaller [1]. We report that pairs of cells with dense plaques of connexin 43 (Cx43), which forms gap junctions, also have their nuclei localized to the cell-cell border region. This phenomenon was observed both in Cx43-YFP-transfected HeLa cells [2] and in the rat hepatocyte cell lineWB-F344 [3], which express endogenous Cx43. Although nuclear polarization is independent of the presence of Cx43, there is a strong correlation between Cx43 polarization towards the cell-cell border and nuclear localization at the cell-cell junction. Furthermore, a DNA-binding dye, DAPI, when injected into the nucleus of such a cell pair crosses rapidly to the nucleus of the adjacent cell. We propose that gap junctions may facilitate transfer of small molecules between the nuclei of adjoining pairs of cells.

Gap junctions are channels made up of six subunits of connexin (Cx) proteins per cellular hemichannel, and co-assemble into dense plaques of several hundred channels at cell-cell borders. Since the channels cross the plasma membranes of two adjacent cells, small ions, metabolites, secondary messengers, and reactive oxygen species can be exchanged by the cells. More recently, gap junctions have been shown to be capable of transporting antigenic peptides between antigen-presenting cells [4], and also of transporting siRNA between cells [5]. These studies have shown that molecules much larger than 1 kDa can, in fact, pass through gap junctions, and that selectivity may be governed more by molecular geometry than molecular weight. All of these examples of gap junction-mediated transport of small molecules involve sharing of cytoplasmic consitutents.

Using two cell lines, one lacking endogenous connexins but transfected with Cx43-YFP (Figure 1A,B), and the other expressing endogenous Cx43 (Figure 1C), we have noticed that nuclei in pairs of cells tend to be more polarized towards cell-cell borders when Cx43 distribution is more intense at the adherens junction. This effect is independent of Cx43 expression, since the nuclei polarize even in untransfected HeLa cells. Furthermore, the effect tends to disappear as cells become confluent and have many neighbors. This indicates that cell-cell contact formation is likely influencing nuclear position. We quantified the polarization of cortical Cx43 distribution and nuclear position (Figure 1D) and found that in cell pairs, when nuclei are polarized, there tends to be a high correlation between the Cx43 and nuclear polarization vectors. In the few isolated cells that have polarized nuclei, this polarization is not matched by high Cx43 and nuclear correlation. Given the striking correlation between nuclear position and Cx43 distribution, we wondered whether there might be any functional consequences for gap junction localization between the closely apposed nuclei of two adjacent cells.

One possible function for gap junctions, under these circumstances, might be to mediate the transfer of nuclear-localized constituents between the nuclei of the adjacent cells. Nuclei contain many macromolecules, such as DNA, unspliced mRNA, and proteins, which are either permanently or reversibly associated with this compartment, but are almost certainly too large to pass through a gap junction channel. Smaller nuclear constituents, could, conceivably shuttle back and forth between nuclei through connexin channels. We used DAPI, which is a small, 280 Da probe that becomes fluorescent upon binding in the minor groove of double-stranded DNA, as a nuclear-localized molecule that should be able to move between cells via gap junctions. By microinjection, we

localized DAPI to the nucleus of one cell of a pair of HeLa cells expressing Cx43, and then observed DAPI fluorescence over time (Figure 2A-D). Within the first minute after microinjection, DAPI clearly left the first cell's nucleus and entered the nucleus of the adjacent cell. As the fluorescence of the acceptor nucleus increased, the donor nucleus fluorescence decreased (Figure 2D), suggesting that there was, in fact, an equilibration of the dye between the two nuclei, rather than simply an excess of injected dye that escaped into the cytoplasm and spread to the second cell. In addition, cell pairs that express Cx43-YFP, but do not have their nuclei localized at the cell-cell border, transferred DAPI much less efficiently from one nucleus to the other. Thus, while a nuclear-localized small molecule can exit one nucleus and reach a second cell's nucleus by diffusing through two cytoplasms, this process would result in a dilution of the molecule throughout the volume of the cytoplasm. Polarized nuclei at the cell-cell junction can share their constituents much more efficiently via gap junctions, making it possible, potentially, for the nuclei of two adjacent cells to have coupled metabolism, transcriptional activities, or signal transduction pathways. Unlike DAPI, a larger nuclear localized molecule, the small double-stranded RNA NRSE [6], labeled with a Cy3 fluorophore, was unable to pass from one nucleus to another through Cx43 gap junctions (Figure 3). Nevertheless, the intriguing possibility remains that other small nuclear RNAs, which are capable of modifying heterochromatin and silencing transcription in fission yeast and plants [7], may be shared between nuclei of adjacent cells via gap junctions.

Nuclei, despite the presence of nuclear pore complexes in the nuclear envelope, which permit many low molecular weight molecules to freely move between the nucleus

and the cytoplasm, still maintain an ionic and redox environment that is distinct from the cytoplasm's. Calcium in the nucleus, for example, can affect gene transcription [8], as well as the activity of the nuclear pore complex [9]. There is also a glutathione gradient between the nucleus and the cytoplasm [10] that may affect the regulation of gene transcription, and perhaps even resistance to damage by reactive oxygen species. As with intercytoplasmic gap junction transport, internuclear gap junction transport could lead to the sharing of either beneficial or deleterious information between cells. Such activity is most likely to be relevant to the interactions of pairs of cells, such as immune cells [11], rather than large aggregates of cells like eplithelial sheets, since nuclei tend to be centrally located in cells with multiple neighbors. In summary, we have shown that the nuclei of adjacent cells are polarized towards cell-cell borders, and is correlated with the degree of Cx43 localization at the cell-cell junction. By microinjection, we have demonstrated that nuclear-localized small molecules can move from one nucleus to the closely apposed nucleus of an adjacent cell through gap junctions. We propose that this may be a mechanism for cells to coordinate nuclear activities such as transcription.

EXPERIMENTAL PROCEDURES

Cell Culture and Transfection

HeLa cells were cultured at 37°C and 5% CO_2 in MEM Eagle's Medium with Earle's BSS, supplemented with 10% Fetal Bovine Serum, Penicillin/Streptomycin, and Non-Essential Amino Acids (UCSF Cell Culture Facility). Cells were transfected with Cx43 in pEYFP [2] (courtesy of Dale Laird) using FuGene 6 (Roche, Indianapolis) according to the manufacturer's instructions. Cells were cultured for 18-48 hours before use in live-cell or fixed cell imaging.

Immunostaining and Imaging of Fixed Cells

Cells were cultured on 12 mm coverslips (Warner Instrument Corp., Hamden, CT) pre-coated with bovine fibronectin (50 mg/ml) and transfected. Cells were fixed with methanol (-20°C) for 5 min, permeabilized with 0.2% Triton X-100 in PBS, and blocked in PBS + 0.1% Triton X-100 + 5% goat serum serum (Jackson ImmunoResearch Laboratories, Inc., West Grove, PA). Rabbit anti-connexin 43 antibody (1:400, Sigma-Aldrich) was diluted into PBS + 0.1% Triton X-100 + 2% serum and incubated at room temperature for 1 hr. Coverslips were washed in PBS, followed by incubation with goat anti-rabbit secondary antibody, conjugated to Alexa 488 (Jackson ImmunoResearch Laboratories, 1:500 dilution in PBS + 0.1 % Triton X-100 + 2 % serum) with 1 □g/ml Hoechst 33342 (Invitrogen, Carlsbad, CA) for 1 hr. at room temperature. Cells were mounted on to microscope slides with GelMount aqueous mounting medium (Biomeda Corp., Foster City, CA). Fixed cells were imaged with either a Nikon E800 epifluorescence microscope equipped with a Spot charge-coupled device digital camera and software (Diagnostic Instruments) or a Nikon TE2000-U inverted fluorescence microscope with Photometrics Coolsnap HQ CCD camera and MetaVue software (Molecular Devices, Sunnyvale, CA).

Quantification of Cx-43 and Nuclear Polarization

Images were analyzed with MetaVue software, and the centroid of the cell area, of the nucleus, and of cortical Cx43 distribution were calculated. The polarization vectors for Cx43 and the nucleus were calculated and correlation was determined by the angle between the two vectors. Data were analyzed for 17 cell pairs and 19 isolated cells.

Microinjection

DAPI (Invitrogen, Carlsbad, CA) at a concentration of 0.2 mg/ml was injected into the cell nucleus using a FemtoJet equipped with FemtoTips (Eppendorf, Hamburg, Germany). NRSE double-stranded RNA [6] labeled with Cy3 (Integrated DNA Technolgies, Coralville, IA) was injected at a concentration of 100 □M. Fluorescence of cells maintained at room temperature was monitored with a Nikon TE2000-U inverted fluorescence microscope with Photometrics Coolsnap HQ CCD camera and MetaVue software (Molecular Devices, Sunnyvale, CA).

References

1. Laird, D. W. (2006). Life cycle of connexins in health and disease. *Biochem J*, 394:527-543.
2. Jordan, K., J. L. Solan, M. Dominguez, M. Sia, A. Hand, P. D. Lampe, D. W. Laird (1999). Trafficking, assembly, and function of a connexin43-green fluorescent protein chimera in live mammalian cells. *Mol Biol Cell*, 10:2033-2050.
3. Tsao, M. S., J. D. Smith, K. G. Nelson, J. W. Grisham (1984). A diploid epithelial cell line from normal adult rat liver with phenotypic properties of 'oval' cells. *Exp Cell Res*, 154:38-52.
4. Neijssen, J., C. Herberts, J. W. Drijfhout, E. Reits, L. Janssen, J. Neefjes (2005). Cross-presentation by intercellular peptide transfer through gap junctions. *Nature*, 434:83-88.
5. Valiunas, V., Y. Y. Polosina, H. Miller, I. A. Potapova, L. Valiuniene, S. Doronin, R. T. Mathias, R. B. Robinson, M. R. Rosen, I. S. Cohen, P. R. Brink

(2005). Connexin-specific cell-to-cell transfer of short interfering RNA by gap junctions. *J Physiol*, 568:459-468.

6. Kuwabara, T., J. Hsieh, K. Nakashima, K. Taira, F. H. Gage (2004). A small modulatory dsRNA specifies the fate of adult neural stem cells. *Cell*, 116:779-793.
7. Bernstein, E., C. D. Allis (2005). RNA meets chromatin. *Genes Dev*, 19:1635-1655.
8. Hardingham, G. E., S. Chawla, C. M. Johnson, H. Bading (1997). Distinct functions of nuclear and cytoplasmic calcium in the control of gene expression. *Nature*, 385:260-265.
9. Stehno-Bittel, L., C. Perez-Terzic, D. E. Clapham (1995). Diffusion across the nuclear envelope inhibited by depletion of the nuclear Ca2+ store. *Science*, 270:1835-1838.
10. Bellomo, G., M. Vairetti, L. Stivala, F. Mirabelli, P. Richelmi, S. Orrenius (1992). Demonstration of nuclear compartmentalization of glutathione in hepatocytes. *Proc Natl Acad Sci U S A*, 89:4412-4416.
11. Matsue, H., J. Yao, K. Matsue, A. Nagasaka, H. Sugiyama, R. Aoki, M. Kitamura, S. Shimada (2006). Gap junction-mediated intercellular communication between dendritic cells (DCs) is required for effective activation of DCs. *J Immunol*, 176:181-190.

Figure 1

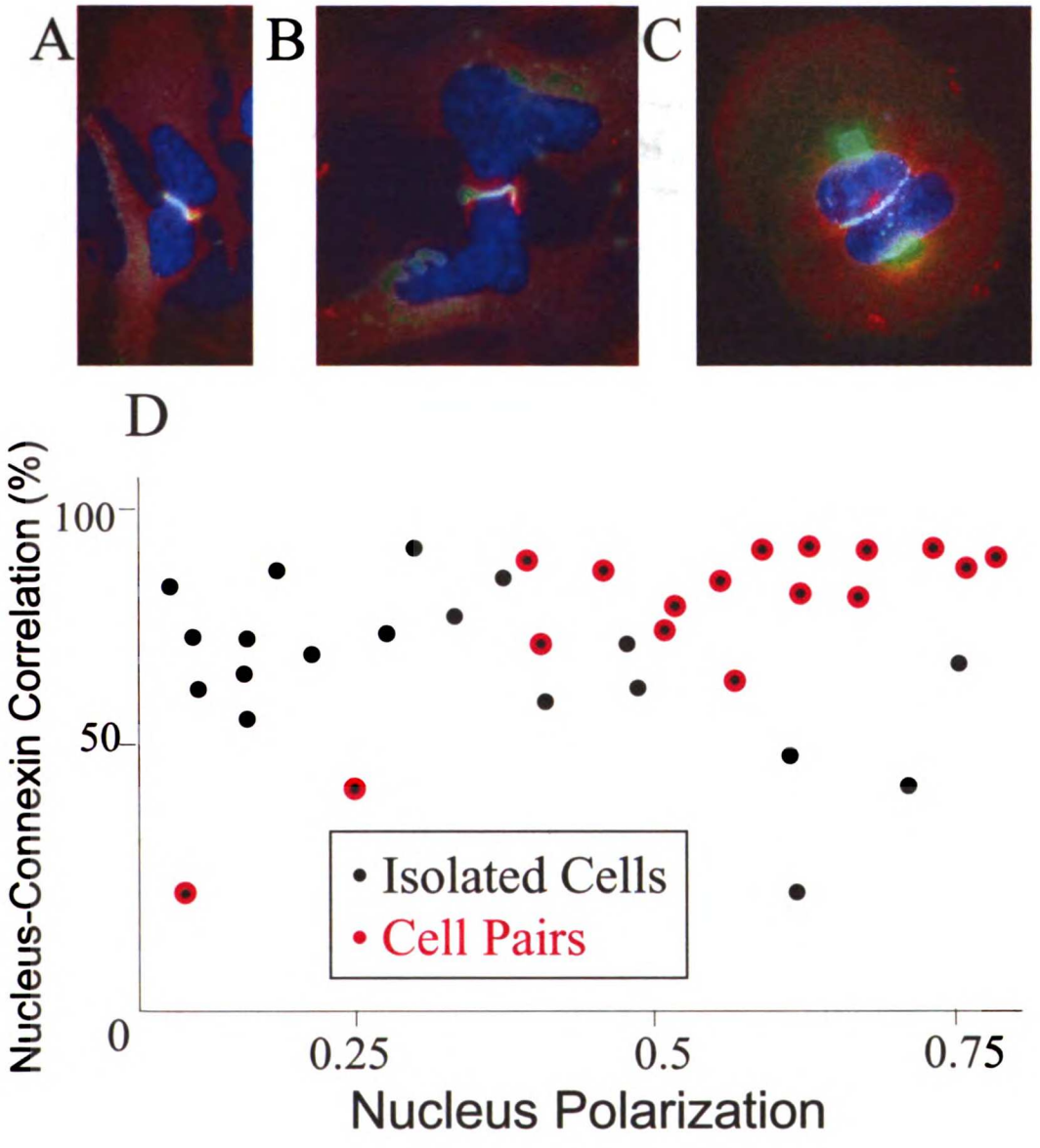

1. Nuclei are Co-Localized at the Cell-Cell Border with Gap Junctions in Cx43-Transfected HeLa Cells (A,B) and in WB-F344 Rat Hepatocytes (C). Cx43 (green) and nuclei (blue). D. Quantification of Nuclear and Cx43-YFP Polarization in Transfected HeLa Cells.

Figure 2

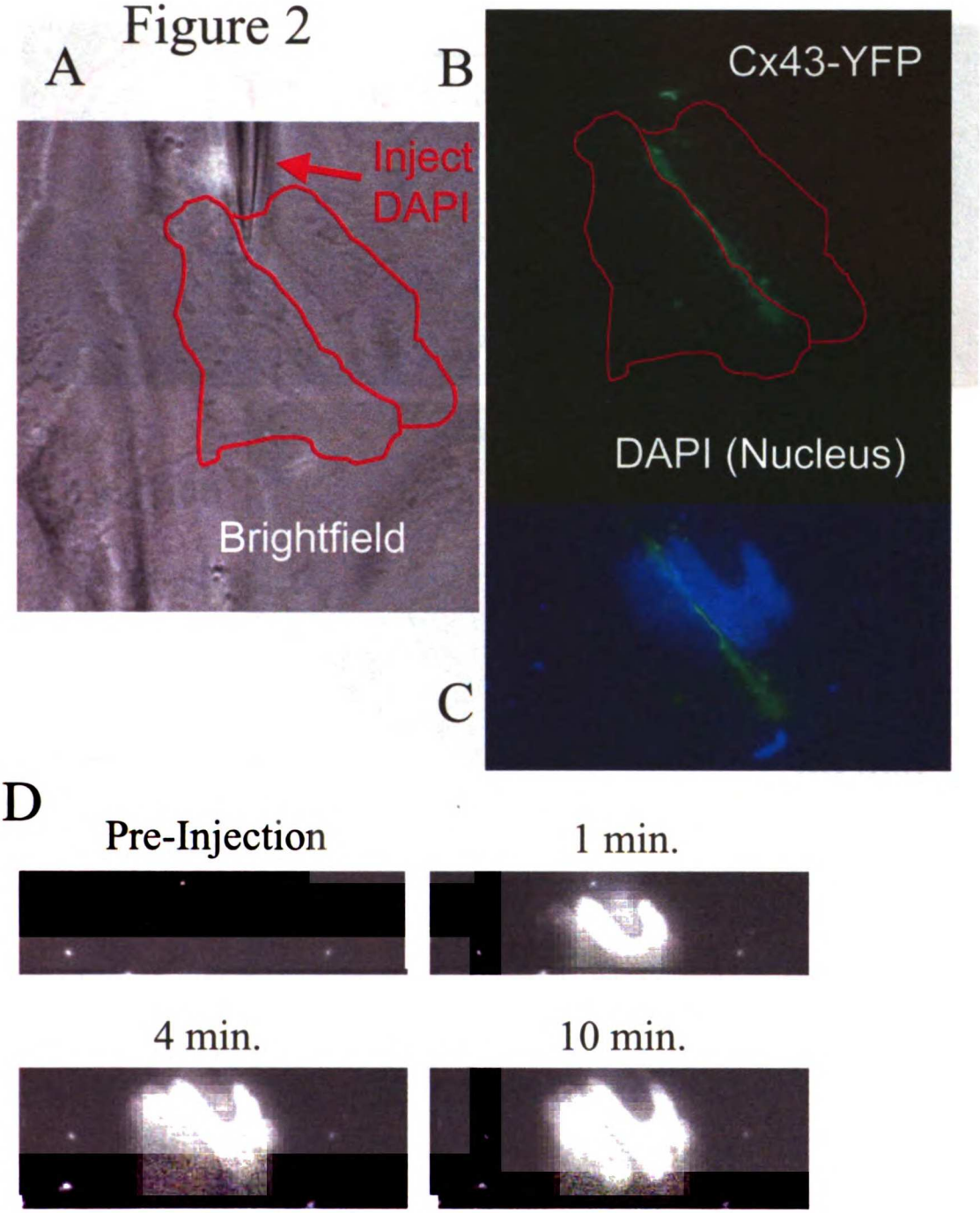

2. Microinjection of Cx43-YFP-Transfected HeLa Cells. A. Brightfield image of pipette positioned above nucleus. B,C. Fluorescence images of Cx43 Plaque (green) and nuclei (blue). D. Time course of DAPI transfer between nuclei.

Figure 3

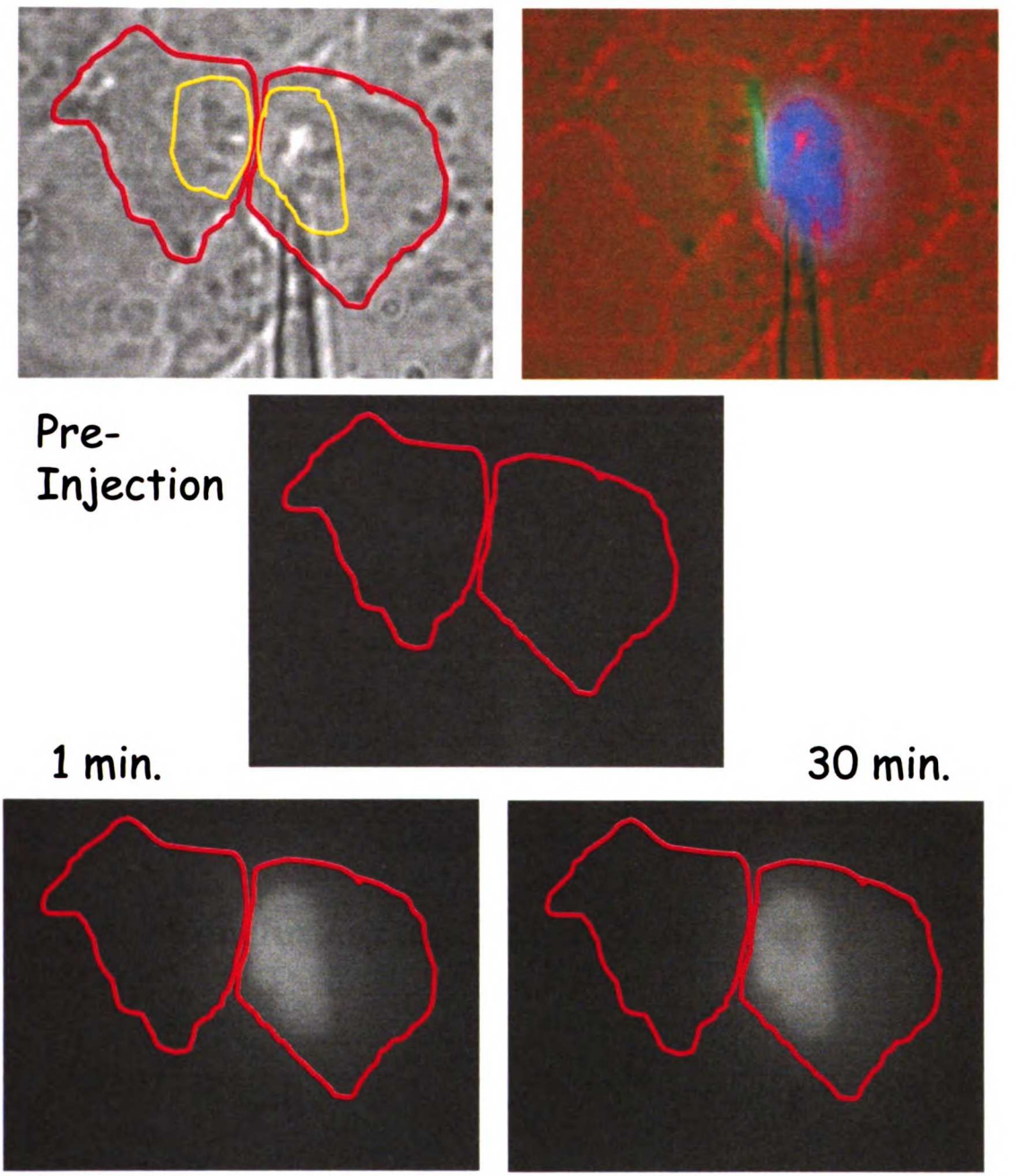

3. Microinjection of Cx43-YFP-Transfected HeLa Cells with NRSE-Cy3 RNA. A. Brightfield image of pipette positioned above nucleus. B. Fluorescence images of Cx43 plaque (green) and injected nucleus (yellow) overlayed with brightfield (red). C. Time points pre- and post-injection..

Chapter 5

Conclusions and Future Directions

Our work with SK channels in neutrophils adds to a growing literature showing the diverse and important roles that ion channels play in immune cells. Ion channels in neutrophils, in particular, have received attention recently with the discovery that the large conductance, calcium-activated (BK) potassium channel is essential for microbial killing [1], and the cloning of the elusive voltage-dependent proton channel [2]. The BK channel discovery was surprising, and controversial, since none of the previous electrophysiological studies of neutrophils [3], eosinophils [4-6], or HL-60 cells [7, 8] have detected the presence of this prominent voltage-dependent current. Nevertheless, Segal and colleagues showed striking effects on killing of *S. aureus, C. albicans, and S. marcescens*, phagosomal pH regulation, and proteolysis of phagocytosed microbes, using both peptide and non-peptide blockers and activators of BK channels [1]. The mechanism that they propose is that the BK current partially compensates for NADPH oxidase electrogenic activity, creating an alkaline, high ionic strength phagosomal environment that promotes protease release from azurophilic granule matrix by ion exchange [1, 9]. While the physiological effects of the BK blockers iberiotoxin and paxilline on neutrophil microbicidal activity are clear, the links to phagosomal potassium content and ionic strength are more tenuous, given the lack of effective probes for making such measurements in live cells.

The recently cloned voltage-gated proton channel [2, 10] should allow for more detailed studies of the neutrophil oxidative burst and its regulation by ionic fluxes, though proton channel studies are still hampered by the lack of specific pharmacological tools. While it has generally been accepted that the proton channel provides the compensatory charge necessary to allow continuous superoxide generation by the voltage-dependent

NADPH oxidase [11], Segal suggested recently that chloride flux through glycine receptor channels is the predominant compensatory current [12]. While the study behind this claim remains unpublished, it seems unlikely that the phagosomal chloride reservoir would be sufficient to counterbalance the large amounts of electrogenic superoxide delivery into the phagosome. However, now that the channels proposed to be involved in neutrophil oxidative activity have been identified, it should be possible to study their necessity in the respiratory burst using conditional knockout mice or by differentiating bone marrow myeloid precursor cells from knockout mice in neutrophils.

Our finding that SK channels modulate granulocyte ROS production not only adds another ion channel to the list of those expressed in immune cells, but also suggests a role in NADPH oxidase-independent ROS generation. Apamin's ability to reduce peroxide accumulation in neutrophils and PLB-985 cells stimulated with the bacterial chemotactic peptide fMLF or with heat-killed, opsonized bacteria shows that SK channels are likely activated by physiologically relevant stimuli. However, the fact that the 1-EBIO and apamin effects remain, even in the gp91*phox* knockout cell line [13], indicates that SK channels are not influencing the respiratory burst, but rather an alternative source of ROS.

Defining precisely the species observed and regulated by SK channel activity is a particular challenge, given the lack of specificity of many fluorogenic ROS probes. Dihydrorhodamine 123, for example, can be oxidized not only by hydrogen peroxide in the presence of a peroxidase, but also by hydroxyl radical and hypochlorous acid [14, 15], alkyl peroxides, and even ROS of uncertain identity. In the highly oxidizing environments of granules and peroxisomes, the endoplasmic reticulum, and the

mitochondria, not only ROS, but also enzymes that produce, modify, and dispose of ROS further complicate detection. The dihydrorhodamine 123 oxidation in the presence of 1-EBIO is likely myeloperoxidase-dependent, since it is present in both undifferentiated and differentiated PLB-985 cells, both of which express myeloperoxidase [16], but not in HeLa cells, which are not promyelocytic and therefore do not express myeloperoxidase. PF1 [17] is a relatively new probe, and while it offers the promise of peroxidase-independent detection of hydrogen peroxide, it has not been well characterized. PF1 can be oxidized by nitric oxide, but not by superoxide or hypochlorous acid. The hypochlorous acid result is complicated by the fact that fluorescein is bleached by HOCl, and the consequent requirement of a peroxidase inhibitor, such as 4-aminobenzoic acid hydrazide [18], when using this probe in myeloperoxidase-positive cells. In fact, the DHR 123 results could be replicated with PF1 only in PLB-985 cells, which have a much lower myeloperoxidase content than neutrophils, presumably due to incomplete myeloperoxidase block by even high concentrations of inhibitor. And so while the consistency of the DHR 123 and PF1 results strongly suggests that both are detecting hydrogen peroxide, the possibility that both are oxidized by another, less well characterized ROS cannot be ruled out.

Dihydroethidine appears to be relatively specific for superoxide [14], and the fact that 1-EBIO increases oxidation of both DHE and peroxide-sensing probes indicates that the source of the ROS is a superoxide-producing pathway. Since 1-EBIO and apamin appear to act on ROS production in a NADPH oxidase-independent pathway, based on our findings in the gp91phox knockout PLB-985 cell line, the mitochondria are the most likely source of superoxide and hydrogen peroxide. That does not necessarily mean,

however, that the hydrogen peroxide-sensitive probes are oxidized in the mitochondria. Hydrogen peroxide can diffuse through membranes, as can the probes used, so oxidation could occur in the lumen of the mitochondria, the endoplasmic reticulum, lysosomes, or granules. In this way, there may be a link between the glutathione cycle [19], the major redox regulator in cells, and the ROS observed in our assays. While our results with MitoSOX [20], showing that 1-EBIO increases mitochondrial superoxide production and reversal of this effect by apamin, do suggest SK channels are influencing mitochondrial ROS, experiments using mitochondrial uncouplers seem to make this conclusion less than satisfactory. Neither 2,4-dinitrophenol nor the protonophore FCCP, both widely used uncouplers, decreased the effect of 1-EBIO, and seemed to, in fact, sharpen the effect of apamin. This could mean that mitochondrial ROS actually are background signal and obscure results with DHR 123. It will be important to clarify which cellular compartment is the source of the species that reduce DHR 123, PF1, and DHE, and these studies are underway. One potential approach will be to co-localize probe oxidation with live-cell markers for the mitochondria, ER, or lysosomes, using deconvolution microscopy.

Apamin, as a peptide toxin, does not cross lipid bilayers, which means that it is unlikely to reach organellar membranes, except by endocytosis. The SK channels affecting ROS production, thus, are almost certainly localized at the plasma membrane. How any depolarization caused by SK block might lead to alteration of an organelle's lumenal oxidative activity is uncertain. Neither apamin nor 1-EBIO had any clear effects on cytoplasmic calcium levels after fMLF stimulation, indicating that SK channels are not influencing calcium release from intracellular stores. It is possible that SK block might lead to depolarization and increased potassium efflux, which could, in turn,

upregulate the Na^+,K^+ ATPase and lead to increased ADP levels and stimulate mitochondrial ATP production. Perhaps 1-EBIO has the opposite effect, and causes the mitochondrial respiratory chain to run in reverse, producing greater amounts of superoxide at complex I or complex III. An alternative explanation is that SK activation leads to complex I or complex III blockade by another pathway. The fact that the complex I blocker rotenone increases DHE conversion to ethidium shows that this probe is capable of sensing mitochondrial ROS production.

Whatever the mechanism of SK modulation of granulocyte ROS production, its most likely consequence would be on downstream effects of ROS production, particularly apoptosis. Indeed, our finding that 1-EBIO increases the percentage of cells undergoing staurosporine-induced apoptosis supports this assertion. Since hydrogen peroxide is a potent apoptotic agent [16, 21], it is likely that 1-EBIO enhances the amount of this reactive metabolite produced by the mitochondria. It seems less likely that SK channels would be involved in microbicidal activity, given that loss of NADPH oxidase is sufficient to abrogate oxidative killing mechanisms [22]. Any other sources of ROS, clearly, are not able to compensate for the loss of the respiratory burst generated by this key enzymatic complex. Differentiation of myeloid precursor cells to neutrophils might also be impacted by SK channel activity, since undifferentiated PLB-985 cells express this channel. Intermediate-conductance, calcium-activated potassium channels (IK) have been found to regulate differentiation of myoblasts [23] and B-cell proliferation [24]. With the identification of SK3 in the myeloid precursor leukemic cell lines PLB-985 and HL-60, and in human neutrophils, and further characterization of the mechanisms of ROS

regulation by channels in these cells, SK channels may be a target for immunomodulatory therapies in the future.

Gap junctions are a class of channels completely unrelated to six transmembrane segment, calcium-activated potassium channels, but they may couple the calcium signals transmitted from cell to cell [25], which modulate the activity of channels such as SK. We have identified the intriguing possibility that ions and other small molecules may be shared not only between the cytoplasms of adjoining cells, but also between nuclei. While it is unlikely that genetic information is shared between nuclei via gap junctions, given these channels' size limitations [26], it is certainly possible that modifiers of gene transcription and other cellular signal transduction pathways could be exchanged between nuclei. Nuclei have discrete pools of calcium [27] and glutathione [28], that are maintained independently of cytoplasmic reservoirs, and which likely influence chromatin regulation [27], and both of these small species could certainly move back and forth through gap junctions. Small RNAs, such as double-stranded siRNAs, though they act predominantly in the cytoplasm, have also been found to be sequestered in the nuclei of fission yeast and plants [29], where they affect gene transcription. Thus, the mechanism of internuclear gap junction communication that we have proposed is ripe for testing in many cell types and various cargoes. Immune cells seem promising, given the observation that nuclei are more likely to be polarized in pairs of cells than in large clusters. With recent work showing a role for gap junctions in antigen presentation [30] and dendritic cell activation [31], it will be interesting to see whether nuclear small molecules are effectors in these processes.

Our findings regarding gap junction localization provide many possible directions to expand our work into other cell types and other membrane proteins. While gap junctions are expressed in many cell types, their functional roles are well characterized primarily in cardiomyocytes [32] and interneurons [33, 34]. Their functions in hepatocytes [35], immune cells [36], and skin cells [37], for example, are still poorly understood, and their impact during the development of the heart [38], the nervous system [38, 39], and other organs remains open questions. The implications of our work on these developmental questions may be of particular interest, given the already well-established role that cadherins play in organogenesis [40, 41].

We have defined a novel mechanism for the targeting of connexin proteins to points of cell-cell contact, a pathway that depends on microtubule plus-ends and plus-end binding proteins, and capture of microtubule plus-ends by adherens junctions. Such a pathway adds significantly to our understanding of how membrane proteins reach different parts of the cell. While selective retention and retrieval are now certainly well-established mechanisms [42] for altering the density of membrane proteins that have reached the cell surface, less attention has been given to the question of how membrane proteins can be selectively delivered to particular domains of the plasma membrane. While polarized epithelial cells have a clear demarcation between the apical and basolateral surfaces, and defined populations of proteins that reach each surface, cardiomyocytes and neurons, too, can be thought of as polarized cells with distinct membrane domains.

Membrane proteins are synthesized and inserted co-translationally into the endoplasmic reticulum, where they fold properly and acquire post-translational

modifications such as glycosylation and disulfide bond formation. After further processing in the Golgi network, vesicles containing these proteins emerge and are transported, presumably by motor proteins along microtubules, to the plasma membrane or to organellar membranes. In general, the steps between the Golgi and the plasma membrane are poorly characterized, since adapter proteins and specific interactions between motor proteins and cargo are unknown, in most cases. Furthermore, the events immediately preceding vesicle fusion with the plasma membrane, namely the interaction of the cytoskeleton with the membrane cortex and off-loading of cargo, are also poorly characterized. Our work explores these events, combining search and capture of microtubule plus-ends, which plays a role in mitotic spindle orientation [43], and preferential off-loading of vesicles from microtubules at specific plasma membrane regions. We propose, specifically, that adherens junction proteins can capture the microtubule plus-ends preferentially, leading to deposition of Cx43-containing vesicles at adherens junctions. Such directed delivery mechanisms have been proposed for zymogen granules to the apical membrane by dynein/dynactin [44] and for minus-end-directed transport of organelles [45]. We cannot say, at this point, whether vesicles fuse directly with the membrane at microtubule plus-ends, or if they are transferred to the cortical actin cytoskeleton for lateral transport before being inserted.

Gap junctions in the nervous system are the key components of electrical synapses, which allow neurons to be electrically coupled and to form synchronized circuits. These electrical synapses, while prevalent during early development, are gradually replaced by chemical synapses postnatally as NMDA receptor activity increases [46]. The electrical synapses that remain are important for oscillatory behavior

of networks of interneurons in the hippocampus [47], for enhanced coordination of motor activity [48], for sharpening visual resolution in the retina [49]. Stem cell transplantation therapies have the potential to repair damaged circuitry, though the complex architecture of brain circuitry makes this an even more challenging problem than for the heart. In addition, delivery of Cx36, the pre-dominant connexin isoform in the brain, to cell-cell contact sites may not be regulated by the same pathway as the one which we characterized for Cx43 .

In the heart, the orientation of cardiomyocytes, which have adherens junction, gap junction, and desmosomal proteins localized at the intercalated disc, but not the transverse side of the cell, is essential for proper electrical conductivity [50, 51]. Changes in membrane potential are transmitted from cell to cell through intercalated disc gap junctions, as the cardiac action potential spreads through the heart. Thus, loss of gap junctional communication [52], or mislocalization of gap junctions to the transverse side of cells, can lead to severe conduction defects, and both of these cases are associated with ischemic damage to the heart [53].

Our work may help to shed some light on the mechanisms of ischemic damage, and points to further experiments to test possible models. If gap junction placement at the adherens junction requires the presence of N-cadherin and β-catenin, as well as capture of microtubule plus-ends at the adherens junction, one can imagine several scenarios that might lead to ischemic mislocalization. Placement of adherens junction proteins might be disrupted, leading to the appearance of N-cadherin and β-catenin at the transverse membrane. This, in turn, could recruit microtubule plus-ends that would

deliver connexin protein to the transverse membrane, leading to improper conduction in the heart and arrhythmogenic activity.

An alternative scenario could be the appearance of another protein at the transverse side, following an ischemic insult, capable of capturing microtubule plus-ends and gathering gap junction proteins in an adherens junction-independent process. Studies showing that the stress-activated protein kinase JNK causes down-regulation of Cx43 without affecting other intercalated disc proteins [54] suggest that this kinase might mediate selective retrieval of Cx43.

A third possibility might rely more on the selective retrieval of connexin proteins from the intercalated disc and transverse membranes: perhaps connexins reach both plasma membrane regions under normal physiological conditions, but are selectively retained at the intercalated disc and/or selectively retrieved from the transverse side. After ischemia, a protein capable of retaining connexins at the intercalated disc might be mislocalized to the transverse side, or retrieval machinery that normally removes any connexin that reaches the transverse membrane could be impaired. These possibilities warrant careful analyses in future studies. The presence of adherens junction proteins at the transverse sides of ischemic cardiomyocytes would support the first model, while the absence of N-cadherin and β-catenin at the transverse membrane could suggest the second model. One might also look for the presence of proteins capable of EB1 capture at the cortex, such as CLASPs [55], in order to determine whether microtubule plus-ends appear more frequently and dwell longer at transverse side cortical sites following ischemic injury. Microinjection of fluorescently-tagged EB1 into cardiomyocytes would facilitate imaging of microtubule plus-end dynamics in these cells that are difficult to

transfect. Studies of altered retention might involve identifying known connexin-binding proteins, such as ZO-1 [56], at post-ischemic transverse membranes, or searching for new connexin-interacting proteins by comparing immunoprecipitation results for normoxic and hypoxic cardiomyocytes. Investigating differences in endocytic rates at the intercalated disc and transverse side would be experimentally more challenging, given the low transfection efficiency of cardiomyocytes, but pulse-chase experiments, using fluorescently tagged antibodies targeted at gap junction extracellular domains, for example, might allow a comparison of connexin endocytosis. Perhaps differential lipid compositions of intercalated disc membranes versus transverse membranes could also be exploited to investigate normal and annular endocytosis rates in healthy and ischemic cardiomyocytes.

Our findings suggest the exciting possibility that hypoxic damage to the heart may be a disease of protein mistargeting, leading to improper electrical conduction and potentially fatal arrythmias. Presumably, ischemic pre-conditioning could prevent connexin mislocalization as part of its protective effect, and identifying key regulatory points for maintaining proper gap junction distribution could form the basis for cardioprotective therapies. In other instances of heart damage, however, gap junction intercellular communication may be deleterious [57, 58], transmitting apoptotic signals or reactive oxygen species from a damaged cell to its neighbor. In such cases, down-regulation of gap junctions may be a protective response by cells in order to limit the spread of toxicity.

Development of the heart, too, requires gap junctions, as evidenced by studies of Cx43 knockout mice [59], and it is likely that rebuilding damaged heart, too, will require

the establishment of gap junctional coupling between heart cells and transplanted cells. Developmentally, the triggers for changes in subcellular localization of connexin during heart formation are still uncharacterized, though Cx43 organization at the intercalated disc follows the appearance of N-cadherin at that region [60, 61]. While gap junctions initially have a relatively uniform distribution around the sarcolemmal membrane postnatally, they gradually begin to co-localize with adherens junctions and desmosomes over the period of 20-90 days postnatal in mice [62-64]. This redistribution is accompanied by increasing density of adherens junction and desmosomal proteins at the intercalated disc, and could depend, according to our model, on the development of microtubule plus-end capture sites at the adherens junction. Concentration of connexins at the intercalated disc allows the establishment of directional conduction and propagation of action potentials, and may offer valuable clues for the remodeling of damaged heart tissue.

Attempts at using stem cell therapy to repair post-ischemic heart tissue have so far been unsuccessful, and the failure of skeletal muscle myoblasts, in particular, may be due to lack of gap junction communication in the transplanted cells. Skeletal muscles are an attractive option for transplantation to congestive heart failure patients, given that they are accessible from the patient's own muscle tissue, are already contractile cells, and are resistant to ischemia [65]. Unfortunately, skeletal muscle cells are arrythmogenic when transferred to the heart [66, 67], a side-effect that may result from their inability to synchronize electrically with the rest of the heart. Perhaps transfecting these cells with Cx43 could lead to gap junction formation between cardiomyocytes and the skeletal muscle cells, and enable greater synchronization and contractile function without

arrhythmia. Our model for gap junction localization would argue for co-transfecting N-cadherin with Cx43, in order to promote adherens junction formation that would correctly localize and orient gap junction proteins for intercellular conduction. Embryonic stem cells, which can be differentiated in vitro to cardiomyocytes with intercalated discs and functional gap junctions [68], or neonatal cardiomyocytes [69] may offer a more promising strategy for cell transplantation.

The intersection of these three projects brings together several fields, and leads to many unexplored questions regarding the roles of channels in immune cell reactive oxygen species production, the ways in which cells communicate and conflict with each other through gap junction intercellular channels and ROS release. Gap junctions have now been shown to play a role in both adaptive and innate immunity, with their functions in the sharing of antigenic peptides between antigen-presenting cells [30] and the activation of dendritic cells [31] and neutrophils [70], for example. Interactions between immune cells are a particularly promising case for internuclear communication through gap junctions, since pairs of cells seem more likely to have polarized nuclei than clusters of cells, based on our findings. Gap junctions may enable such cells to rapidly share modifications in transcriptional responses mediated by small, nuclear-localized molecules. Beyond transcriptional regulation, gap junctions may allow signals for regulating ROS or NOS production to spread from cell to cell, perhaps by modifying the activities of ion channels such as SK, BK, or the voltage-gated proton channel. These reactive oxygen species may then be targeted against pathogenic microbes, or may be the agents of inflammatory damage to host tissue. Such oxidant-mediated destruction of

cardiac or brain tissue, by as yet unknown mechanisms, may trigger apoptotic or necrotic cell death in some cells, and ischemic damage in other cells. In the heart, gap junction proteins are downregulated and mislocalized following an ischemic insult, leading to impaired propagation of action potentials and potentially fatal arrhythmias. The prospect of using stem cells, expressing the appropriate complement of gap junction and adherens junction proteins, to repair infarcted tissue is an enticing, but still distant goal. In the meantime, my work on granulocyte ROS production and gap junction formation and communication points to several steps for limiting inflammatory destruction: immune cell activation, the sharing of information between immune cells, the release of reactive oxygen species by granulocytes, and the alterations in gap junction trafficking that follow ROS-mediated damage.

1. Ahluwalia, J., A. Tinker, L. H. Clapp, M. R. Duchen, A. Y. Abramov, S. Pope, M. Nobles, A. W. Segal (2004). The large-conductance Ca2+-activated K+ channel is essential for innate immunity. *Nature*, 427:853-858.
2. Ramsey, I. S., M. M. Moran, J. A. Chong, D. E. Clapham (2006). A voltage-gated proton-selective channel lacking the pore domain. *Nature*.
3. Krause, K. H., M. J. Welsh (1990). Voltage-dependent and Ca2(+)-activated ion channels in human neutrophils. *J Clin Invest*, 85:491-498.
4. Tare, M., S. A. Prestwich, D. V. Gordienko, S. Parveen, J. E. Carver, C. Robinson, T. B. Bolton (1998). Inwardly rectifying whole cell potassium current in human blood eosinophils. *J Physiol*, 506 (Pt 2):303-318.
5. Saito, M., R. Sato, I. Hisatome, T. Narahashi (1996). RANTES and platelet-activating factor open Ca2+-activated K+ channels in eosinophils. *Faseb J*, 10:792-798.
6. Saito, M., R. Sato, N. M. Munoz, A. Herrnreiter, M. Oyaizu, H. Kasugai, T. Narahashi, A. R. Leff (1997). Association of granular exocytosis with Ca(2+)-activated K+ channels in human eosinophils. *Am J Physiol*, 273:L16-21.
7. Varnai, P., N. Demaurex, M. Jaconi, W. Schlegel, D. P. Lew, K. H. Krause (1993). Highly co-operative Ca2+ activation of intermediate-conductance K+ channels in granulocytes from a human cell line. *J Physiol*, 472:373-390.
8. Wieland, S. J., Q. H. Gong, R. H. Chou, L. H. Brent (1992). A lineage-specific Ca(2+)-activated K+ conductance in HL-60 cells. *J Biol Chem*, 267:15426-15431.

9. Reeves, E. P., H. Lu, H. L. Jacobs, C. G. Messina, S. Bolsover, G. Gabella, E. O. Potma, A. Warley, J. Roes, A. W. Segal (2002). Killing activity of neutrophils is mediated through activation of proteases by K+ flux. *Nature*, 416:291-297.
10. Sasaki, M., M. Takagi, Y. Okamura (2006). A Voltage Sensor-Domain Protein is a Voltage-Gated Proton Channel. *Science*.
11. DeCoursey, T. E., D. Morgan, V. V. Cherny (2003). The voltage dependence of NADPH oxidase reveals why phagocytes need proton channels. *Nature*, 422:531-534.
12. Segal, A. W. (2005). How neutrophils kill microbes. *Annu Rev Immunol*, 23:197-223.
13. Zhen, L., A. A. King, Y. Xiao, S. J. Chanock, S. H. Orkin, M. C. Dinauer (1993). Gene targeting of X chromosome-linked chronic granulomatous disease locus in a human myeloid leukemia cell line and rescue by expression of recombinant gp91phox. *Proc Natl Acad Sci U S A*, 90:9832-9836.
14. Walrand, S., S. Valeix, C. Rodriguez, P. Ligot, J. Chassagne, M. P. Vasson (2003). Flow cytometry study of polymorphonuclear neutrophil oxidative burst: a comparison of three fluorescent probes. *Clin Chim Acta*, 331:103-110.
15. Crow, J. P. (1997). Dichlorodihydrofluorescein and dihydrorhodamine 123 are sensitive indicators of peroxynitrite in vitro: implications for intracellular measurement of reactive nitrogen and oxygen species. *Nitric Oxide*, 1:145-157.
16. Wagner, B. A., G. R. Buettner, L. W. Oberley, C. J. Darby, C. P. Burns (2000). Myeloperoxidase is involved in H2O2-induced apoptosis of HL-60 human leukemia cells. *J Biol Chem*, 275:22461-22469.
17. Miller, E. W., A. E. Albers, A. Pralle, E. Y. Isacoff, C. J. Chang (2005). Boronate-based fluorescent probes for imaging cellular hydrogen peroxide. *J Am Chem Soc*, 127:16652-16659.
18. Kettle, A. J., C. A. Gedye, M. B. Hampton, C. C. Winterbourn (1995). Inhibition of myeloperoxidase by benzoic acid hydrazides. *Biochem J*, 308 (Pt 2):559-563.
19. Schafer, F. Q., G. R. Buettner (2001). Redox environment of the cell as viewed through the redox state of the glutathione disulfide/glutathione couple. *Free Radic Biol Med*, 30:1191-1212.
20. Lieven, C. J., M. J. Hoegger, C. R. Schlieve, L. A. Levin (2006). Retinal ganglion cell axotomy induces an increase in intracellular superoxide anion. *Invest Ophthalmol Vis Sci*, 47:1477-1485.
21. Kasahara, Y., K. Iwai, A. Yachie, K. Ohta, A. Konno, H. Seki, T. Miyawaki, N. Taniguchi (1997). Involvement of reactive oxygen intermediates in spontaneous and CD95 (Fas/APO-1)-mediated apoptosis of neutrophils. *Blood*, 89:1748-1753.
22. Thrasher, A. J., N. H. Keep, F. Wientjes, A. W. Segal (1994). Chronic granulomatous disease. *Biochim Biophys Acta*, 1227:1-24.
23. Fioretti, B., T. Pietrangelo, L. Catacuzzeno, F. Franciolini (2005). Intermediate-conductance Ca2+-activated K+ channel is expressed in C2C12 myoblasts and is downregulated during myogenesis. *Am J Physiol Cell Physiol*, 289:C89-96.
24. Wulff, H., H. G. Knaus, M. Pennington, K. G. Chandy (2004). K+ channel expression during B cell differentiation: implications for immunomodulation and autoimmunity. *J Immunol*, 173:776-786.

25. Wolszon, L. R., V. Rehder, S. B. Kater, E. R. Macagno (1994). Calcium wave fronts that cross gap junctions may signal neuronal death during development. *J Neurosci*, 14:3437-3448.
26. Moreno, A. P. (2005). Connexin phosphorylation as a regulatory event linked to channel gating. *Biochim Biophys Acta*, 1711:164-171.
27. Hardingham, G. E., S. Chawla, C. M. Johnson, H. Bading (1997). Distinct functions of nuclear and cytoplasmic calcium in the control of gene expression. *Nature*, 385:260-265.
28. Bellomo, G., M. Vairetti, L. Stivala, F. Mirabelli, P. Richelmi, S. Orrenius (1992). Demonstration of nuclear compartmentalization of glutathione in hepatocytes. *Proc Natl Acad Sci U S A*, 89:4412-4416.
29. Bernstein, E., C. D. Allis (2005). RNA meets chromatin. *Genes Dev*, 19:1635-1655.
30. Neijssen, J., C. Herberts, J. W. Drijfhout, E. Reits, L. Janssen, J. Neefjes (2005). Cross-presentation by intercellular peptide transfer through gap junctions. *Nature*, 434:83-88.
31. Matsue, H., J. Yao, K. Matsue, A. Nagasaka, H. Sugiyama, R. Aoki, M. Kitamura, S. Shimada (2006). Gap junction-mediated intercellular communication between dendritic cells (DCs) is required for effective activation of DCs. *J Immunol*, 176:181-190.
32. Severs, N. J., S. R. Coppen, E. Dupont, H. I. Yeh, Y. S. Ko, T. Matsushita (2004). Gap junction alterations in human cardiac disease. *Cardiovasc Res*, 62:368-377.
33. Galarreta, M., S. Hestrin (2001). Electrical synapses between GABA-releasing interneurons. *Nat Rev Neurosci*, 2:425-433.
34. Kiehn, O., M. C. Tresch (2002). Gap junctions and motor behavior. *Trends Neurosci*, 25:108-115.
35. Gonzalez, H. E., E. A. Eugenin, G. Garces, N. Solis, M. Pizarro, L. Accatino, J. C. Saez (2002). Regulation of hepatic connexins in cholestasis: possible involvement of Kupffer cells and inflammatory mediators. *Am J Physiol Gastrointest Liver Physiol*, 282:G991-G1001.
36. Oviedo-Orta, E., W. Howard Evans (2004). Gap junctions and connexin-mediated communication in the immune system. *Biochim Biophys Acta*, 1662:102-112.
37. van Steensel, M. A. (2004). Gap junction diseases of the skin. *Am J Med Genet C Semin Med Genet*, 131C:12-19.
38. Wei, C. J., X. Xu, C. W. Lo (2004). Connexins and cell signaling in development and disease. *Annu Rev Cell Dev Biol*, 20:811-838.
39. Sohl, G., S. Maxeiner, K. Willecke (2005). Expression and functions of neuronal gap junctions. *Nat Rev Neurosci*, 6:191-200.
40. Lecuit, T. (2005). Adhesion remodeling underlying tissue morphogenesis. *Trends Cell Biol*, 15:34-42.
41. Nose, A., M. Takeichi (1986). A novel cadherin cell adhesion molecule: its expression patterns associated with implantation and organogenesis of mouse embryos. *J Cell Biol*, 103:2649-2658.
42. Rodriguez-Boulan, E., G. Kreitzer, A. Musch (2005). Organization of vesicular trafficking in epithelia. *Nat Rev Mol Cell Biol*, 6:233-247.

43. Lee, L., J. S. Tirnauer, J. Li, S. C. Schuyler, J. Y. Liu, D. Pellman (2000). Positioning of the mitotic spindle by a cortical-microtubule capture mechanism. *Science*, 287:2260-2262.
44. Kraemer, J., F. Schmitz, D. Drenckhahn (1999). Cytoplasmic dynein and dynactin as likely candidates for microtubule-dependent apical targeting of pancreatic zymogen granules. *Eur J Cell Biol*, 78:265-277.
45. Vaughan, P. S., P. Miura, M. Henderson, B. Byrne, K. T. Vaughan (2002). A role for regulated binding of p150(Glued) to microtubule plus ends in organelle transport. *J Cell Biol*, 158:305-319.
46. Arumugam, H., X. Liu, P. J. Colombo, R. A. Corriveau, A. B. Belousov (2005). NMDA receptors regulate developmental gap junction uncoupling via CREB signaling. *Nat Neurosci*, 8:1720-1726.
47. Hormuzdi, S. G., I. Pais, F. E. LeBeau, S. K. Towers, A. Rozov, E. H. Buhl, M. A. Whittington, H. Monyer (2001). Impaired electrical signaling disrupts gamma frequency oscillations in connexin 36-deficient mice. *Neuron*, 31:487-495.
48. Placantonakis, D. G., A. A. Bukovsky, X. H. Zeng, H. P. Kiem, J. P. Welsh (2004). Fundamental role of inferior olive connexin 36 in muscle coherence during tremor. *Proc Natl Acad Sci U S A*, 101:7164-7169.
49. DeVries, S. H., X. Qi, R. Smith, W. Makous, P. Sterling (2002). Electrical coupling between mammalian cones. *Curr Biol*, 12:1900-1907.
50. Shaw, R. M., Y. Rudy (1997). Ionic mechanisms of propagation in cardiac tissue. Roles of the sodium and L-type calcium currents during reduced excitability and decreased gap junction coupling. *Circ Res*, 81:727-741.
51. Gros, D. B., H. J. Jongsma (1996). Connexins in mammalian heart function. *Bioessays*, 18:719-730.
52. Kaprielian, R. R., M. Gunning, E. Dupont, M. N. Sheppard, S. M. Rothery, R. Underwood, D. J. Pennell, K. Fox, J. Pepper, P. A. Poole-Wilson, N. J. Severs (1998). Downregulation of immunodetectable connexin43 and decreased gap junction size in the pathogenesis of chronic hibernation in the human left ventricle. *Circulation*, 97:651-660.
53. Peters, N. S., J. Coromilas, N. J. Severs, A. L. Wit (1997). Disturbed connexin43 gap junction distribution correlates with the location of reentrant circuits in the epicardial border zone of healing canine infarcts that cause ventricular tachycardia. *Circulation*, 95:988-996.
54. Petrich, B. G., X. Gong, D. L. Lerner, X. Wang, J. H. Brown, J. E. Saffitz, Y. Wang (2002). c-Jun N-terminal kinase activation mediates downregulation of connexin43 in cardiomyocytes. *Circ Res*, 91:640-647.
55. Mimori-Kiyosue, Y., I. Grigoriev, G. Lansbergen, H. Sasaki, C. Matsui, F. Severin, N. Galjart, F. Grosveld, I. Vorobjev, S. Tsukita, A. Akhmanova (2005). CLASP1 and CLASP2 bind to EB1 and regulate microtubule plus-end dynamics at the cell cortex. *J Cell Biol*, 168:141-153.
56. Toyofuku, T., M. Yabuki, K. Otsu, T. Kuzuya, M. Hori, M. Tada (1998). Direct association of the gap junction protein connexin-43 with ZO-1 in cardiac myocytes. *J Biol Chem*, 273:12725-12731.

57. Garcia-Dorado, D., A. Rodriguez-Sinovas, M. Ruiz-Meana (2004). Gap junction-mediated spread of cell injury and death during myocardial ischemia-reperfusion. *Cardiovasc Res*, 61:386-401.
58. Rodriguez-Sinovas, A., D. Garcia-Dorado, M. Ruiz-Meana, J. Soler-Soler (2006). Protective effect of gap junction uncouplers given during hypoxia against reoxygenation injury in isolated rat hearts. *Am J Physiol Heart Circ Physiol*, 290:H648-656.
59. Lo, C. W. (2000). Role of gap junctions in cardiac conduction and development: insights from the connexin knockout mice. *Circ Res*, 87:346-348.
60. Kostin, S., S. Hein, E. P. Bauer, J. Schaper (1999). Spatiotemporal development and distribution of intercellular junctions in adult rat cardiomyocytes in culture. *Circ Res*, 85:154-167.
61. Li, J., V. V. Patel, I. Kostetskii, Y. Xiong, A. F. Chu, J. T. Jacobson, C. Yu, G. E. Morley, J. D. Molkentin, G. L. Radice (2005). Cardiac-specific loss of N-cadherin leads to alteration in connexins with conduction slowing and arrhythmogenesis. *Circ Res*, 97:474-481.
62. Gourdie, R. G., C. R. Green, N. J. Severs, R. P. Thompson (1992). Immunolabelling patterns of gap junction connexins in the developing and mature rat heart. *Anat Embryol (Berl)*, 185:363-378.
63. Fromaget, C., A. el Aoumari, D. Gros (1992). Distribution pattern of connexin 43, a gap junctional protein, during the differentiation of mouse heart myocytes. *Differentiation*, 51:9-20.
64. Angst, B. D., L. U. Khan, N. J. Severs, K. Whitely, S. Rothery, R. P. Thompson, A. I. Magee, R. G. Gourdie (1997). Dissociated spatial patterning of gap junctions and cell adhesion junctions during postnatal differentiation of ventricular myocardium. *Circ Res*, 80:88-94.
65. Menasche, P. (2003). Skeletal muscle satellite cell transplantation. *Cardiovasc Res*, 58:351-357.
66. Menasche, P., A. A. Hagege, J. T. Vilquin, M. Desnos, E. Abergel, B. Pouzet, A. Bel, S. Sarateanu, M. Scorsin, K. Schwartz, P. Bruneval, M. Benbunan, J. P. Marolleau, D. Duboc (2003). Autologous skeletal myoblast transplantation for severe postinfarction left ventricular dysfunction. *J Am Coll Cardiol*, 41:1078-1083.
67. Smits, P. C., R. J. van Geuns, D. Poldermans, M. Bountioukos, E. E. Onderwater, C. H. Lee, A. P. Maat, P. W. Serruys (2003). Catheter-based intramyocardial injection of autologous skeletal myoblasts as a primary treatment of ischemic heart failure: clinical experience with six-month follow-up. *J Am Coll Cardiol*, 42:2063-2069.
68. Westfall, M. V., K. A. Pasyk, D. I. Yule, L. C. Samuelson, J. M. Metzger (1997). Ultrastructure and cell-cell coupling of cardiac myocytes differentiating in embryonic stem cell cultures. *Cell Motil Cytoskeleton*, 36:43-54.
69. Cai, J., G. Lin, H. Jiang, B. Yang, X. Jiang, Q. Yu, J. Song (2006). Transplanted Neonatal Cardiomyocytes as a Potential Biological Pacemaker in Pigs with Complete Atrioventricular Block. *Transplantation*, 81:1022-1026.
70. Saez, J. C., M. C. Branes, L. A. Corvalan, E. A. Eugenin, H. Gonzalez, A. D. Martinez, F. Palisson (2000). Gap junctions in cells of the immune system:


UC
San Francisco
LIBRARY
UNIVERSITY OF CALIFORNIA · UNIVERSITY OF CALIFORNIA